AD-A096 696 CALIFORNIA UNIV LIVERMORE LAWRENCE LIVERMORE LAB F/G 12/1
CHARACTERIZATION OF ERRORS INHERENT IN SYSTEM EMP VULNERABILITY--ETC(U)
OCT 80 R M BEVENSEE, H S CABAYAN W-7405-ENG-48
UNCLASSIFIED UCRL-52954

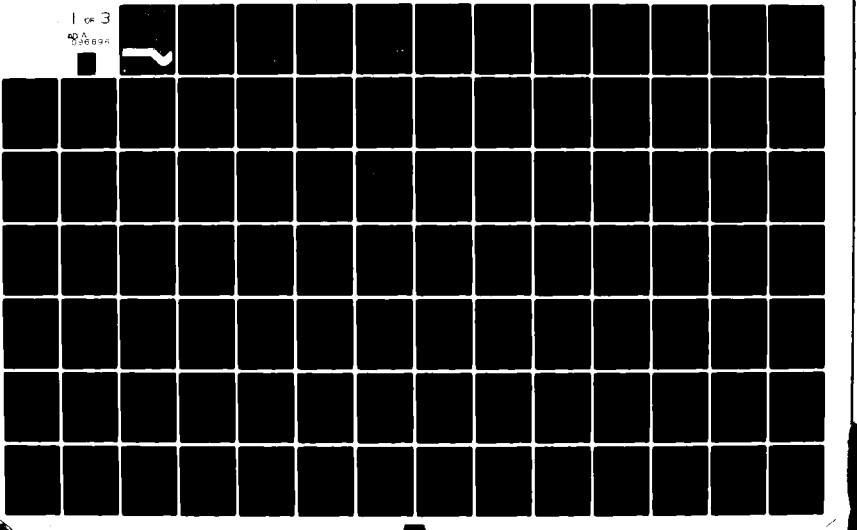

LEVEL II

12

UCRL-52954

Characterization of errors inherent in system EMP vulnerability assessment programs

R. M. Bevensee

H. S. Cabayan

F. J. Deadrick

L. C. Martin

R. W. Mensing

October 1, 1980

Lawrence Livermore Laboratory

DISCLAIMER

Work performed under the auspices of the U.S. Department of Energy by Lawrence Livermore National Laboratory under Contract W-7405-Eng-48.

UCRL-52954
Distribution Category UC-38

Characterization of errors inherent in system EMP vulnerability assessment programs

R. M. Bevensee
H. S. Cabayan
F. J. Deadrick
L. C. Martin
R. W. Mensing

Manuscript date: October 1, 1980

LAWRENCE LIVERMORE LABORATORY
University of California • Livermore, California • 94550

Available from: National Technical Information Service • U.S. Department of Commerce
5285 Port Royal Road • Springfield, VA 22161 • $15.00 per copy • (Microfiche $3.50)

PREFACE

In recognition of the fact that the highest confidence test of systems' survivability to EMP (exposure to an atmospheric nuclear detonation) is not advisable, one seeks to optimize available EMP test and analysis techniques. A first step is to understand and acknowledge the differences between currently used EMP assessment techniques and the ultimate nuclear threat. This report documents Phase I of a two-phase effort to investigate the uncertainties and confidence associated with system EMP vulnerability assessment.

Under Phase I, Lawrence Livermore Laboratory has surveyed assessment techniques in order to illuminate sources of uncertainty and their present treatment in the course of determining system vulnerability.

The Phase II effort will evaluate methods for quantifying and reducing uncertainties.

ACKNOWLEDGMENT

Many individuals have provided us with material and valuable comments in conjunction with this project. Without that generous help, it would have been impossible to conduct the type of survey we undertook. We take this opportunity to thank them all, and list them by affiliation.

Air Force Weapons Laboratory
Chris Ashley
Phil Castillo
Dick Hays
Bill Herman
Bob Pelzl

Braddock, Dunn & McDonald
Alan Malmberg
Don Wunsch

Boeing
Walt Curtis
Don Egelkrout

Defense Nuclear Agency/VLIS
Capt. Frank Eisenbarth
Capt. Mike King

EG&G
J. Keller
G. Sower
Tom Wilson

EM Applications
Dave Merewether

General Electric
Manny Espig (DISIAC)
Hugh O'Donnell
Dante Tasca

General Semiconductor
Mel Clark

Harry Diamond Laboratories
Bob Gray
Bruno Kalab
Joe Kreck
Ting Mak
Bob McCoskey
Joe Miletta
Bob Oswald
Bill Petty
Bob Pfeffer
Charles Ruzic
Dan Spohn
Mike Vrabel
Bob Williams
Tal Wyatt

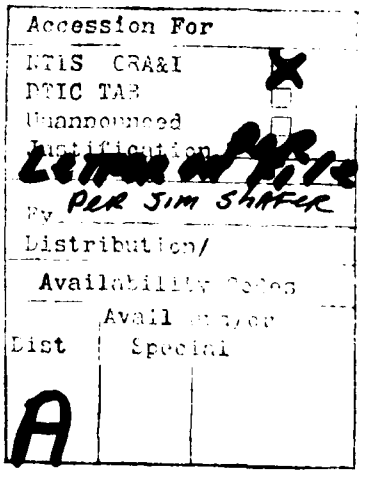

Air Force Weapons Laboratory
Illinois Institute of Technology Research Institute
Irv Mindel

Microwave Assoc.
Yoginder Anand
Gerry Rousseau

Mission Research Corp.
K. Kunz
Jim Prewitt

Naval Reasearch Laboratory
Martin Tanenhaus

NSWC-DL
Vince Puglielli

Naval Surface Weapons Center-WOL
Lloyd Diehl
Bill Emberson
Dave Koury
Lou Libelo
Neil McElroy
Marcella Petree
Ed Rathbun

General Electric
Research and Development Assoc.
John Bombardt
Byron Gage

Reynolds Industry
Ed Malone

Rockwell International
Charles Juster
Jim Locasso
John Wagner

SRI International
Ed Vance

Sylvania
Art Murphy

TRW
Chuck Lear
Bob Pattern
Gus Soux
Bob Webb

Univ. of Michigan
Val Liepa

We greatly appreciate the continuing interest and support of George Baker of the Defense Nuclear Agency.

The authors also wish to thank Toni Bryant, Raylene Cooper, Lisa Lopez, and Debbie Papazian for typing this report and Bob Condouris for his editing.

GLOSSARY

To make this report more nearly self-contained and clear, we include a list of definitions of specialized terms, as applied to the study of the survival of an electronic system subject to an EMP and as used in this report.

Achilles I; II - Air Force simulators, electric dipole (vertically polarized); hybrid (with ground plane reflection).

ADSET - Data processing system similar to DASET.

AESOP - Army simulator.

A-extrapolation - Extrapolation of system response from simulator to threat field by the ratio of these two fields.

ALECS, ARES - Air Force parallel-plate transmission line simulators, vertically polarized.

ATHAMAS I; II - Air Force simulators, hybrid with earth reflection; vertically polarized electric dipole.

ATLAS I; II - Air Force parallel-plate transmission line simulator of horizontal; vertical polarization.

Confidence - With regard to a statement, it is an expression of the probability that the method used to develop the statement led to a true statement. The exact interpretation of confidence will depend on the context of the use of the term probability.

Confidence Interval - An estimate of an interval which has a specified confidence of containing the unknown value (s) of a parameter (s) of interest. The confidence is a statement about the probability that the method

used to construct the interval does provide an estimate which contains the parameter value.

DASET - A data processing system composed of sensor cable, integrator or differentiator, microwave transmitter, dielectric waveguide, receiver, and a recording system.

EMP - Electromagnetic pulse from a nuclear explosion.

EMPRESS - Navy dipole simulator of vertical polarization.

FD - Finite difference, a type of computer code which solves Maxwell's time-dependent field equations by time-stepping, with the differential equations replaced by space-time difference equations.

FREFLD - HDL computer code for long cable response to an incident electromagnetic wave.

Functional Analysis - A detailed study of how the parts (circuits, subsystems, components, etc.) of a system work together to perform their overall function.

HEMPS - Army horizontal electric pulse simulator with vertical electric field, composed of two tapered transmission lines in an inverted V above a wire mesh on ground.

HPD - Air Force horizontally polarized dipole simulator.

Judgmental Uncertainty - Uncertainty associated with the measurements of a process, introduced through the use of subjective opinions, feeling or hunches, due to lack of complete knowledge of parameters, models, etc.

Mission Critical - A designation given to a system, subsystem, component, etc., which must function within certain limits in order for the overall system, of which it is a part, to perform its mission.

MSEP - Multiple systems evaluation program.

POE - Point(s) of entry of EMP through the exterior envelope of a system.

PREMPT - A Boeing Aerospace program for evaluating EMP system hardness.

PRESTO - A Boeing Aerospace code for computing EMP-induced internal current with transmission line and network analyses.

Probability of survival, P_s - Probability that a process (system, component, etc.) will perform its designed function when subject to stresses caused by an EMP.

Random Uncertainty - Basic variation in the measurements associated with a process (system, components, etc.) due to the undeterminable variations in the physical characteristics of the process and the measurement system; it is the inherent variation found in the most measured variables which is outside the control of the researcher. Random variation is usually described by a probability distribution.

"Reasonable and "achievable" - A phrase denoting an error or uncertainty in a measured or computer quantity which has been reached or bettered by at least one organization and which is neither extremely optimistic nor extremely pessimistic relative to many organizations.

REPS - Army repetitive electromagnetic pulse simulator, horizontal dipole with pulser at center.

rss - root sum square.

SCIT - Surface current injection technique of simulating EMP external current response by injection of current of appropriate frequency content.

Screenbox - A recording system consisting basically of sensor, cable, power splitter, attenuator, integrator or differentiator, and oscilloscope(s).

SRF - Air Force horizontally polarized simulator.

Survivability - A measure of the ability of a system with a known vulnerability level to complete a given mission while encountering a defined threat.

Susceptibility - The response of individual components, equipment packages, discrete subsystems, or complete systems to a broad range of electromagnetic stimuli.

Systematic Uncertainty - Uncertainty in the measurements associated with a process due to modeling of processes; modeling of the probability distributions for random uncertainties; calibration of a measurement system; etc. This type of uncertainty is usually within the control of the researcher and can be reduced by improved models, calibration, etc.

TEFS - Army transportable electromagnetic field source, consisting of a horn array, horizontal (HAT) or vertical (VAT), with conducting side screen(s).

TEMPS - HDL transportable electromagnetic pulse simulator, often positioned above ground.

VEMPS - Army vertically polarized simulator.

VPD - Air Force vertically polarized dipole simulator.

Vulnerability - The characteristic of a system which causes it to degrade in performance as a result of having been subjected to a certain level of effects from the environment.

WIRANT - A Boeing Aerospace method-of-moments computer code for frequency domain EMP-induced current in thin-wire structures.

Worst-Case Assessment (analysis, design, etc.) - An assessment which is performed using actual values of parameters, where those values are known, and using a limiting value (usually estimated) in the detrimental direction for those parameters where the value is not known for the specific assessment case being considered.

CONTENTS

Appendices

CHARACTERIZATION OF ERRORS INHERENT IN SYSTEM EMP VULNERABILITY ASSESSMENT PROGRAMS*

ABSTRACT

The overall objectives of the DNA-funded program at LLL are to provide a measure of accuracy of currently used EMP vulnerability assessment methodology. In addition, system tools are to be provided to improve the confidence in assessment efforts, which in turn will result in improved confidence in establishing hardening requirements. During Phase I, assessment techniques currently used by the EMP community are surveyed and the sources of uncertainty are identified. Typical data are presented for quantifying the major sources of uncertainty in all phases of the assessment effort.

During this phase, a statistical methodology to assess the impact of uncertainty on the survivability of a system has been partially validated with a simple system test.

*This work sponsored by the Defense Nuclear Agency under subtask Code R99-QAXEC-301 "Data Collection and Assessment," work unit code 83 "S/V Confidence Evaluation," prepared for Director, Defense Nuclear Agency, Washington, D.C. 20305.

1. INTRODUCTION

"There are three types of lies: Lies, damn lies, and statistics."
B. Disraeli

1.1 PURPOSE AND SCOPE

The purpose of the DNA-sponsored effort at LLL for error and uncertainty quantification is to investigate and characterize sources of uncertainty and their impact on the high-altitude EMP assessment of military systems. The effort is intended to assist system assessment efforts in the following manner:

- Provide the government, the service laboratories and their contractors with system tools that can be used to improve the confidence in results of EMP vulnerability assessment of large systems.

- Provide a measure of the accuracy of currently used EMP system assessment techniques.

- Improve confidence in establishing hardening requirements.

- As part of the Phase I effort, assessment methodologies currently used by the EMP community including HDL, AFWL, NSWC, TRW, EG&G, Rockwell International, and Boeing have been surveyed and the sources of uncertainties identified. In addition, a large amount of data pertaining to uncertainty in the EMP environment, coupling, and susceptibility have been compiled and, except for the environment, are presented in this report to give an indication of the magnitude of real uncertainties. The uncertainties inherent in evaluating the environment due to high-altitude EMP are discussed in a separate

classified report.* In addition, during Phase I, LLL started the validation of tools for the evaluation of the impacts of uncertainties on the vulnerability assessment efforts.

- The approach uses a statistical framework where both random and systematic uncertainties are treated separately. The eventual aim is to determine the sensitivity of system survivability to underlying database uncertainties.

During the follow-on Phase II, the tool validation effort started during Phase I will be completed and the methodology applied to military systems already assessed. In addition, methods will be evaluated that can quantify and reduce uncertainties in assessment efforts.

1.2 BACKGROUND

Almost all stages in an EMP assessment program include variables that are random, rather than deterministic, in nature. Conventional solutions generally result in an uncertainty between performance and prediction, which is usually accounted for by safety factors or margins. A more realistic view is to incorporate the random nature of the engineering variables in the EMP assessments. These variables fall within a spectrum of possible values, and no single value can be realistically singled out as representing a reliable solution to the assessment program.

There is a great need at the present time to reduce or eliminate the uncertainty (both overdesign and underdesign) that results from safety margins. A probabilistic approach answers this need. Instead of hiding the possibility of failure behind a safety margin, the probabilistic approach realistically recognizes that inevitably there is a finite possibility of failure.

---

*H. S. Cabayan and D. Smith, Expected Ranges in Weapons Gamma Output and High Altitude EMP, Lawrence Livermore Laboratory, UCID-18639 (title U, report SRD) (1980).

Unfortunately, engineering random variables in EMP assessment cannot always be described by well-defined probability distributions. Instead, distributions associated with some variables carry their own degree of uncertainty. Here are some typical uncertainties:

- Uncertainty is always inherent in the definition of the EMP environment.

- The transformation of the EMP environment into cable currents is subject to uncertainty (e.g., introduced by simplifying assumptions concerning the degree of complexity of the system being illuminated).

- Uncertainties arise when component burnout data are limited due to testing a finite or small sample.

- Properties of cable shielding, grounding, component behavior, etc. may be influenced in an unknown way by time and other environmental effects and thus introduce uncertainty.

- Questions of quality of the workmanship in system installation and maintenance arise and lead to an element of uncertainty.

These uncertainties represent factors of "ignorance" that prevent an absolute solution to the assessment problem. A question arises as to whether such uncertainties should or can be resolved or reduced. Usually, sensitivity analyses are required to evaluate any potential savings in the hardening program for comparison with the cost of further study to remove or reduce an uncertainty.

1.3 SUMMARY AND CONCLUSIONS

This effort provides the EMP community with certain analytical approaches and tools necessary for studying quantitatively the impact of uncertainty on EMP assessment. Furthermore, it will identify those sources of uncertainty

that have maximum impact on assessment as an aid for identifying areas where additional investigations are needed.

To meet those objectives stated in Section 1.1, the major emphasis in the present effort was in ascertaining and establishing the necessary groundwork tools. The following task objectives during Phase I were accomplished:

- Examine assessment approaches used by the service laboratories and some of their contractors and identify sources of uncertainty.

- Validate applicabilities of system tools for evaluating the impact of uncertainties with a simple, well-controlled experiment.

In conclusion, this effort has shown that a reasonable, statistically oriented effort to evaluate the impacts of uncertainties is just as easy to implement as a zeroth-order worst-case analysis regardless of the complexity of the system under consideration. Furthermore, a statistical approach that takes into account an honest or realistic appraisal of uncertainties will provide decision makers with much more useful output from which to make intelligent and rational decisions about complex and costly hardening schemes.

1.4 ORGANIZATION OF THIS REPORT

In Section 2, some of the pertinent technical issues are briefly discussed and issues related to uncertainty and vulnerability assessment are cast within a statistical framework. The results of our survey to quantify sources of uncertainty are tabulated and summarized in Section 3. The statistical issues involved in EMP vulnerability assessment are discussed in Section 4. In Sections 5 and 6, we go in greater detail into the uncertainties of coupling and subsystem and component susceptibility technology. Some of the uncertainties involved in protection and hardening are included in Section 7. The system tools validation results are presented in Section 8. In Section 9, we present conclusions and recommendations based on this phase of work on errors and uncertainties in assessment for EMP effects.

2. TECHNICAL APPROACH TO UNCERTAINTY IMPACT EVALUATION

2.1 INTRODUCTION

Uncertainty considerations in EMP assessment have a major impact in any hardening program. Methods currently used by researchers introduce factors of uncertainty at every step of the assessment starting from the incident EM fields to circuit failure analysis.

As adequate identification and quantification of these errors are usually not attempted, a very conservative approach to hardening generally results, an approach which can lead to excessive hardening costs. A conservative approach to hardening is one which is based on the abundant use of safety factors at each point of protection design. A worst-case viewpoint is usually taken and certain parameters will be set at limiting values. Such type of designs will normally require, for example, use of heavier shields, more shielded cables, larger-than-required transient suppressors, more than the required number of protection devices, replacement of components, and other such design additions or changes which are the result of the worst-case viewpoint. Such conservation is not necessarily bad from a functional point-of-view, although it can be very costly in other respects. Dollar cost and tradeoff of weight for performance in an aircraft or missile is an example.

We outline one candidate approach for performing failure analysis using statistical techniques. The technique allows the introduction of both random and systematic uncertainties in survivability analysis. It provides a powerful tool for ranking sources of uncertainty in order of their impact on system reliability determination.

To overcome the above weaknesses, a probabilistic-based system analysis study is proposed in order to develop tools for quantifying uncertainties and to study their impact on the overall EMP hardening approach.

In the following sections, we briefly touch on those technical aspects of this work that warrant special attention. In Section 2.2 the nature of uncertainties as they apply to high-altitude EMP assessment is discussed. The disadvantages of the classical approach, where safety margin criteria are used, are outlined in Section 2.3. Casting the issue of system assessment in a probabilistic framework is discussed. In Section 2.4 the very important issue of the interpretation of probability is presented. Finally, in Section 2.5, the applicability of a failure analysis computer code to EMP vulnerability assessment is outlined.

2.2 NATURE OF UNCERTAINTIES IN HIGH-ALTITUDE EMP VULNERABILITY ASSESSMENT

Uncertainties arise in all phases of an EMP vulnerability assessment analysis. These include uncertainties in the external threat definition; in coupling (both exterior and interior); component, subsystem, and system susceptibilities; and system models. There are several ways to include these uncertainties into the vulnerability assessment analysis. This study treats uncertainties by considering many of the input and system parameters as variables rather than deterministic constants. For example, it is recognized that the source of a high-altitude EMP will not be the same at each occurrence and location. Similarly, the input into a critical component within a system due to the EMP will vary because of the variation of the physical properties of the system components contributing to the coupling of the EMP to the interior of the system. Also, with regard to the vulnerability assessment analysis, this input will have an additional uncertainty due to uncertainties in evaluating the coupling through modeling and/or testing. Thus, the assessment methodology is based on variable inputs and the result of the assessment is generally expressed in terms of a probability of survival (or failure) rather than just that it will survive (or fail).

Generally, in risk assessment programs, uncertainties are classified into two types, random and systematic uncertainties. There does not seem to be general agreement on the definitions of these terms and there frequently is

only a "fine" difference between these two types of uncertainties. Thus, it is appropriate that these terms be defined relative to the assessment problem. The following definitions express the use of these terms in this report.

- Random uncertainties--variations due to inherent "natural" worst-case analysis and probabilistic analysis. The latter approach accounts for the variations in physical properties and operation or behavior. Thus, the inherent variation in the threshold value (stress at which failure occurs) of similar units is considered random variation. Similarly, the variations in the incident electric field from an EMP due to environmental variations, "natural" source differences, etc. are considered random uncertainties.

- Systematic uncertainties--variations (biases) due to inadequate modeling, testing, design, analysis, etc. An example of a systematic uncertainty is the uncertainty introduced in coupling modeling. Any mathematical model (analytic and/or computer) is only an approximation to the actual coupling relationship. Thus, the coupled response at an interior point is subject to a bias due to the modeling inadequacy. This uncertainty is considered a systematic uncertainty. Similarly, if the coupling is evaluated by field testing, there is variation in the results of the tests. This uncertainty in the coupled response due to the test variation is considered a systematic uncertainty.

Random uncertainties are generally expressed in terms of a probability. In particular, the probability of the random variable, e.g., X, not exceeding a specific value, e.g., x, is given for all values x. That is

$$Pr(X \leq x)$$

is generally stated. If the family of probability distribution of X is well known (e.g., X is known to have a Gaussian or normal, exponential, uniform, etc. distribution) then it is sufficient to specify only the probability

density function, f(t), since

$$Pr(X \leq x) = \int_{-\infty}^{x} f(t)dt \quad .$$

Alternatively, only the constants of the distribution; e.g., the mean, μ, and standard deviation, σ, in the case of a Gaussian random variable, need be given.

Although it is appropriate to state a systematic uncertainty by a probability, this is not always the form in which these uncertainties are expressed. Frequently, systematic uncertainties are stated as a deviation from a nominal value. Thus, if x_0 is the nominal value of the random variable X, and uncertainty, Δ, is reported by the statement

$$x_0 - \Delta \leq X \leq x_0 + \Delta \quad .$$

Unfortunately, the deviation, Δ, does not always have a consistent interpretation, which can lead to considerable confusion when comparing alternative assessment analysis. The systematic uncertainty is often transformed into a probability statement by introducing a Beta probability distribution to describe the uncertainty. The constants of the Beta distribution are related to the deviation Δ.

It should be clear from the above discussion that probability is an important ingredient in the assessment of vulnerability. It is an important input in terms of describing uncertainties and it is the output of a probabilistic analysis of vulnerability assessment. Thus, it is important for understanding the results of an assessment that the use of the term "probability" be clearly described. This is discussed in Section 2.4.

To illustrate the role of uncertainties in assessment, consider the problem of coupling estimation. The various methods used and their interrelationships are shown in Fig. 2.1. Figure 2.1(a) shows the real system in the natural environment of a high-altitude burst. At this level of

assessment, the only uncertainty is random uncertainty. There is random variation in the incident electric field at the point of entry into the system as well as random variation in the physical properties and/or operation of all parts of the system from the point of entry to the "black box" within the interior of the system. Thus, the stress on the black box due to an EMP will be subject to random uncertainty.

In Fig. 2.1(b) the "real" system is shown in a simulated environment. Often the "real" system in (b) is not an exact replica of the real system in (a). Problems that arise in interpreting the data from (b) for assessment include uncertainties in extrapolation and translatability. Both are analysis type of uncertainties and therefore contribute to a systematic component of uncertainties and to a systematic component of uncertainty for assessment purposes. The uncertainties involved in extrapolation arise from trying to infer responses in (a) from the simulated fields in (b). The nonlinearities that arise from frequency dependency (i.e., shielding and circuit responses) and from field magnitudes (i.e., nonlinear circuit responses) give rise to uncertainties in the interpretation of the data. Similarly, the extension of the data in (b) from one environmental setting (ground properties, grounding, etc.) give rise to what we call uncertainties in transferability.

Figures 2.1(c) and (d) represent coupling estimation in the model world. In (c), we sketch the scale model method commonly used for "external" and "internal" coupling determination. Uncertainties in data interpretation as discussed above are more severe in this case. "External" and "internal" coupling can also be determined using analytical/numerical models. In both (c) and (d), the issue of model order reduction (i.e., how complex should the model be) has great bearing on characterizing uncertainties.

Examination of the interrelationships among the four blocks should illustrate the role of uncertainty in an EMP system assessment. This illustration should also provide insight into the uncertainty characterization needed for vulnerability assessment. The problem of uncertainties and the need to characterize uncertainties arise in all other phases of the assessment problem and are similar to that shown by the external coupling estimation problem.

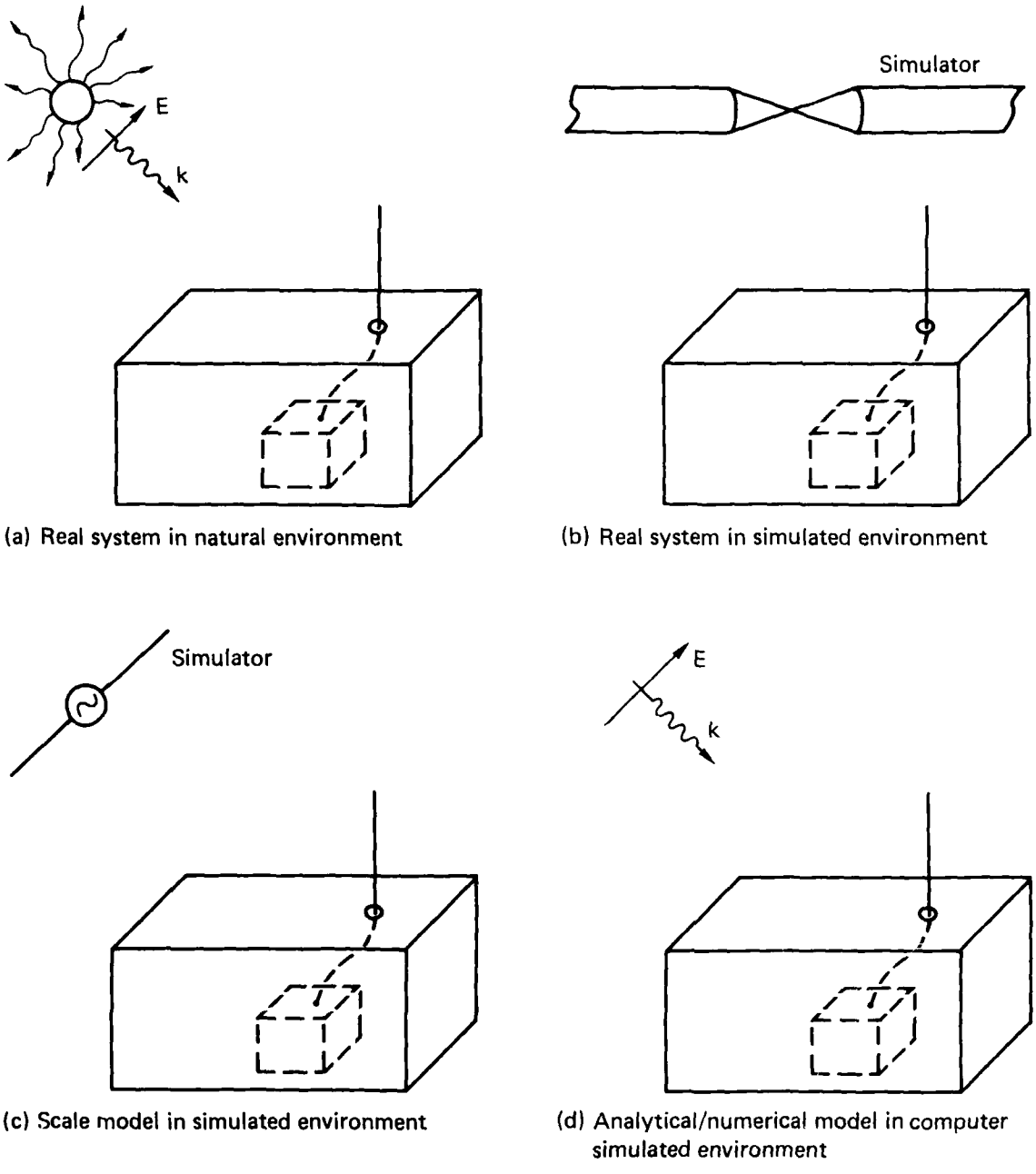

FIG. 2.1. Interrelationships among various phases of EMP system assessment. (a) and (b) represent the real world; (c) and (d) represent the model world.

2.3 A PROBABILISTIC APPROACH TO UNCERTAINTY IMPACT EVALUATION

2.3.1 Introduction

Because of the complexity of the system EMP assessment problem, a probabilistic approach is a viable and adequate alternative to a classical deterministic approach. In many fields, the concept of a probabilistic notion of reliability that admits the possibility of failure is commonly used to quantify system performance under stress. This concept can also be used to great advantage in system EMP assessment. EMP reliability becomes an inherent attribute of a system just as is the system's capacity or power rating.

In this section, we briefly describe reliability theory and investigate its relationship to the classical notion of safety factors. We point out the deficiencies of invoking safety factors in making design decisions. Issues of errors and the types of information needed are also discussed.

2.3.2 Reliability Analysis

The entire process of getting engineering data and building engineering models of phenomena is oriented to performing cost-effective designs that meet general requirements and that are reliable or survivable in the intended environments. To be cost-effective, it is not often possible to resort to worst-case designs in general--as worst-case calculations of EMP-induced signals have demonstrated. As mentioned earlier, hardening designs which are based on worst case and which go above and beyond the limits of normal reliability operating regimes usually result in excessive costs because of the additional safety factors involved. Thus, it is quite reasonable to consider the complex interaction and coupling problem in the context of the operating reliability aspects of the system and the subsystems and components which make up its hierarchical structure.

In the analysis used here, the component or subsystem reliabilities are considered to be constants with time. The basis of the concept of reliability is that a given component or subsystem has a certain capacity to withstand EMP-induced energy; if the energy exceeds this capacity, failure results. In order to determine the reliability, both the EMP-induced energy and component or subsystem susceptibility distributions must be determined as shown in Fig. 2.2. Once these two distributions are determined, the component reliability can be easily calculated. That is, this approach expresses the component (or subsystem) reliability as a function of the induced internal EMP energy and component/subsystem susceptibility.

If S denotes the susceptibility random variable and E the EMP-induced internal energy random variable, the random variable $Y = S - E$ is then related to the reliability, R, of the component/subsystem by

$$R = P(Y \geq 0) \quad . \tag{2.1}$$

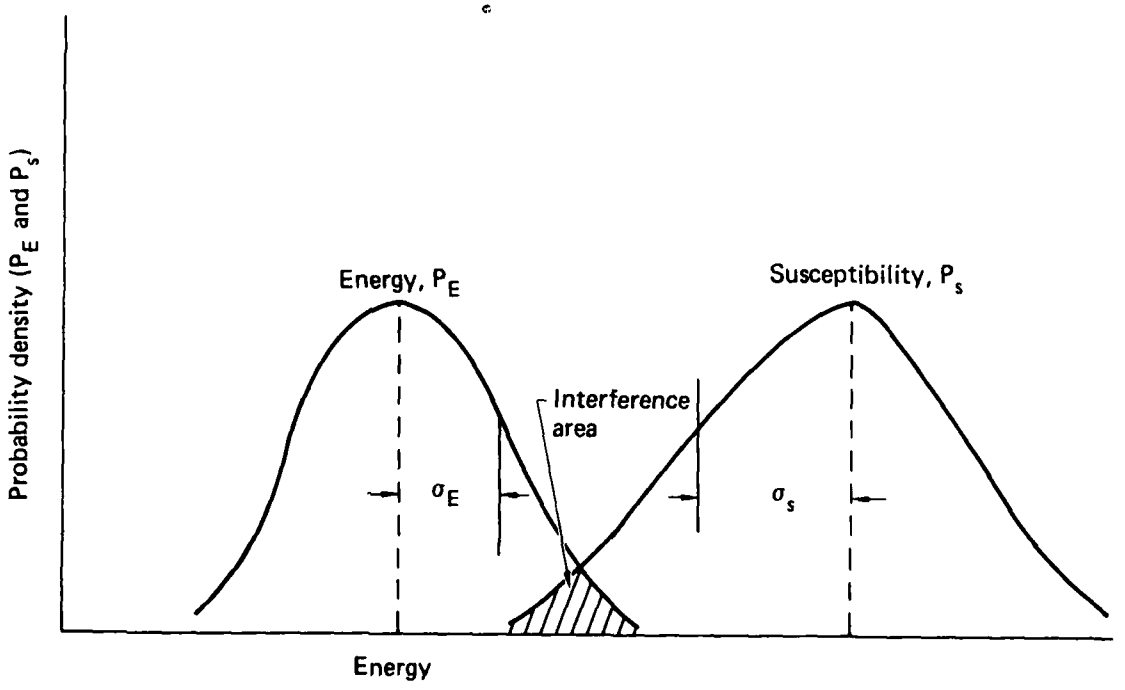

FIG. 2.2 An illustration of internal energy levels and component/subsystem susceptibilities showing energy-susceptibility interference.

For example, when E and S are normal random variables, Y is normally distributed and the reliability, R, is given by

$$R = \frac{1}{\sqrt{2\pi}} \int_{-z_0}^{\infty} e^{-z^2/2} dz \quad , \tag{2.2}$$

where

$$z_0 = \frac{\mu_S - \mu_E}{\sqrt{\sigma_S^2 + \sigma_E^2}} \quad . \tag{2.3}$$

Here μ_S is the mean value of the susceptibility, μ_E is the mean value of the energy, and σ_S and σ_E are the standard deviations of susceptibility and energy, respectively.

2.3.3 Relationship Between Reliability and Factors of Safety

The conventional design approach, which is based on somewhat arbitrary multipliers such as safety factors and safety margins, gives little indication of the failure probability of the component/subsystem. This conventional design approach is not adequate from a reliability standpoint. The factor of safety, n, given by the ratio

$$n = \mu_S/\mu_E$$

depends only on the mean energy and mean susceptibility and not on the variability of these variables. Table 2.1 indicates how reliability and safety factor are affected by different mean levels and variability in the susceptibility and energy random variables. Energy and susceptibility are assumed to be normal random variables. The units are arbitrary.

It is not always possible to determine the probability density curves with any high degree of accuracy. Usually these curves are estimated with either experimentation or analysis and are, therefore, prone to errors and uncertainties. These give rise to systematic variations inherent in establishing the best-estimate curves. The effects of these uncertainties on reliability are shown schematically in Fig. 2.3(a) for changes in the mean level of E and Fig. 2.3(b) for changes in the variability of E. The estimate of reliability, R, varies for different levels of μ_E and σ_E. Uncertainties in (μ_S, σ_S) have a similar effect on the value of R. Thus, instead of a single estimate of reliability, a distribution of values of R exists due to the uncertainties in the parameters of the distributions of E and S. Consequently, the output of a reliability analysis would be a probability distribution for R as shown in Fig. 2.4.

TABLE 2.1. Safety factors and reliability (the energy and susceptibility are assumed to be normally distributed). Units are arbitrary.

Case No.	Mean susceptibility, μ_S	Mean energy, μ_E	Susceptibility standard deviation, σ_S	Energy standard deviation, σ_E	Factor of safety, $n=\mu_S/\mu_E$	Reliability, R
1	50,000	20,000	2,000	3,500	2.5	1.0
2	50,000	20,000	8,000	3,000	2.5	0.9997
3	50,000	20,000	10,000	3,000	2.5	0.9979
4	50,000	20,000	8,000	7,500	2.5	0.9965
5	50,000	20,000	12,000	6,000	2.5	0.987
6	25,000	10,000	2,000	2,500	2.5	0.99999
7	25,000	10,000	1,000	1,500	2.5	0.999999
8	50,000	10,000	20,000	5,000	5.0	0.9738
9	50,000	40,000	2,000	2,500	1.25	0.99909
10	50,000	10,000	5,000	5,000	5.0	1.0
11	50,000	20,000	20,000	20,000	2.5	0.8554

For a given value, R_0, of R as shown, the corresponding shaded area C is the probability that R is greater than R_0; i.e., $Pr(R > R_0) = C$. Hence R_0 is an estimate of a lower bound for R, and C can be used as a figure of "confidence" in this estimate. Section 8 illustrates the principles expressed in this section for a very simple system.

Note that, for example, in cases 1 and 9 the factor of safety doubles and yet there is no change in reliability. That is, an improvement in n, often at considerable expense, need not lead to an improvement in reliability. Conversely, comparing cases 1 and 11, there is a significant change in the reliability even though the factor of safety remains constant. For fixed mean levels, as variability increases, reliability decreases. Clearly, a design decision based solely on the factor of safety is inadequate. Such a decision must take into consideration the variability of energy and susceptibility as well as the mean levels of these variables.

2.3.4 Effects of Systematic Errors on Reliability

To indicate the effect of uncertainties on reliability in the distribution of the input variables, consider again the case of E and S, and hence Y, having a normal distribution. Let $\mu_y = 40$ and $\sigma_y = 10$. Then the unreliability (probability of failure) is 3×10^{-5}. Suppose the mean and the standard deviation of Y are in error by 10%. Then, as is shown by the second entry in Table 2.2, the unreliability can change rather significantly. It is evident that uncertainties in the values of μ_y and σ_y can lead to divergent estimates of reliability.

2.4 INTERPRETATION OF "PROBABILITY" IN SYSTEM EMP VULNERABILITY ASSESSMENT

Important to the acceptance of the probabilistic approach to vulnerability assessment by the EMP community is a clear understanding of the

meaning of the term "probability". Probability is an important element of the input into the assessment since it is the vehicle for describing random variation. It also can be used to describe systematic uncertainty. In addition, one of the outputs of the assessment is a statement of the "probability of system survival" given an EMP. Thus, to use the probabilistic approach to assessment, both in terms of the inputs and in understanding the output, it is important that the meaning of the term "probability" be clarified.

One of the difficulties in discussing probability is the fact that there are several interpretations which have been used that lead to the possibility of a misinterpretation of the results of an assessment. In addition, the applicability of an interpretation may depend on the frame of reference for the analysis. In particular, it may be important, in interpreting the results, to distinguish between the case in which inferences are to be made to a large family of nominally identical systems and the case in which the inferences are relative to a unique system.

TABLE 2.2 Sensitivity of Unreliability to Errors in Input.

μ_Y	σ_Y	Unreliability
40	10	3×10^{-5}
36	11	53×10^{-5}
44	9	5×10^{-5}

Objective Probability. Perhaps the earliest accepted view of probability, referred to in the literature as "objective" probability, treats probability as a measure of the "long run relative frequency of occurrence" of the outcome of interest. Thus, this interpretation is based on the realization (or, at least, conceptual realization) of the event under nominally identical conditions.

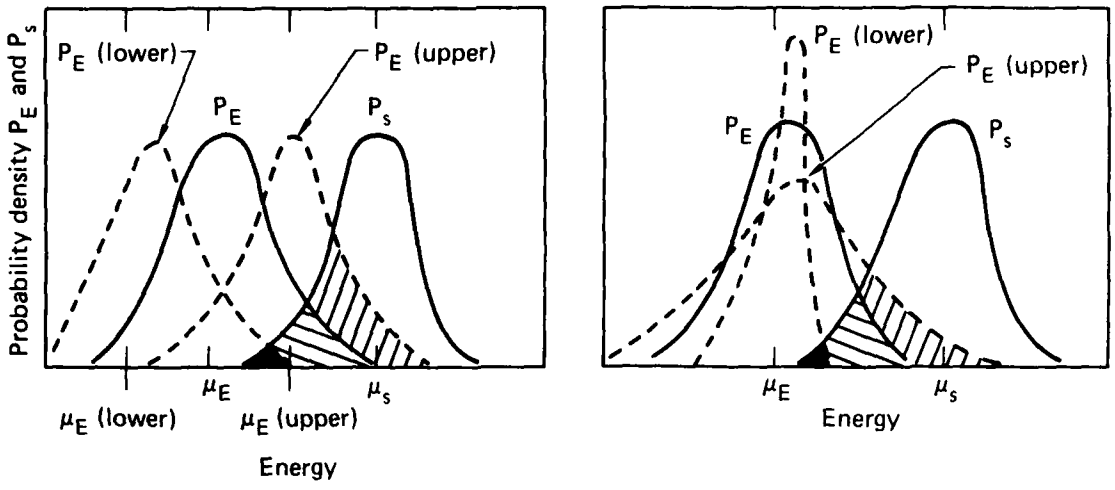

FIG. 2.3. Effects of systematic error on reliability.

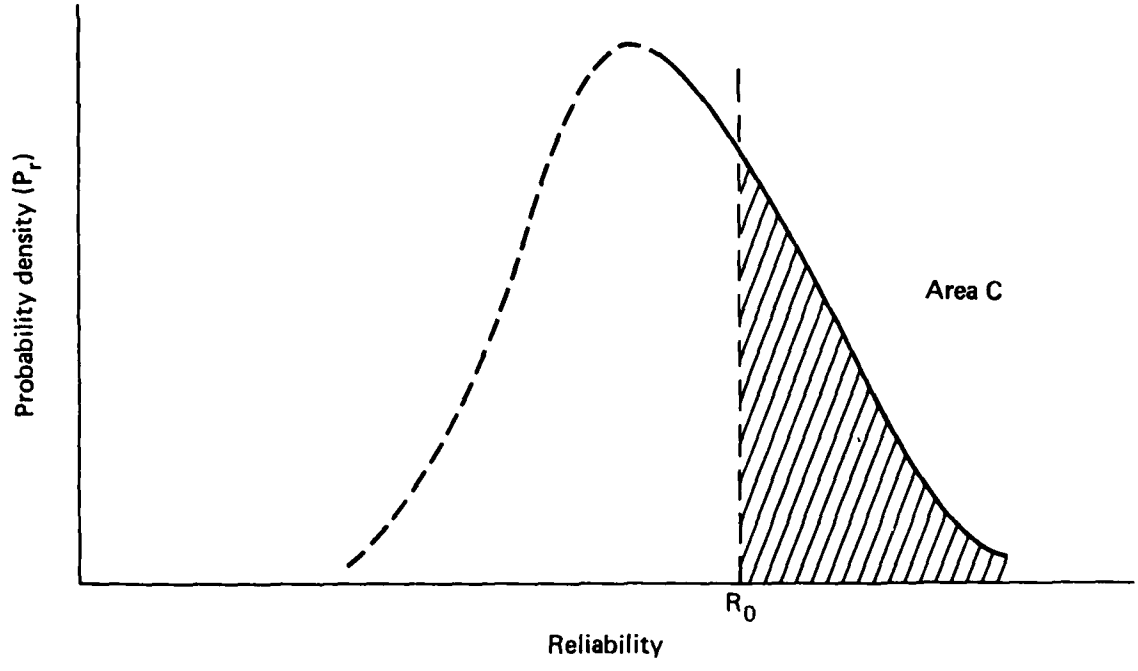

FIG. 2.4. An illustration of the systematic error bounds and resulting probability distribution of reliability.

The use of objective probability can arise, for example, in measuring the susceptibility of a component. Suppose a type of component is said to fail with probability 0.05 at an input voltage of 50 V. The objectivistic interpretation of this statement means that among all such like components (assuming a very large or "infinite" collection) 5% of the units would fail at 50 V. An individual component is then thought of as a component chosen "at random" from the large collection, and hence, is assigned a failure probability (at 50 V) of 0.05. This view of probability is sometimes referred to as the "frequency" view of probability. It is not completely satisfactory for use in vulnerability assessment because its frame of reference is a large class of nominally "identical" systems. Frequently, vulnerability assessment is relevant to a unique system. On the other hand, many of the statistical techniques used to analyze data and which provide some of the necessary inputs into a vulnerability assessment have their theoretical basis on the "frequency" view of probability.

Subjective Probability. A more recent interpretation of probability, referred to in the literature as "subjective" probability, views probability as a measure of one's "degree of belief" or state of knowledge about the occurrence of an uncertain event. An important point to note here is the fact that the frame of reference is not to an event which occurs, at least conceptually, a large number of times but refers to the single occurrence of an uncertain event. This does not mean that subjective probability cannot be used for an event which can happen repeatedly, but rather that the statement is relevant to a single occurrence of the uncertain event, not the frequency of occurrence over many trials. This interpretation of probability is particularly useful for vulnerability assessment because (1) many of the probability inputs into the assessment analysis cannot be based on a large number of replicated trials (time, cost, practicality, etc.), (2) many probabilistic inputs concerning uncertainties are based on individual or group judgments, and (3) the frame of reference for much of the assessment work is a unique system rather than a collection of similar systems.

Even within the classification of subjective probability there seems to be two views as to what is really being stated by an individual. One view

treats a probability assignment as a "state of knowledge" (i.e., property of the mind rather than a property of the "real" world consistent with the frequency concept) that is independent of the personality of the individual. Thus, it is an expression of a logical, rational, or necessary degree of belief.[1,2] Another view[3] treats probability as a measure relative to the individual expressing the probability and is based on how the individual would act in a betting situation. Thus, the latter view allows for differences between individuals. This view is sometimes referred to as "judgmental" probability because it can be thought of as an individual's judgment of the occurrence of an uncertain event. Certainly, given the present state of the information regarding the reliability of components, external and internal coupling, and basic environmental conditions, "judgmental" probability will play an important role in many of the inputs into a vulnerability assessment. Thus, it is important that the role of this type of probability in a probabilistic vulnerability assessment be investigated and clearly documented. This will be done during Phase II.

2.5 APPLICATION OF A FAILURE ANALYSIS COMPUTER CODE TO EMP VULNERABILITY ASSESSMENT

The FAST algorithm (Failure Analysis by Statistical Techniques)[4] was implemented into a computer program by TRW and is applied to the vulnerability analysis of strategic systems. A version of this code is available and running on the LLL computer network system. It has wide potential applicability to the hardness survivability evaluation of many military systems.

In FAST, the free field environments are transformed by transfer functions to establish local system responses to the environment, which are, in turn, used to predict component failure probabilities. Component probabilities of failure are combined in system equations to compute system reliability. The code accepts finite uncertainty in modeling environments, transfer functions, and component susceptibilities. The uncertainties can either be random or systematic. In Fig. 2.5, we show a simple system

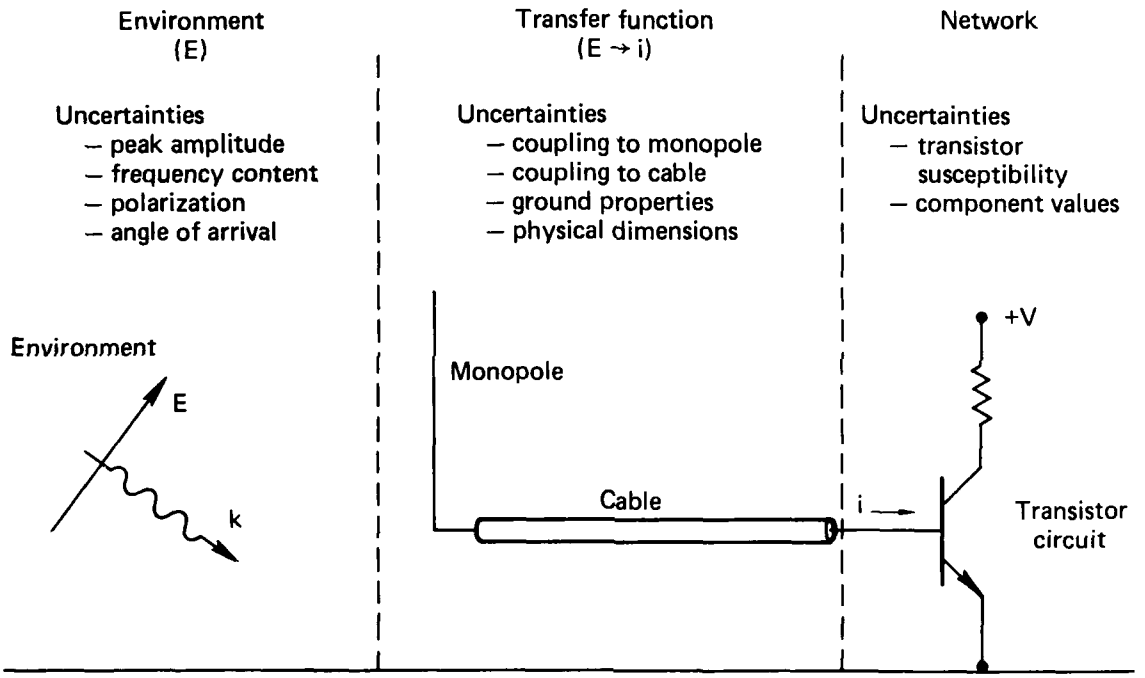

FIG. 2.5. FAST methodology applied to EMP assessment of a simple system.

(monopole/transistor circuit) and the various quantities used in the FAST methodology. The code combines component failure probabilities into subsystem and system failure probabilties based upon the system network.

The FAST code combines the probabilistic representations of environments, transfer functions, and susceptibilities in accordance with the system reliability (i.e., survivability). The Monte Carlo technique is used in performing the survivability calculations. Random variations affecting system survivibility are appropriately averaged by the process, while the systematic variations are propagated through the calculations to indicate the level of confidence in the system reliability result. The code selects bias values from the systematic variation distributions for the environments, transfer functions, and susceptibilities. For each such value, the mean probability of failure is computed from values selected from the random variation distributions for the environment, transfer function, and susceptibility.

The probability of failure data is accumulated in histogram format. System reliability with an associated confidence can be determined as a function of the parameters of an incoming EMP field, the system coupling and the component susceptibilities. A more detailed analysis of FAST is provided in Section 4.

2.6 REFERENCES

1. J. Keynes, A Treatise on Probability, (Macmillan, New York, 1921).

2. H. Jeffreys, Theory of Probability, 3rd Ed., (Oxford, New York, 1961).

3. F. Ramsey, Truth and Probability, reprinted in Studies on Subjective Probability, Kyberg and Smokler, Eds., (John Wiley and Sons, New York, 1964).

4. Failure Analysis by Statistical Techniques, User's Manual, Vol. I, TRW Systems Group, DNA3336F-1, September, 1974.

3. OVERVIEW OF SECTIONS 4 THROUGH 7

One of the goals of the first phase of this study was to assemble the available information on uncertainty in high-altitude EMP assessment. Many of the service laboratories and their contractors were contacted in gathering the data on uncertainties. A portion of the results of this survey are summarized in this section. In Section 3.2, the uncertainties in testing, data gathering and processing, and data analysis relating to estimating currents and voltages are shown. Uncertainties in component and subsystem susceptibility are included in Section 3.3. In Secton 3.1, several vulnerability assessment techniques are summarized. Special attention is given to how these techniques deal with uncertainties. Finally, uncertainties in protection and hardening are summarized in Section 3.4.

3.1 VULNERABILITY ASSESSMENT TECHNIQUES

Vulnerability assessment methods range from very deterministic analyses not using probability concepts to methods which rely heavily on probability, although almost all methods do recognize some kind of uncertainty in the inputs and/or models used throughout the assessment analysis.

The assessment methodology developed by HDL in the Multiple Systems Evaluation Program (MSEP)[1] is an illustration of a nonprobabilistic technique. This methodology is strong on modeling and makes heavy use of analytically oriented coupling and circuit code models. Uncertainties in the input, coupling and circuit parameters, and components are all considered in attempting to develop safety margins which are realistic.

TRW developed for AFWL[2] a methodology for assessing the vulnerability of an aircraft which is based on using EMP simulators. The methodology involves presystem tests and analyses, a system test, a post test analysis and a final assessment analysis all leading to a statement of a probability of

survival. Uncertainties are recognized throughout the analysis and are stated in probabilistic terminology.

Rockwell International developed a method for assessing the EC-135 aircraft.[3] The method relies on simulated environments to determine wire currents throughout the system. These are extrapolated, using functions based on analytic codes or scale model tests, to a criterion level and are compared with threshold currents to determine the safety margin. Uncertainties in the inputs and extrapolation functions are combined using statistical methods. The output of the assessment is expressed in terms of reliability-confidence interval.

Boeing Aerospace Corp.[4] has developed an assessment methodology for communication facilities which employs both functional and electrical models to simulate the signal at "critical" circuits. The safety margin is estimated by comparing the response signal with the circuit threshold. Uncertainties in the analysis are introduced through a factor called "data quality". More detailed descriptions of these techniques are given in Section 4.

3.2 COUPLING

In this section, typical uncertainties in the various coupling assessment techniques are reviewed. Emphasis is placed on "reasonable and achievable" accuracies based on well-run tests and/or analyses. The emphasis is on uncertainties in amplitude in the time-domain since electronic vulnerability is usually much more sensitive to changes in amplitude than to small changes in frequency content.

3.2.1 Full-Scale System Tests

The uncertainties here may be categorized as due to the following:

- Measurement Errors.

- Extrapolation of test data.
- Intrasystem and intersystem variations.

Each of these areas will be considered separately.

Measurement Uncertainties. These include simulation variation error (shot-to-shot), instrumentation error, and data processing errors.

Simulator field errors appear to be due primarily to shot-to-shot variations in the discharge circuits, waveform variation, and nonprincipal ($1/R^2$-$1/R^3$) components. The latter two appear to be minor. Examination of a dozen or so simulators suggests a "reasonable and achievable" error due to simulator field uncertainty is ± 2 dB.

Instrumentation errors include those in current and charge sensors; circuit elements such as cables, altenators and power dividers; integrators and differentiators; oscilloscopes, recorders; and such subsystems as microwave telemetry, screenboxes, and data acquisition systems. A well-controlled and calibrated instrumentation system has about the smallest error and uncertainty of any aspect of a coupling assessment, according to studies of several companies. For example sensor errors can be held to 1-dB, as can integrator and differentiator errors up to 50 MHz; oscilloscope errors can be made almost negligible. A good microwave telemetry or screenbox system will have less than 1-dB error over its dynamic range; an ADSET or DASET data acquisition system can be similarly designed.

An overall error of ± 3 dB is not unreasonable for an entire instrumentation system.

Data processing errors occur from the recorded raw data through the data manipulations of digitization, Fourier transformation, etc., to the final oscilloscope, film, or recorded f- or t-domain responses. Most of the individual errors are small.

Data processing error estimates have ranged from ±6 dB in one system to essentially zero in another system in frequency intervals extending to 1 GHz. The upperbound error in a DASET or ADSET processing system is about ±3 dB if nonlinear effects, which can in principle be removed from the data, are absent. This seems to be a "reasonable and achievable" figure.

Extrapolation Uncertainties. The measured wire currents from a test program must be extrapolated to threat conditions and this usually causes additional uncertainties. The extrapolation provides corrections for incident field amplitude and waveshape, incidence angle, and polarization and for whatever is necessary to account for the presence of the ground plane. The ground plane correction can be important for aircraft assessment when in-flight currents are to be extrapolated from test data. Ground conductivity effects can also be important when the system to be tested is to be deployed in physical environments quite different than that in the simulator site. For instance, estimates of the effect of ground conductivity on the reflected wave for various angles of the incident wave and antenna height indicate they all could cause a 4-dB change or more in coupling response.

For an aircraft where free-field penetration into the interior through points of entry (POE) is the critical means of internal excitation, Rockwell[5] has used the surface magnetic field (H_s) at the POE as the extrapolation quantity. When more than one POE may be driving a given internal wire to an unknown extent compared to other POE, the resultant uncertainty is referred to by Rockwell as the POE location error, an additional source of extrapolation uncertainty.

In Rockwell's assessment method 1 (by computer program), the estimate of the extrapolation ratio H_s (free space threat) /H_s (simulator) is made by computer programs, and the inherent error has been evaluated by comparison with AFWL simulator data to be ±7.2 dB. For the EC-135, Rockwell estimated the POE error as varying from wire to wire over a range of ±6 to ±10 dB. These errors should be treated as independent to arrive at the extrapolation error.

In Rockwell's assessment method 2 (by scale model aircraft data), an estimate of the extrapolation ratio error was not separated from the POE error; the net error in predicted threat wire currents due to both sources was computed to lie in the range of ±7 to ±12 dB depending on the orientation of the aircraft. (This was called "simulation error.")

EMP-induced wire changes occur by the power-on vs power-off operations modes. In addition, variations have been observed in EMP couplings to the same circuits in identical systems. Even within a given system, variations in internal coupling occur day-to-day due to changes in physical layout and changes in electrical configuration. These variations have been reported for aircraft, but it is very likely that they apply to other systems as well. These variations are very system dependent and existing data on them is rather scarce.

For the EC-135, Rockwell reports a power on-off uncertainty of ±10 dB. Morgan[6] reports a spread of 10 dB in specific measurement points from different samples of one aircraft type.

3.2.2 Computer Simulation

Computer simulation has been used to make predictions for both external and internal coupling. In terms of uncertainty however, better results have been achieved in external coupling. In the following, computer simulation predictions are compared to measured values and the differences are attributed to prediction errors. In the previous section, full-scale system test errors were discussed and quantified. These included simulator variation, instrumentation, and data processing errors which can add up to a total rss uncertainty between ±5 to ±6 dB.* The adequacy of any computer simulation technique should be judged with this in mind.

---

*Measurement and data processing errors are independent random variables and are combined in the usual fashion (i.e., square root of sum of squares). Instrumentation errors are not random and are added linearly.

In external coupling, antennas, cables, and external envelopes of systems have received much attention. Antennas have been analyzed in free space and over ground (both lossy and perfect) with integral equation techniques. [4] A review of such simulation performed by HDL and LLL shows that peak response time-domain errors in current should be no higher than 4 dB. Computer code prediction of surface current on aircraft tends to have an error range somewhat higher than this.

Cable coupling has been performed using transmission line theory. Cables over perfect and lossy grounds have been modeled. The largest uncertainty in specifying the parameters of the model has been a knowledge of the terminating impedances. It appears that 3-dB accuracies can be achieved in predicting the EMP-induced current entering a system on a single coaxial or multiwire shielded transmission line, although in many cases only 6-dB accuracies have been reported. Skin currents and charges induced on the exterior metallic envelope of systems have been computed with integral equations (i.e., wire mesh models) and finite difference schemes. Objects in free space and over ground have been considered. In particular, aircraft have been extensively analyzed in this fashion. If the modeling is done well, uncertainties can be considerably less than 10 dB. Cases have been reported where errors of 3 dB have been obtained for aircraft with finite difference codes.

Interior coupling predictions have been made by first computing the currents and charges induced on the exterior envelope of the system as described in the previous paragraph. These are used to define equivalent sources (both electric and magnetic) on apertures, which in turn drive internal cable systems. These attempts have been characterized by large uncertainties because of the difficulty in modeling complex apertures and random-run multi-branch cables. In addition, it is often not possible to characterize precisely the load impedances. Error intervals for internal aircraft cable currents computed analystically by Rockwell,[5] from computer program, Bethe theory aperture penetration, and circuit analysis have been large, typically 10 dB and more.

3.2.3 Scale Model Tests

For several reasons, scale model tests have not experienced as much popularity in EMP coupling assessment as full scale system simulator tests and analysis. Chief among these reasons is the difficulty of taking measurements in the picosecond time regime. Furthermore, the scaling laws for non-metallic objects such as dielectrics with finite conductivity are nonlinear in frequency and, therefore, very difficult to scale. Most reliable results are achieved for metallic objects either in free-space or over perfectly conducting ground planes. Until recently, scale model tests have been used for making external coupling measurements only. Recently, internal coupling predictions for a ship have been performed by LLL and the predictions compared to full-scale simulator test data. Scale model tests have been used for aircraft predictions by the University of Michigan.

The scale model transient facilities are prone to measurement uncertainties. LLL reports a peak time domain uncertainty in the simulator field less than ± 1 dB. Instrumentation plus data processing errors are estimated to be less than ± 4 dB. The University of Michigan test facility is reported to have a simulator field uncertainty less than ± 1 dB over the frequency range of 0 to 2 GHz (and probably about the same up to 6 GHz) with model-facility interactions plus instrumentation errors less than ± 3 dB up to 6 GHz. Because scale models are usually larger than about 1/700 size, this frequency range scales to more than 8.5 MHz for the full-size aircraft. Data processing errors in this facility appear to be negligible over 0 to 6 GHz.

The comparison of LLL predictions and full simulator measurements for the Canadian ship Huron show a discrepancy between ± 7 and ± 10 dB for the antennas (due to measurement errors) and between ± 2 and ± 20 dB for internal cables when compared to NSWC data.[7]

3.2.4 Current Injection Tests

Surface current injection testing has been performed on such systems as aircraft so as to excite the first one or two natural modes with reasonable accuracies compared to EMP. But the surface current response has been well matched over only part of the EMP spectrum. The meager amount of published data on systems suggests a "reasonable and achievable" error of 6 dB in derived EMP surface temporal response.

3.2.5 LLL Modular Data

These modular data have been generated by LLL[8] for various generic classes of structures using both computer modeling and scale model tests. These modules are intended for quick-look external coupling estimates to provide induced quantities of interest such as current, voltage, power and energy. The data is provided in parameterized form and can be easily scaled. Generic classes considered include straight wires and loops in free space, whips and loops on boxes and ships, and loops on cylinders. When compared to actual system test results, the model prediction accuracies ranged from a low of 1 dB to a high of 9 dB. The accuracy is best for structures that deviate little from the generic form and gets worse as this deviation increases.

3.3 SUSCEPTIBILITY ASSESSMENT UNCERTAINTIES

These uncertainties are those which are most prevalent at the subsystem, circuit, and component level of the system structure. Susceptibility implies a response. Performance may or may not be degraded to a recognized point of failure. There are uncertainties involved in knowledge of the levels at which components fail. There are also uncertainties in determining at what level a subsystem or circuit will fail. Not all uncertainties need to be known at the same level of confidence. In a subsystem assessment, for example, there may

be only the objective to do some simple screening of circuits which have identifiable susceptible components. Uncertainty in the model representation of a component or circuit plays a different role in assessment situations which require a highly refined and detailed analysis supported by tests of various kinds. Clearly, the meaning of errors takes on a different significance according to the objectives of the assessment.

This overview provides a listing of some of the major uncertainties. Quantitatively only a few tables are presented, as many component reports are in themselves quantitative summaries. The purpose here is to attempt to show concisely the ranges encountered.

The locations of susceptibility uncertainties in circuits and subsystems and in components are summarized below.

- Circuits and subsystems

  - Circuit parameters, specific devices/circuits.
  - Transformer coil nonlinear effects.
  - High-level, solid-state device models/response.
  - Nonlinear models, in general.
  - Indirect coupling to buried circuits.
  - Configuration details, in general.
  - Simultaneous pin or port excitation effects.
  - Power-on vs power-off effects.
  - Functional definitions.
  - Stray circuit elements.

- Components

  - Damage prediction with theoretical models.
  - Waveform differences (system vs test).
  - Distribution of thresholds.
  - Definitions of integrated circuit damage.
  - Failure modes not expected.
  - Lot-to-lot, manufacturing-to-manufacturing variations.

- Effect of lead inductances in testing.
- Unipolar step-stressing quantization error (level at failure is quantized).

Typical uncertainties in susceptibility parameters, as expressed by range in ratios of standard deviation (σ) to mean (μ), are in Table 3.1.

TABLE 3.1. Typical uncertainties in susceptibility parameters in components.

	σ/μ range
Diodes:	
Forward conduction direction	1.16 - 2.24
Reverse direction	1.58 - 2.51

Digital circuits (TTL, ECL, DTL, RTL):

	σ/μ	$2\sigma/\mu$
Power, P	1.78 - 3	3.9 - 5.5
Current, I	1.8 - 2	
Resistance, R.	1.7 - 2.1	

Linear devices (Op amplifiers, comparators):

	σ/μ	$2\sigma/\mu$
Power, P	3.4 - 4.3	8.3
Current, I	2.3 - 3	
Resistance, R	2.6	

Data is available which shows correlation of transistor and diode tests with predicted failure (K factors) constants. For example, the data of Table 3.2 is given for the range of ratios of test K factors to predicted K factors for the junction capacity model predictions.[9]

TABLE 3.2 Transistor and diode test correlation.

	Ratio of test K factors to predicted K factors								
	Collector-base			Base-emitter			Diodes		
Junction capacity model	Min	Max	Range	Min	Max	Range	Min	Max	Range
Power (K_D)	0.78	19	24	0.16	9.2	58	0.014	1.7	121
Current (K_I)	0.35	23	66	0.05	2.1	42	0.010	1.0	100
Sample size			16			16			6

Evidence of errors present in predictions of thresholds at pins would, in part, show up in validation or supporting tests. In both the EC-135 and AABNCP assessment programs, there were box pin tests performed for several boxes. The EC-135 assessment, which is the more recent of the two, includes a summary of box level data points for both assessment programs. Table 3.3 reproduces this summary.

TABLE 3.3. Summary of box level data points.

	Number of Data Points					
Program	No. of boxes tested	Burnouts> predicted	Burnouts< predicted	Test stopped> prediction	Test stopped< prediction	Total data points
EC-135 assessment	9	8	0	71	27	106
AABNCP GFE assessment	15	39	1	65 total		105

The EC-135 predictions data include effects of bulk resistance and the AABNCP data do not include this parameter. The data from the table indicate that the calculated threshold levels are a reliable lower bound on the time thresholds, as supported by the test data.

3.4 EMP PROTECTION

There are many approaches to the hardening or protection of systems. The general objective is to somehow reflect, divert, or absorb the interfering energy, induced in the system by the EMP, away from the vulnerable parts of the system. Protection can also be accomplished in some cases by use of circumvention which effectively removes the distrubance until it has ceased. Also, design selection of nonsusceptible, out-of-band components such as fiber optics or microwave links is also possible.

The following list includes many of the general techniques employed in EMP protection.

- Shielding practices.
- Amplitude and spectrum limiting.
- Circumvention and disconnects.
- Coding of signals.
- Microwave or optical transmission.
- Component selection.
- System layout practices.
- Cabling and connecting practices.

Notice that many of these general techniques are also used in connection with other electromagnetic issues, such as lightning protection. The task of electromagnetic compatibility (EMC) is to ensure that systems will operate in their intended operational environments without either being unacceptably degraded or causing unacceptable degradation to other systems. There is very little resolution of the issues of errors and uncertainties in the EMP hardening and protection literature. In this overview only a few qualitative issues are presented.

3.4.1 Systems Viewpoint

Many approaches to protection are possible for different systems. Uncertainties in each approach will influence tradeoff decisions. Apportionment of protection to various levels of the system depends on some relative confidence in each type of protection element. Shielding technology is important to EMP protection from the systems viewpoint, as frequently the construction of the system includes inherent shielding features which may be augmented to provide a desired level of shielding. Similarly, proper layout and grouping of subsystems and circuits provide opportunity for inherent reduction of susceptibilty. Large uncertainties can exist if protection relies solely on inherent features, such as structural shielding.

3.4.2 Shielding

The use of shields to enclose susceptible subsystems and circuits totally will substantially reduce the EMP-induced signals. The thickness of the shielding material does not introduce significant uncertainty in the shielding effectiveness. Uncertainties are introduced by the manner of construction (welds, bolt joints, rivets, etc.) and by imperfections in the material. Uncertainties are also introduced with the use of necessary apertures and penetrations. Conductors which penetrate a shielded enclosure require specific treatment measures to avoid violation of shield continuity. Sources

of error therefore include the manner of evaluation of degradation of shielding, the use of small loops and dipoles to measure shielding effectiveness for transient phenomena, and the use of a planar theory of shielding for complex three-dimensional objects.

3.4.3 Amplitude and Spectrum Limiting

A terminal protection device (TPD) is frequently used to limit the amplitude of an EMP-induced transient. Such devices exhibit uncertainty in their operating parameters: reaction time, switching time, threshold level, energy dissipation, and loading effects. A TPD such as a silicon transient suppressor will have device-to-device variations in threshold levels within ±5%. Voltage clamping characteristics will vary with amplitude of current in the device. Data show (refer to Fig. J.3 of Appendix J) that such variations are well within a factor of 1.5 over a range of pulse test current of 30 to 120 A. For typical low clamping levels of 10 V, the range is from 9 to 11 V. A TPD also influences the spectrum of the EMP transient, since its nonlinear nature will introduce spectral components not present in the original transient, but which are not present possibly to disrupt sensitive circuitry. Such signals are an additional source of uncertainties in estimating the effects of protective devices.

3.5 REFERENCES

1. Multiple System Evaluation Program (MSEP) reports, for example, J. R. Miletta, Component Damage from Electromagnetic Pulse (EMP) Induced Transients, Harry Diamond Laboratories,Woodbridge, VA, HDL-TM-77-22, October 1977.

2. HPD/VPD II Analytical Integration Project Interim Report, Vol. I, CDRL A009, AFWL Contract F29601-76-C0112, TRW, Redondo Beach CA, January 1977.

3. C. F. Juster, et al., EC-135 EMP Assessment Program, Final Program Report, AFWL-TR-77-2666, Rockwell International, Autonetics Strategic Systems Division, Anaheim, CA, May 1978.

4. V. K. Jones, T. P. Higgins, Survivability/Vulnerability Safety Margin Assessment Final Report, DNA 3859Z, The Boeing Co., Seattle, WA, September 1975.

5. J. V. Locasso, et al., EC-135 EMP Assessment Program, Final Assessment Report, AFWL-TR-77-254 Rockwell International, Autonetics Division, Anaheim, CA, November 4, 1977.

6. G. E. Morgan, Consideration for the Proper Determination of EMP Design Margins for Aeronautical Systems, Rockwell International, private memo, October, 1976.

7. F. J. Deadrick, et al., EMP Coupling to Ships, Lawrence Livermore Laboratory, Livermore, CA, UCRL-52803 (1980).

8. R. M. Bevensee, et al., External Coupling of EMP to Generic System Structures, Lawrence Livermore Laboratory, Livermore, CA, M-090, (1978).

9. Advanced Airborne Command Post GFE Assessment Program Executive Summary Report, TRW Systems Group, Redondo Beach, CA, AFWL Contract F29601-74-C-0035, December 15, 1975.

4. VULNERABILITY ASSESSMENT TECHNIQUES

4.1 INTRODUCTION

This section examines very briefly some of the assessment techniques currently employed. The emphasis is on a general discussion of the approach (Section 4.2) and on the statistical aspects relating to uncertainties (Section 4.3).

4.2 DESCRIPTION OF ASSESSMENT TECHNIQUES

Vulnerability assessment commonly refers to a process of determining margin-of-safety of performance of a system to an EMP threat scenario situation. A certain level of vulnerability will exist for a given situation. This level, a number, will necessarily be probabilistic in nature, although it might not be treated as such in assessment methods. System survivability, a measure of its capability to perform a mission, will depend to a great extent on the generality and completeness of the vulnerability assessment and its extension to mission situations. Vulnerability, of course, refers to essential weaknesses that the system may have in the presence of certain threats. A given mission situation may not tax the vulnerability limits. Some specific missions may possibly be a calculated risk in that vulnerability levels might be exceeded intentionally due to unforseen situations. A probability of survival could then be quite small, but still acceptable due to the circumstances. Vulnerability assessment expressed in probabilistic terms would provide this type of mission-oriented survivability guidance. A flat go/no-go situation would theoretically prohibit any type of mission flexibility in combat situations. Ideally, one would prefer to have considered all missions and all threat situations, but this is unlikely in the press of battle and unforseen circumstances.

4.2.1 Present Methodologies

The Service EMP Lead Laboratories (HDL, NSWC, AFWL) exhibit their EMP activities through their development and sponsorship of development of technology and participation in specific programs. In this task work, we have contacted the Service Laboratories and some of their major contractors to obtain the essential ingredients of their approach. We recognize that assessment methodology is not stationary and frequently, if not always, has an ad hoc form for a particular program. The nature of the program will dictate whether there is to be extensive emphasis on the basic ingredients and how much of each. Therefore, in some programs, the interaction and coupling aspects would dominate the assessment. In others, hardening may be the critical issue, and all emphasis is placed upon the implementation of hardware. Still others may be faced with a horrendous problem of system description or mission definition to the extent that assessment of vulnerability to the component or unit interface level is meaningless. All of tnese situations are important and in general have been recognized, but not necessarily accounted for, in assessing the effects of EMP.

The point here is that different types of uncertainties play major roles in various systems. It is really up to the investigator to determine what is most essential or what is dominating his assessment problem.

Vulnerability assessment can be tied in with a hardening program. Clearly, there are reasons both for knowing vulnerability and for hardening systems to improve the vulnerability. System vulnerability assessment methodology is controlled by several factors. Consider the following:

- Development state of the system.
  - New system.
  - Deployed system.
  - Upgraded or added-to system.

- Level of technology in EMP.
- Available tools, and resources.
- Monies, expertise, and time
- Other constraints such as availability of system for testings, etc.

The development state of the system has a great influence on the methodology for assessment. A new system is developed for hardness. Assessment is geared to specification of hardness. Modeling and experience are the basis. Exact configuration is not available. The nature of EMP and its relative newness implies many existing systems without specific neclear hardness. Thus assessment is necessary to meet this new threat. Methodology is based then on other factors, with the tradeoffs necessary for a given program. Without knowing the type or range of uncertainties, the investigation may focus too much attention on the wrong part of the problem. For example, minor variations in coupling levels may pale in comparison to variations of overall system design. A methodology which does not recognize or accommodate these basic problems is inadequate. Within the present state of the art, it is not possible to quantify the range of uncertainties present without a great deal of experimentation and control of variables for specific cases.

4.2.2 HDL Assessment Methodology

The assessment methodology developed and used by HDL in the MSEP makes heavy use of analytically oriented coupling and circuit code models. A block diagram of these general vulnerability analysis procedures is shown in Fig. 4.1. Additional details are illustrated in Fig. 4.2, and the computer-oriented nature is shown in Fig. 4.3. DAMTRAC is a circuit code. NET2, Version 9, for the IBM system is now being used by HDL. There are also specialized codes for both cables and antennas. Usually, the codes depend on specialized analysis or testing to determine input parameters. MSEP systems

and indeed many Army systems are faced with significant lengths and quantities of multiconductor transmission lines as well as antenna coupling.

This methodology is strong on modeling, but the modeling is not meant to be too strongly system-specific. Uncertainties appear at all stages, from the system description all the way through to comparisons of calculated power into devices with experimental failure powers. (Uncertainties in coupling and in circuits and components are discussed in Sections 5 and 6.) The methodology is not statistically oriented, but uses detailed modeling and calculations to obtain worst-case soluations.

4.2.3 TRW Assessment Methodology

An effort performed by TRW for AFWL[3] formulated a methodology for performing an assessment of the survivability of an aircraft system to EMP. Phase II of this work developed a number of assessment concepts (philosophies) oriented to a specific aircraft and to identify the data and technology required to implement these concepts. The emphases is placed on assessment methodologies for aircraft which have been intentionally designed to survive and EMP threat, though much of the methodology may be applied to unhardened aircraft as well. The assessment methodology is based on the EMP simulators and technology being developed in AFWL programs.

A matrix of assessment concepts is presented whereby each concept is defined by a set of decisions in seven areas.

1. The type of survivability statement (assessment answer) desired (safety margin, probability statement, etc.).

2. The technical basis for such statement of survivability.

3. A threshold concept.

4. An extrapolation (to threat) concept.

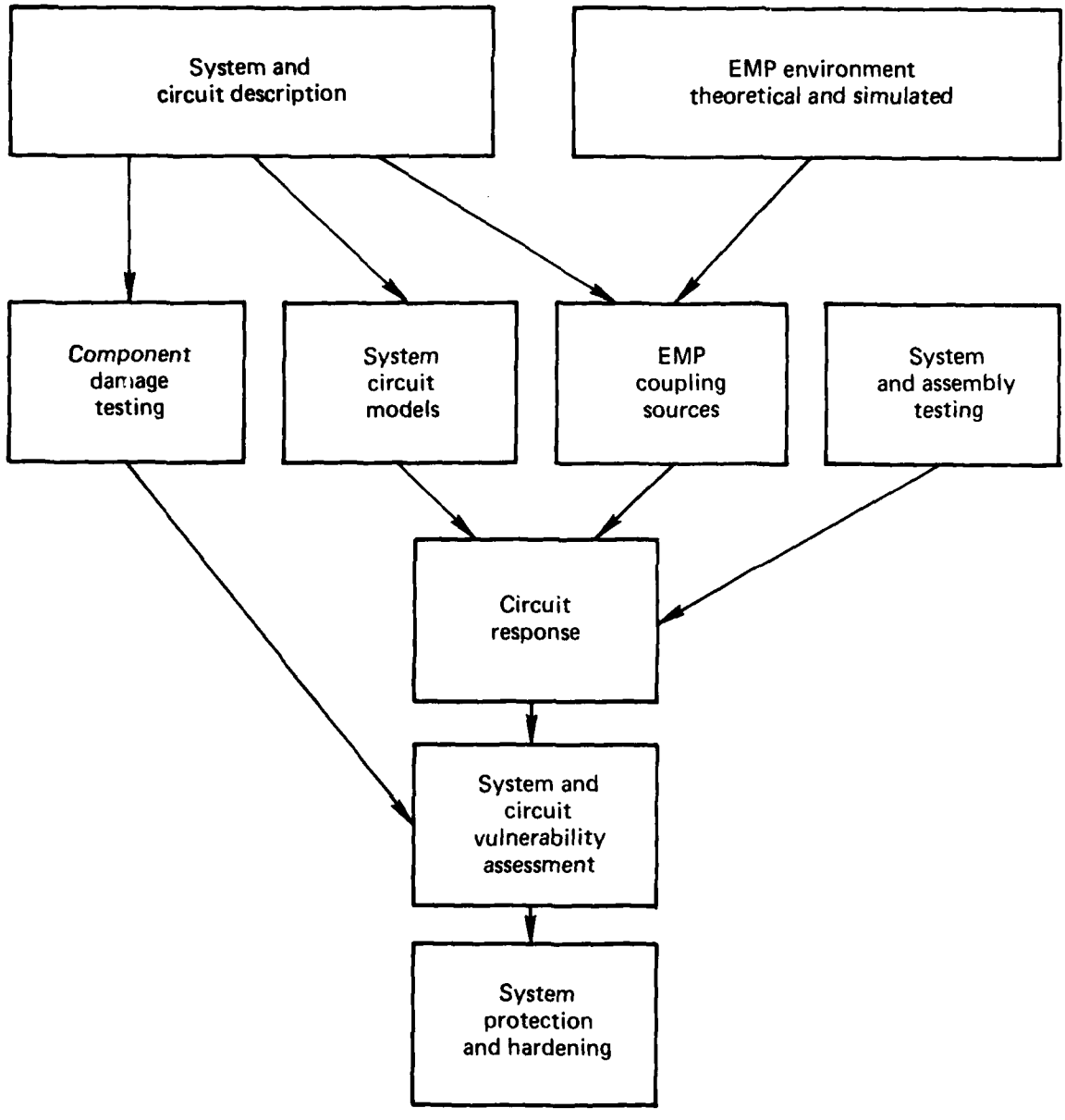

FIG. 4.1. General procedures in MSEP (Ref. 1).

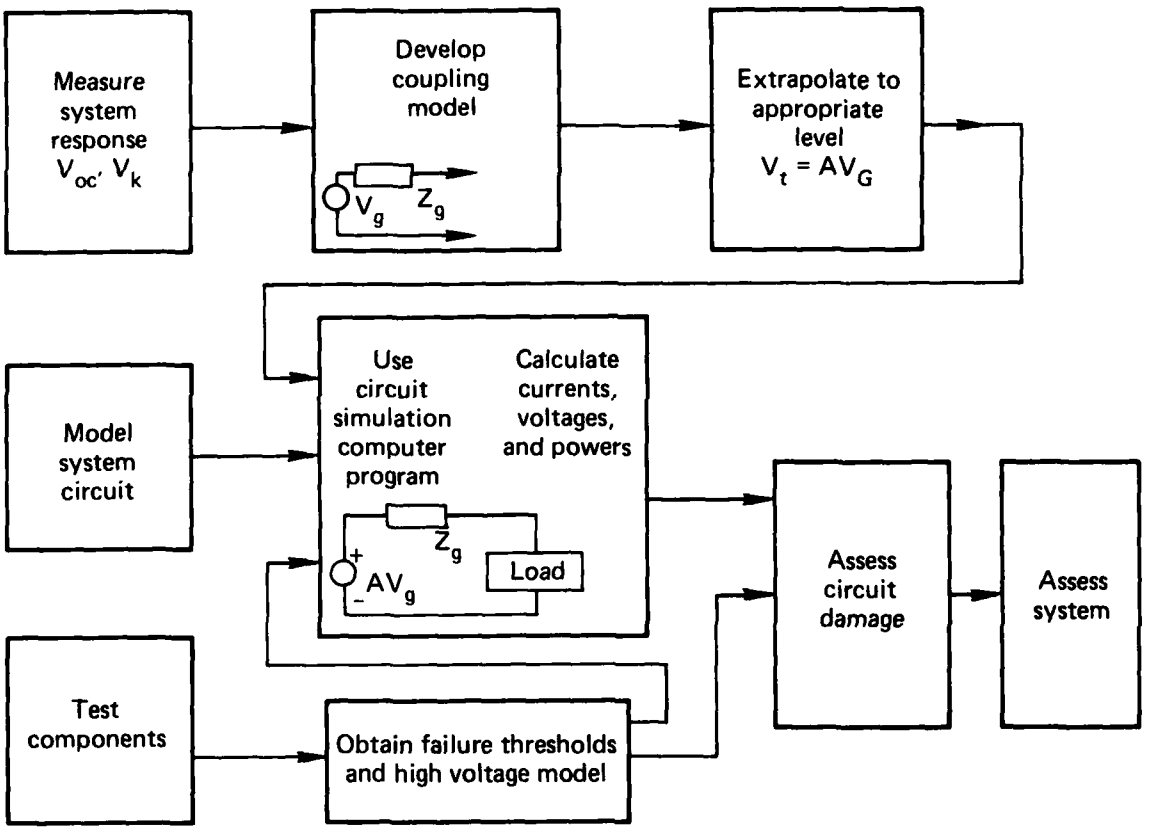

FIG. 4.2. Details of system assessment (Ref. 1).

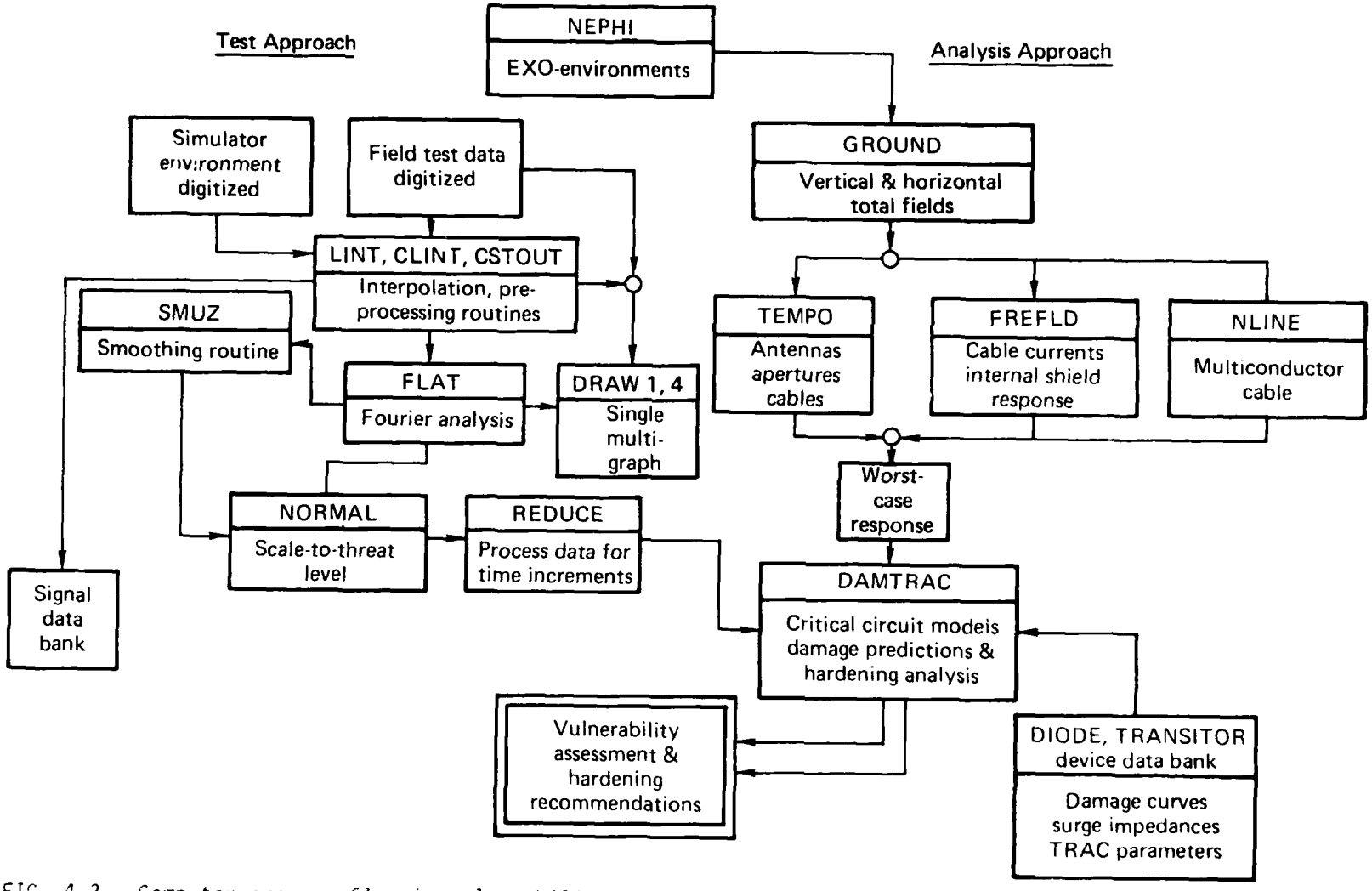

FIG. 4.3. Computer program flow in vulnerability assessment (Ref. ?).

5. A concept for confining threshold and coupled signals to obtain the survivability statement.

6. An EMP simulator concept.

7. The test object (aircraft, etc.) configuration utilized.

Table 4.1 lists three possible threshold reference locations (aircraft oriented) and four possible extrapolation concept alternatives with the matrix of "top level" concepts. There are a number of issues involved in a development of a candidate methodology for aircraft. Briefly, some of these are (1) test operations, logistics, and safety; (2) configuration; (3) concepts and methodologies for extrapolating to threat; (4) concepts and methodologies for determining assessment completeness; (5) concepts and methodologies for treating nonlinear effects; (6) concepts and methodologies for uncertainty analysis; (7) special problems related to special antennas; (8) point-of-entry (POE) isoloation and instrumentation; (9) direct drive requirements; (10) fuel system vulnerability. Assessment tasks are shown in Fig. 4.4. A representative or example flow diagram for assessment is shown in Fig. 4.5. Although this methodology has not been employed, it does deal with most of the major ingredients of an aircraft system.

More detailed descriptions of these techniques are given in Section 4.

4.2.4 The Rockwell Assessment Methodology for the EC-135

To determine how the EC-135 aircraft responds in an EMP environment, Rockwell International conducted an assessment of the aircraft.[4] Briefly, the transient currents and voltages in the aircraft while in the simulator environment were measured, and these were mathematically extrapolated to threat levels. Finally, the susceptibility of the electronics to these extrapolated currents and voltages were determined. The wire current I_W

TABLE 4.1 Eleven top level assessment concepts (Ref. 3).

Extrapolation concept / Threshold reference location	By analytical model	By hybrid analytical model	Direct extrapolation of system test data (by scalar multiplier)	Threat level direct drive of portions of system based on results of subthreat excitation of total system
Pressure hull interface	1[a]	2	3	4
Pressure hull damage thresholds, subsystem box interface for upset thresholds	5	6	7	8
Subsystem box interface	Not considered viable due to state-of-the-art limitations in internal coupling analyses	9	10	11

[a] Numerical designation of top level assessment concepts.

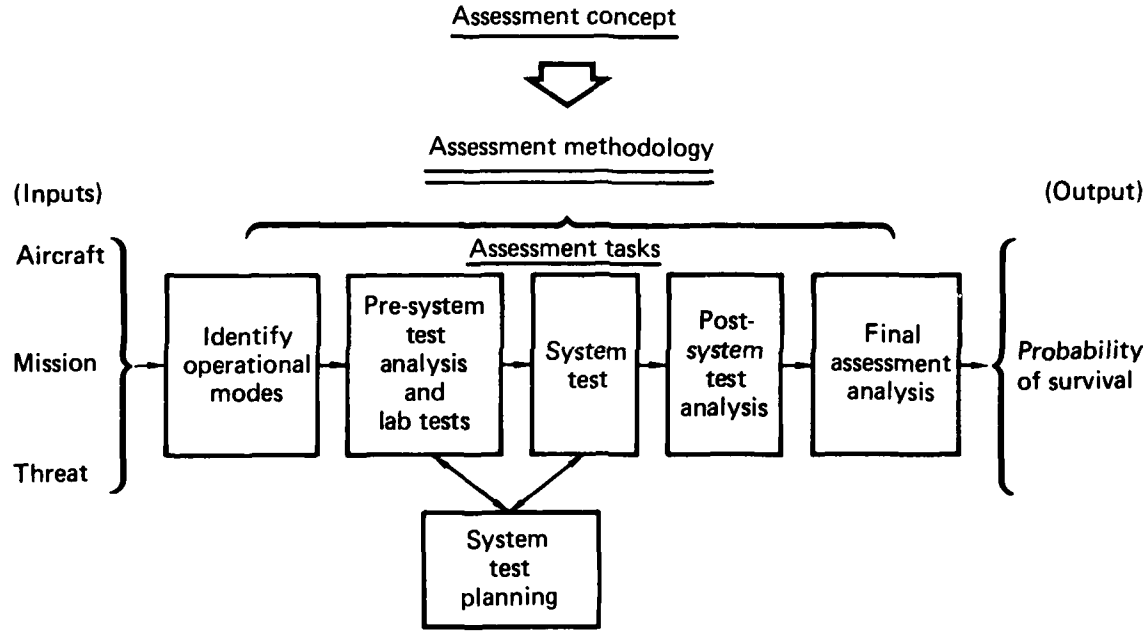

FIG. 4.4. Typical tasks in assessment (Ref. 3).

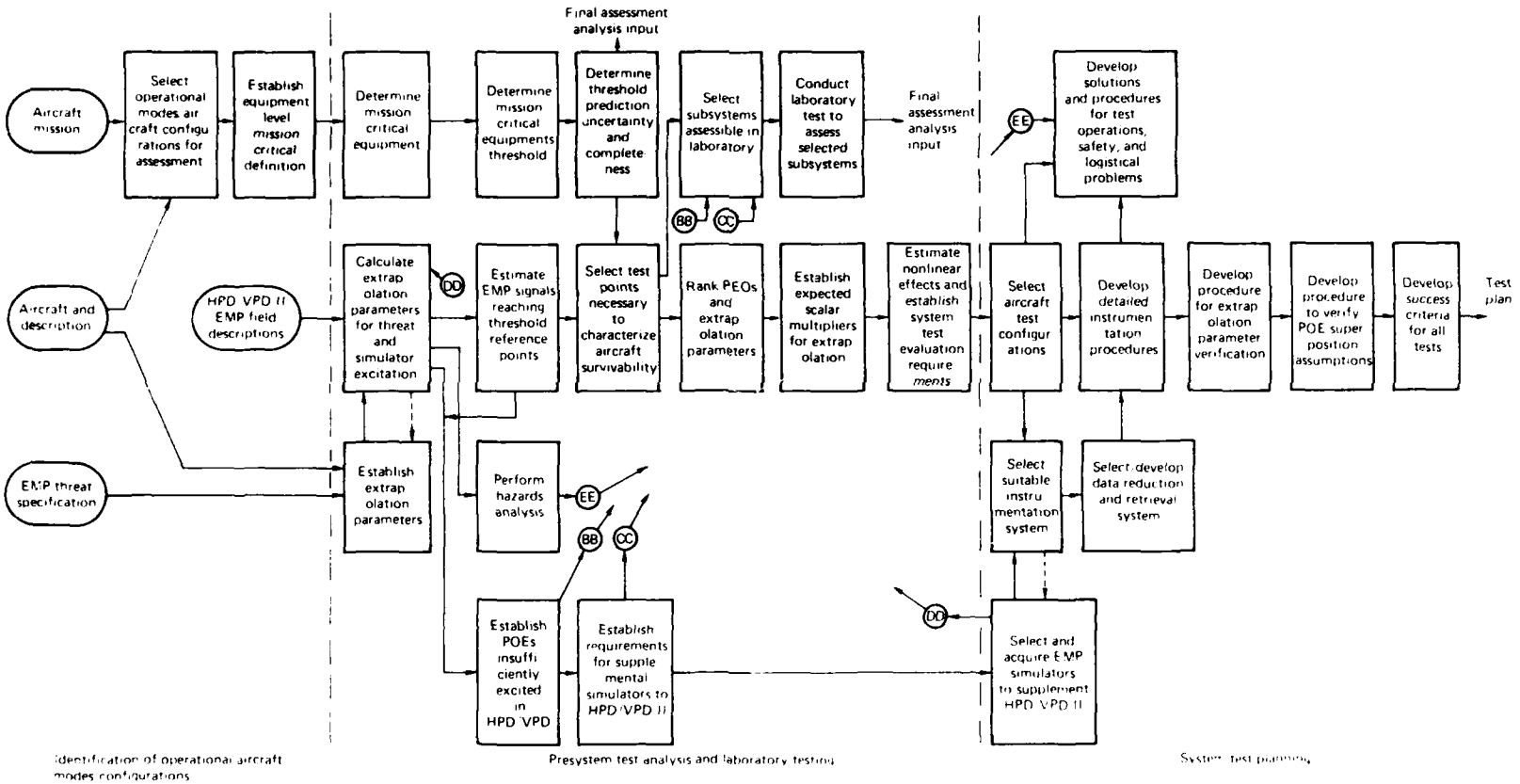

FIG. 4.5. Example assessment plan flow (Ref. 3).

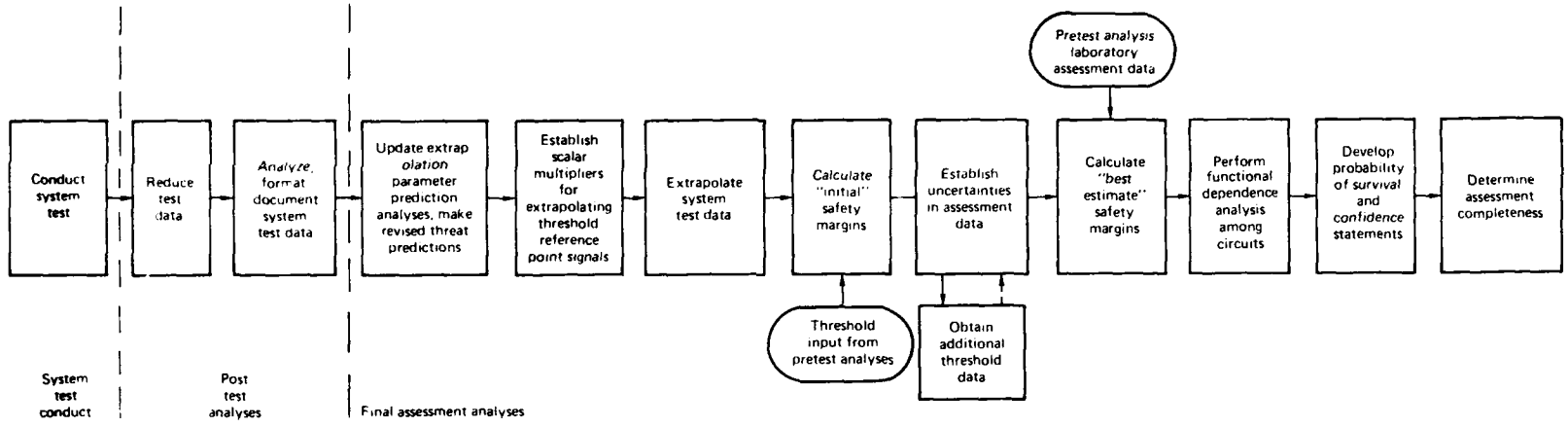

FIG. 4.5. (Continued).

caused by the EMP and the threshold current I_T are used to calculate the "hardness margin" of the pin level with margin defined as

$$M = 20 \log \frac{I_T}{I_W} \text{ dB} \quad .$$

Error estimated in both I_T, I_W, and M are folded into the predictions. (For detailed errors and uncertainties uncovered in the EC-135 program, the reader is referred to Section 5 of this report.)

Two methods were used in performing the assessment. In method No. 1, a single point of entry (POE) for each wire is used to compute the extrapolation to criterion level; and in method No. 2, Rockwell used scale model results and 3C extrapolation methods.[5] Statistical methods are used to characterize errors, to combine error sources, to account for random threshold variations, and to develop hardness conclusions.

A flow diagram of the major steps in method No. 1 is shown in Fig. 4.6. The major purpose of the preliminary assessment was to identify all pins with potentially low hardness margins. These pins then became candidates for detailed wire current extrapolation from simulator levels to high altitude burst (HAB). The analytical coupling predictions used in the extrapolation were obtained using wire stick models. For details of the extrapolation method, please refer to Ref. 4.

A flow diagram for the extrapolation method No. 2 is shown in Fig. 4.7. This method was used in addition to method No. 1 as an independent check to increase the confidence in the results. The extrapolation to criterion for each aircraft orientation was calculated by taking the geometric mean of the extrapolation functions at several representative points on the aircraft. (See Ref. 5). Only four functions, one for each orientation, were used to extrapolate all the wire currents to the criterion level. As in method No. 1, a preliminary assessment was performed to identify critical pins.

In conclusion, the Rockwell vulnerability assessment methodology consists in extrapolating test data to criterion level using extrapolation functions determined either with codes or with scale model tests. The two methods are similar in philosophy and differ in how the extrapolation function is determined.

The Boeing Aerospace Corporation in work sponsored by DNA[6] has developed a prediction technique for communication facility response. The method employs both functional and electrical models. The electrical model represents EMP coupling down to the component level. The external environment is an input which provides the source for the predicted waveforms at the components of interest. These waveforms are compared with failure thresholds to come up with probabilities of disruptions. The functional model relates these probabilities with various functional response paramenters to discuss communication impairment.

The nature of the analytical model is shown in Figure 4.8. EMP coupling to ground based communication facilities includes that from power, communications, and grounding conductors which penetrate the facility, as well as other conductors such as a microwave relay tower. Coupling paths may be direct, with transmission line models carrying the effect of this coupling to the critical component. Within a site, there may be cross-coupling elements. The waveforms appearing at circuit cards will be transferred to components with the aid of circuit analysis programs, if necessary, in order to perform upset and damage prediction. Damage levels are based on the Wunsch constants for devices. The number of components predicted to be damaged depends on the distribution of damage threshold levels of components and upon the distribution of the EMP-induced levels at various points in the system containing the components.

4.3 STATISTICAL ASPECTS OF ASSESSMENT METHODS

4.3.1 Description of How Specific Techniques Handle Uncertainties.

The survivability of a system to an EMP event will depend on many factors such as the environment (magnitude, direction, etc.) surrounding the EMP, the response (coupling) of the components within the system to the EMP, and the susceptibility (fragility) of the components and/or system to an EMP. Thus,

to assess the survivability of a system, it is necessary to accumulate information concerning these factors. This information is not always known exactly, thus, is subject to uncertainty. For example, in the environment, the exact magnitude of the electric field and/or the location of the EMP are unknown quantities. Likewise, the input current of an individual component within a system is unknown exactly because of uncertainties in the coupling of the EMP to the component. Finally, the ability of a component to withstand high voltages is unpredictable and varies from component to component. Thus, exact information is unavailable and what information is available is based on testing, measurements, data analysis, modeling, etc., which are all subject to uncertainties.

In general, there are two types of uncertainties that should be recognized in assessment studies. These are random variation and systematic uncertainty. A review of these uncertainties in describing the environment, coupling, and component and/or system susceptibilities are given in the appropriate sections of this report. The description of the assessment techniques outlined in this section concentrates on how random and systematic uncertainties are incorporated into the assessment. The method of incorporating uncertainties into the assessment differs considerably between the various assessment techniques, although most techniques make an attempt to include an uncertainty analysis. The techniques reviewed are outlined below.

TRW. The TRW assessment analysis[7] is based on using a computer simulation code (FAST or SURVIVE) to estimate the survivability. (Note: The description below of the code input, capability, etc. is based on an adaptation of FAST to EMP assessment analysis. We did not have access to SURVIVE.) Inputs into the code include:

a. Environment: The environment can be characterized by several variables (e.g., for EMP assessment, the environment may be described by (1) the electric field peak amplitude (V/m), (2) angle of incidence, θ, and (3) pulse width, Γ, etc.). Each variable is assumed to be either a normal or lognormal random variable. Thus, the random variation in the environment is defined by two parameters, the nominal or mean values

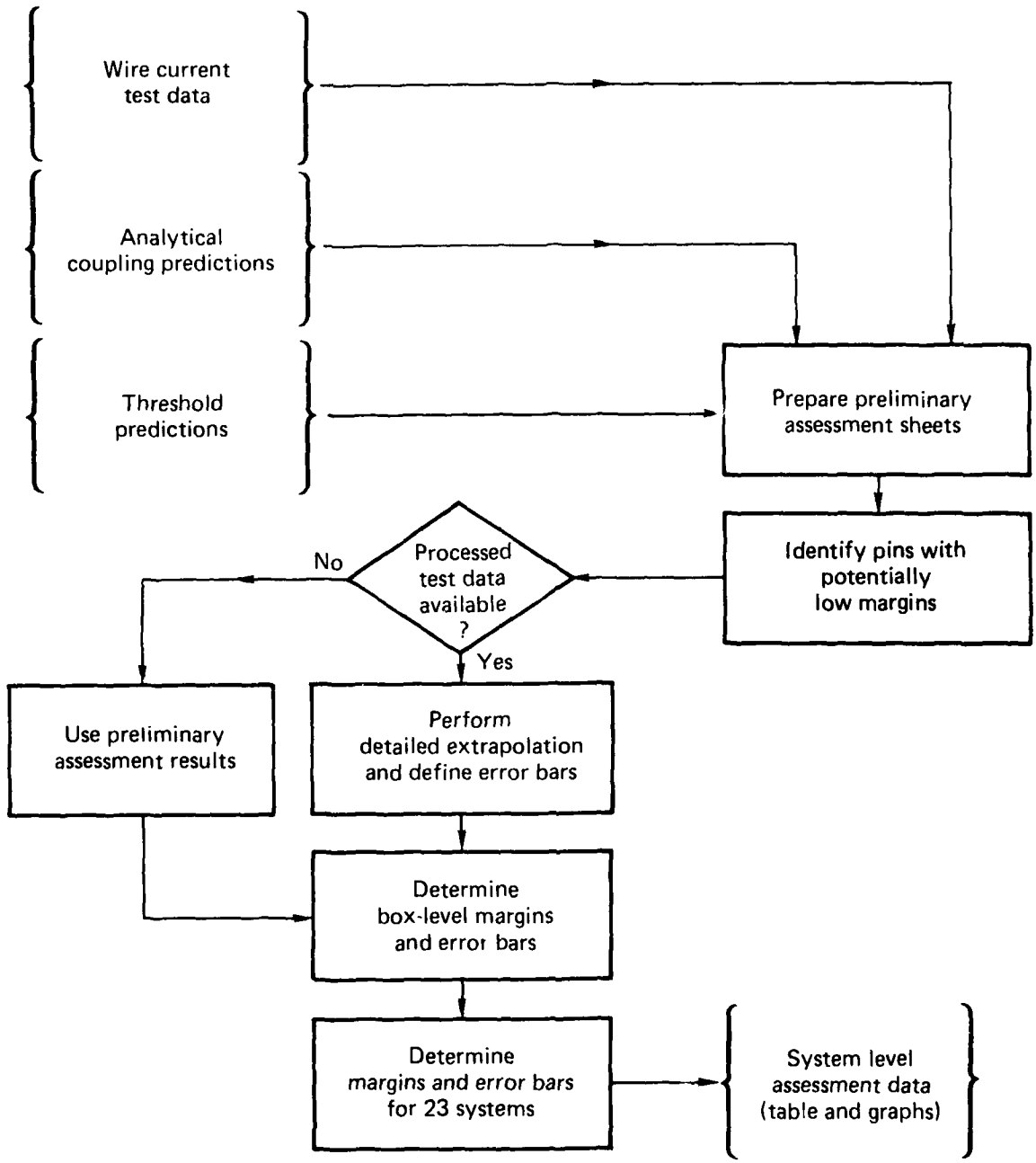

FIG. 4.6. Assessment flow chart for method No. 1. (Ref. 4).

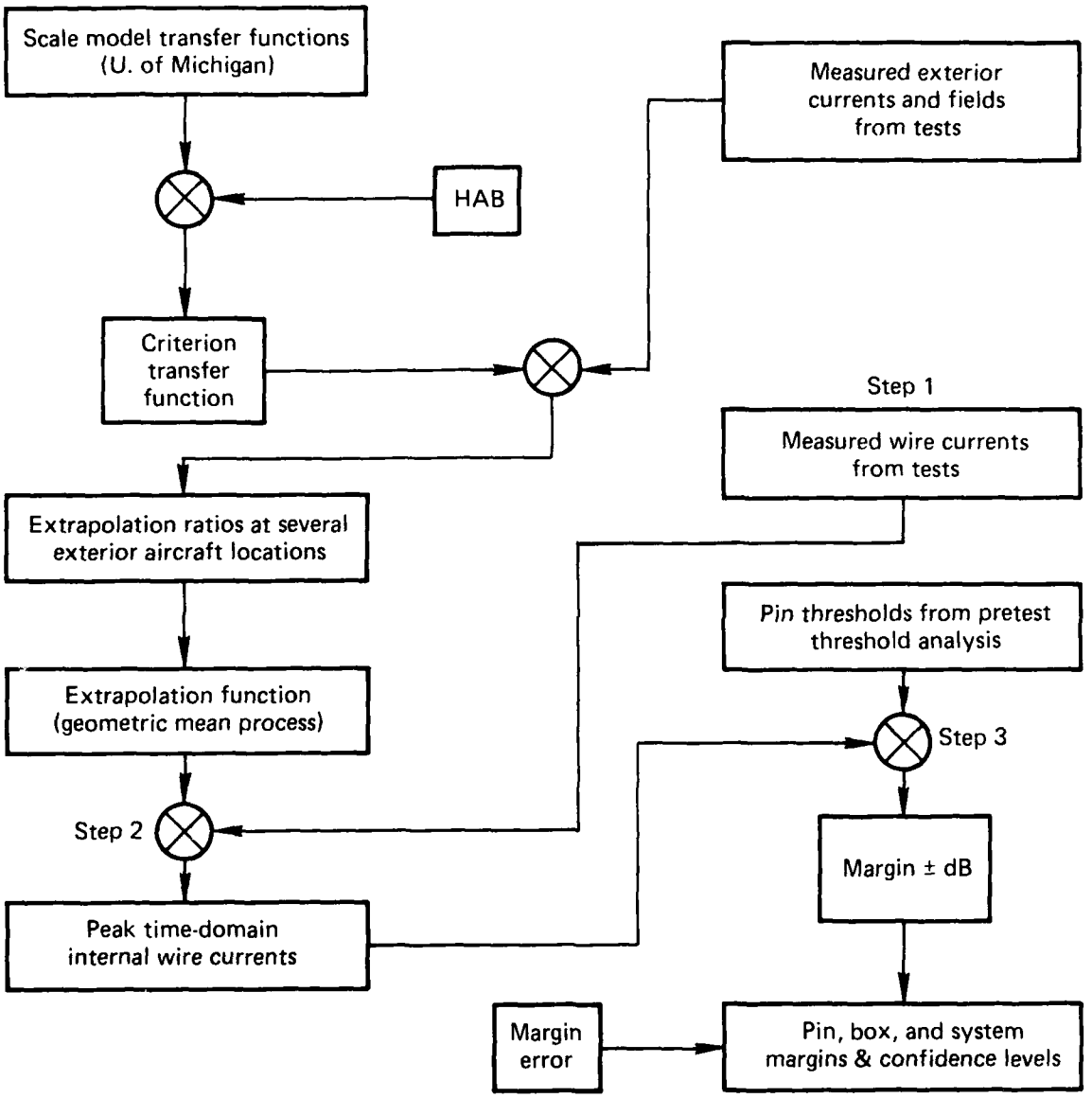

FIG. 4.7 EC-135 assessment overview for method No. 2 (Ref. 4).

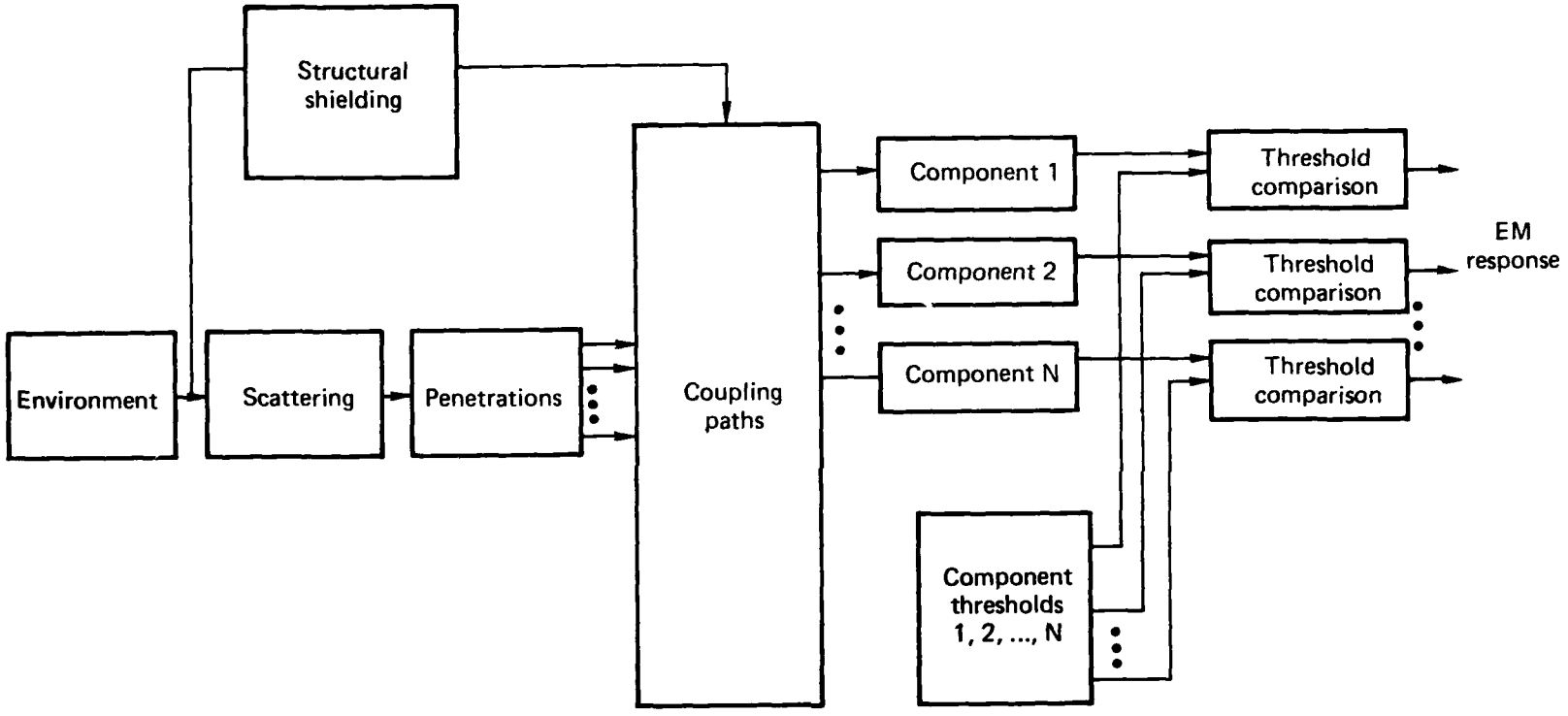

FIG. 4.8. Model used in PREMPT analysis program. (Ref. 6).

(denoted ULN) and the variances and covariances (denoted S) of the environmental variables. In addition, systematic uncertainty in ULN is specified by a factor K, which determines a Beta distribution.

FAST has the capability of handling an environment which is described by several possibly correlated random variables (in a random environment). Further, uncertainty in the specification of the distribution of the environmental variables due to modeling (e.g., transfer from gamma-ray to electric field), testing (e.g., estimating electric field output from sampled events) is included in the systematic error. A not uncommon source of systematic uncertainty is the many subjective judgements made in estimating the environment.

b. *Transfer function:* The coupling of the environment to the response of a component (subsystem, system) is assumed to be described by a transfer function. This transfer is currently assumed to be described by a linear function, so the response is

$$R = \sum_{j=1}^{k} A_j E_j \quad ,$$

where the E_j's denote the environmental variables and the A_j's are specified coefficients. Uncertainty in the transfer function is introduced by assigning systematic uncertainities to the coefficients A_j. This uncertainty is assumed to be described by a Beta distribution.

FAST presently assumes the response (e.g., input to a component) to be a linear combination of the environmental variables. This capability could likely be extended to allow (1) nonlinear transfer functions and (2) vector responses as a function of the vector of environmental variables.

c. Fragility curves: The probability of a failure of a component, etc., as a function of the response, is assumed to be described by a cumulative distribution function, F (r), which is a piecewise linear function such as shown in Fig. 4.9.

The systematic error is described by the error bounds (shown in Fig. 4.9) and is approximated by a Beta distribution within the code.

Although the present version of FAST is restricted to empirical distribution functions described by straight line functions, this can easily be extended to include other functions with well-defined analytical expressions. Also, the response is a scalar, but this should be readily extended to allow vector responses.

d. System functional model (network): The system is assumed to be modeled by a parallel-series functional model of "independent" component (subsystems). The system network is inputted by describing the relationships between various components and subsystems.

Once the environmental variables, transfer functions, fragility curves, and system models are inputted, the FAST code uses a two-cycle simulation procedure to evaluate a probability distribution of P_f, the system probability of failure. For a given transfer function, the environment is selected at random from a fixed environmental distribution and the probability of failure for each component (subsystem) is determined for a fixed fragility curve. These are inputs into the system analysis, which are used to determine the system failure probability, P_f. This value is a consequence of the random uncertainties in the inputs. Simulating (based on the systematic uncertainties) a new environmental distribution, transfer function, and fragility curve, provides a new value P_f. The simulation is repeated (up to N=50 iterations) until a distribution of values of P_f is accumulated. The output of the analysis is this distribution of P_f or correspondingly a confidence interval for the probability of system survival.

Boeing. Boeing, like TRW, bases its system assessment on computer simulation[8]. Its code, PRESTO, uses environmental data from an EMP scenario, along with a model of the system as inputs, and computes the response signal at "critical" circuits. The response signal is compared with the circuit threshold to compute an estimated safety margin, which in turn is used to estimate the failure probability for the circuit. These are combined in a systems analysis to estimate the probability of system survival.

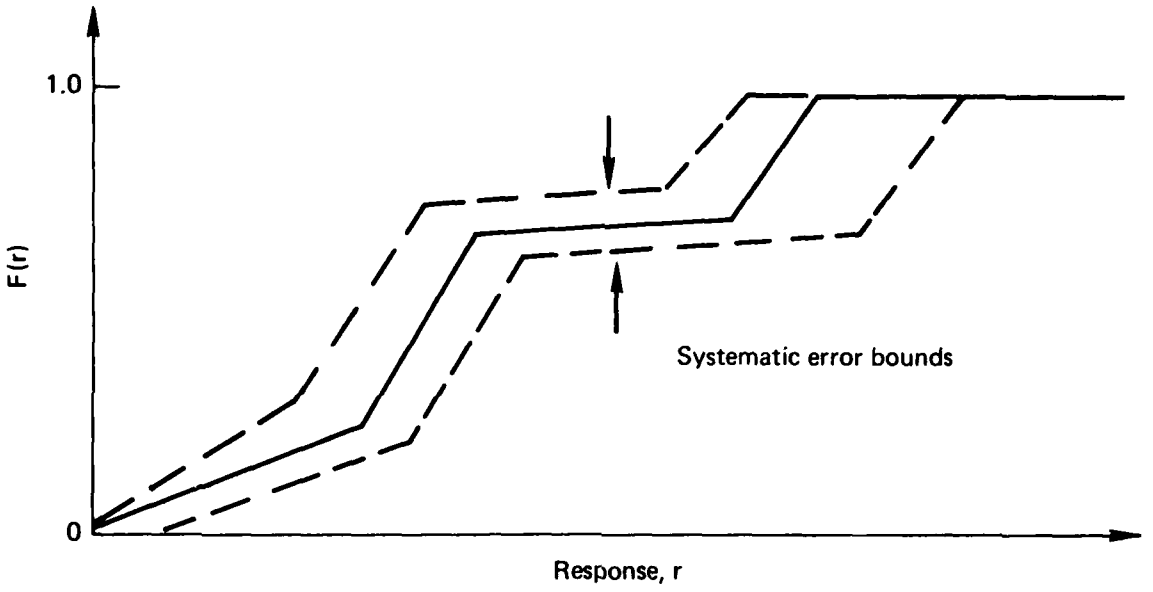

FIG. 4.9 Fragility curve with systematic error bounds.

Uncertainties in the assessment variables are introduced through a factor called data quality (DQ), which is a measure of uncertainty in the estimated safety margins. Three types of uncertainties are considered:

(1) Random variations among similar type units, assuming "true" population safety margin, is known.

(2) Systematic variation in safety margin for the specific unit under test, (i.e., uncertainty due to modeling, testing, etc.).

(3) Systematic plus random variation in observed safety margin.

Models for the uncertainties in the safety margin include the normal, lognormal, uniform, Weibull, and extreme-value distributions.

The measures of survivability, corresponding to the three types of uncertainties, are the probability of survival in (1) and the "confidence", given in terms of a probability, that the safety margin is greater than zero,

i.e., the "confidence" that the component survives in (2) and (3). Given a system network, these probabilities can be combined to evaluate the corresponding measure of system survivability.

Rockwell International. Whereas TRW and Boeing rely on computer simulations for evaluating the survivability of a facility, the assessment technique outlined in (Ref. 9) relies heavily on an analytic determination of a survivability measurement using test data. The basic quantity used to accommodate uncertainties is a reliability-confidence interval defined as follows:

> Definition: A $\beta 100\%$ - reliability-confidence interval for a variable I is given by $\pm \Delta I$ and means that, based on test data, if I_0 is the "nominal" value of I, then one is $\gamma 100\%$ confident that at least $\beta 100\%$ of the values of I within the appropriate population will be in the interval.
>
> $$(I_0 - \Delta I,\ I_0 + \Delta I)$$

Thus, reliability-confidence intervals permit statements of bounds between which a high percentage of the values of a variable can be expected to lie and the "quality" of the methods used to determine these bounds are expressed in the confidence statement.

The basic inputs to the assessment methodology in (Ref. 10) are reliability-confidence intervals for all of the necessary variables (e.g., component thresholds, simulated currents, E-field, etc.). These variables and inputs are analytically combined to evaluate the safety margin and corresponding reliability-confidence intervals for individual components within a system. These, in turn, are combined into box, subsystem and, finally, system safety margin reliability-confidence interval statements. The final output of the analysis is an estimated lower bound for the probability that the system safety margin is greater than zero, where the estimate is given with a specified level of confidence.

The analytical expressions used to evaluate the inputs (energy, current, etc.) at individual components were based on the expressions used to extrapolate environmental data (e.g., E-field) into inputs at the components. The interval widths, ΔI, are based on uncertainties that surround the basic input variables. These uncertainties are due to testing, modeling, simulation, etc. Uncertainties are assumed either to be normal (lognormal) or otherwise. Thus, two types of intervals are used, one based on the normal model and the other a nonparametric estimate used if the uncertainties are non-normal. The intervals are combined based on a root-sum-of-squares methodology.

The method used in (Ref. 9) does not differentiate between random and systematic variations. Rather both types of uncertainties would be combined into a single statement $\pm \Delta I$, for the reliability-confidence interval limits for a variable I.

4.3.2 Discussion of Assessment Techniques from a Statistical Point of View

Perhaps the item of greatest concern encountered in reviewing the different assessment techniques from a statistical viewpoint is the lack of consistency between techniques in the use of statistical terminology, concepts and methods. Thus, although most of the techniques reviewed used such terms as random and systematic errors, confidence, and reliability, these have been interpreted, used, etc. in quite different ways. Hence results from different techniques are not necessarily comparable (e.g., a 90% lower confidence bound for the probability of system survivability given an EMP event).

The description, classification, applications, combination, etc. of uncertainties is one area of inconsistency. As discussed in the previous section, there are two types of errors or uncertainties which are generally recognized in assessment work. Although not all methods use such a classification, one meaningful clarification of uncertainties is into two types, random uncertainty and systematic uncertainty.

Without making formal definitions, random uncertainty is generally viewed as the inherent variation that is associated with a random variable. Primary sources of such random variation are the result of variation in measuring processes, of operational environment differences of like units within a system, of manufacturing differences between like units, etc. The primary application of random uncertainty in assessment is in describing the properties (peak amplitudes, phase, angle of incidence, etc.) of the EMP, which affects the inputs into the system and/or components, and in describing the failure (fragility) properties of the individual components. Such random variation is recognized by either specifying a probability distribution and/or lower and upper bounds for the random variation.

Systematic uncertainty is generally viewed as the uncertainty in knowing the exact value of a "parameter" (non-random variable). Such "parameters" include the form (normal, uniform, etc.) and parameters (μ, σ etc.) of the probability distribution of a random variable, the form of the model (function) relating several variables, the computational method used, and others. In assessment work, systematic uncertainties include uncertainties in the form and/or parameters of the probability distributions for the properties of the EMP and the failure (threshold) properties of the components (subsystems, etc.). Also, uncertainties in functions (e.g., relating the input at a component to the properties of the EMP) are systematic errors; related to this is the uncertainty in using a complex computer code to model the coupling between the EMP electric field and the inputs into individual components. Systematic uncertainty is introduced into the assessment method in a way analogous to random variation. Thus, a collection of possible values of the "parameter" is considered and a relative weighting of the values in the collection is specified. This weighting is usually in the form of a probability distribution (or error bounds) and describes the relative likelihood of a value being the "correct" value of the parameter.

These two types of uncertainties are treated differently in the three techniques (TRW, Boeing, and Rockwell) discussed in the previous section. TRW makes a clear distinction between the two types of uncertainties. The evaluation of the probability of failure, P_f, is based on the random variation for a fixed value of the parameters (i.e., a fixed systematic

error). This evaluation is then repeated for different parameter values (different systematic errors) where the systematic error is chosen according to its specified probability distribution. Thus, a distribution of P_f values is accumulated. Boeing's three cases correspond to (i) no systematic error, (ii) no random error, and (iii) systematic and random errors combined into one error. In all three cases only a single value, either a probability of failure or a confidence, is estimated. Rockwell, in using reliability-confidence intervals, does not recognize some systematic errors (e.g., fagility curve uncertainties) and those that are included are combined with random uncertainties to get one measure of uncertainty. The output is a lower bond for P_f, estimated with a stated confidence. Treated properly, it would be possible to develop comparable estimates of P_f using either the TRW approach of separating the random or systematic errors or the Boeing and Rockwell approaches of combining ramdon and systematic errors.

Another item of concern with regard to uncertainties is the methods used to combine uncertainties. Boeing assumes that a single measure of the combined uncertainty is available--this seems an unlikely possibility. For the Rockwell approach, if y is a function of two variables x, w, i.e.,

$$y = f(x,w) \quad ,$$

then the measure of uncertainty for y, denoted Δy, is derived from the relationship

$$y = \sqrt{(\Delta y_x)^2 + (\Delta y_w)^2} \quad ,$$

where Δy_x, Δy_w are defined to be the uncertainty in y due to an uncertainty in x and w, respectively. Thus, the method is always to combine uncertainties by a root sum of squares method. This is possible given the definitions of uncertainties due to x and w. This approach, basically a difference method, is not the most effective measure of uncertainty in y when x, w are random variables. In particular, the effects of correlation and higher-order variations are not included in this method. Also, the more usual situation is that uncertainties in x and w (not uncertainties in y due to x and w) are well known. Then, the uncertainty in y, expressed in terms of the

uncertainties in x and w, is a bit more complex. For example, suppose the function relationship is

$$y = xw \quad ,$$

where x, w are both random variables. Suppose μ_x, and μ_w, σ_w denote the expected value and standard deviation of x and w, respectively, where the standard deviation is the measure of random uncertainty. Then, assuming x and w are independent,

$$\mu_y = \mu_x \mu_w$$

and

$$\sigma_y^2 = \sigma_x^2 \sigma_w^2 + \mu_x^2 \sigma_w^2 + \mu_w^2 \sigma_x^2 \quad .$$

Further research into methods for combining uncertainties appropriate to vulnerability assessment will be considered during Phase II.

A specific problem associated with the Rockwell approach of using reliability-confidence intervals, which was recognized by Chris Ashley[10] and which is related to the comments made above, is how reliability-confidence intervals for several variables should be combined. Since two types of reliability-confidence intervals are used, one based on the variable having a normal or lognormal distribution and the other based on a nonparametric procedure for variables having any other type of distribution, the question asked is "what is the appropriate method to combine the two types of intervals?" That question is apparently still unanswered. The method used in the EC-135 study appears to be a conservative procedure with regard to the confidence that can be associated with the combined intervals. The question of the confidence level that can be associated with combined reliability-confidence intervals also needs to be researched.

Another point of inconsistency between the three assessment methods reviewed is the use of the term "confidence" with regard to the estimate of

failure or survivability. Although the same term is used in all three methods, it has a different meaning in each case. For example, in the TRW method it is common to use, say, the 5th and 95th percentiles, $P_{f,5}$ and $P_{f,95}$, from the output histogram of the failure probabilities as a 90% "confidence" interval for P_f. That is, since

$$P_r(P_{f,5} < P_f < P_{f,95}) = 0.90 \quad , \tag{4.1}$$

a 95% "confidence" interval for P_f is

$$(P_{f,5}, P_{f,95}) \quad .$$

The probability in Eq. (4.1) and hence the "confidence" statement is derived from the systematic uncertainties. Thus, an interval of values, instead of a single value, is used to estimate P_f because of the systematic errors, i.e., because the "parameters" (fragility curves, distribution of environments, and transfer function) are not known exactly. This is not the usual statistical usage of the term confidence.

The output of the Boeing method of assessment is

$$P_s \equiv P_r(SM > 0) \quad , \tag{4.2}$$

where SM denotes the safety margin. That is, the value evaluated is the probability that the safety margin is greater than zero or the probability that the system will survive (assuming SM > 0 means system survival). If the only uncertainties are random uncertainties, then P_s is considered to be the probability that a randomly selected unit will survive [case (i)]. If a systematic error exists, then P_s is considered to be the "confidence" that the unit under study [case (ii)] or a randomly selected like unit [case (iii)] will survive. Here, the probability in Eq. (4.2) is derived from the systematic uncertainty in [case (ii)] and the combined random and systematic uncertainty in [case (iii)]. The use of "confidence" by Boeing is not a confidence in the value of the probability of survival but a measure of the probability of survival itself.

The term "confidence" as used by Rockwell in the reliability-confidence interval or as a confidence that the probability of survival is greater than some specified lower bound has yet another interpretation. The use of confidence by Rockwell is a statement about the estimation procedure used to construct the reliability-confidence intervals or the lower bound of the probability of survival. This is consistent with the use of the term in classical statistics. Thus, confidence here means that if additional samples are taken and the same estimation procedure is used to construct the lower bound for P_s, then γ % (the confidence level) of the time the stated bound will be a lower bound (and $(1-\gamma)$ % of the time the actual value of P_s will be below the stated bound).

In summary, with regard to the confidence statements associated with the different techniques, it is important that the user of the results of the analysis understand the basis for the statement. One could easily be led to a misinterpretation of the results.

The points mentioned here are just a few of the questions that arose while reviewing the three assessment techniques which incorporated uncertainties into the analysis. Certainly there are other questions which could be discussed such as "how can uncertainties be dealt with if the input variables (environment, etc.) are multivariate or the transfer functions are nonlinear?" or "how does one model complex systems with many dependencies and common cause failures?" There are many aspects of the assessment techniques which need to be further analyzed and researched beyond what we were able to do in our limited review. Minimally, though, an effort should be made to define and standardize the usage of many of the statistical terms and methods used throughout all the assessment methods.

4.4 REFERENCES

1. Various MSEP reports, e.g.; J. R. Miletta, Component Damage from Electromagnetic Pulse (EMP) Induced Transients, Harry Diamond Laboratories, Washington, D.C., HDL-TM-77-22, October 1977.

2. T. V. Noon, Implementation of the Device Data Bank on the HDL IBM Computer, Harry Diamond Laboratories, Washington, D.C., HDL-TR-1819, October 1977.

3. HPD/VPD II Analytical Integration Project Interim Report, Vol. I, CDRL A009, AFWL Contract F29601-76-C-0112, TRW, Redondo Beach, CA, January 1977.

4. C. F. Juster, et.al., EC-135 EMP Assessment Program, Final Program Report, AFWL-TR-77-2666, Rockwell International, Autonetics Strategic Systems Div., Anaheim, CA, May 1978, (title U, report SRD).

5. C. E. Baum, Extrapolation Techniques for Interpreting the Results of Tests in EMP Simulators in Terms of EMP Criteria, AFWL Sensor Simulation Note 222, March 1977.

6. W. W. Cooley, D. W. Mahaffey, and A. Rudzitis, "DNA PREMPT Program Communication Facility EMP Response-Prediction Techniques," 1977 IEEE Intern. Symp. on Electromagnetic Compatibility, pp 353-362.

7. HPD/VPD II Analytical Integration project Interim Report, Vol. II, CDRL A009, AFWL Contract F29601-76-C-0112, TRW, Redondo Beach, CA, January 1977.

8. V. K. Jones and T. P. Higgins, Survivability/Vulnerability Safety Margin Assessment, Final Report, DNA 3859Z, The Boeing Company, Seattle, WA, September 15, 1975.

9. J. V. Locasso, et al, EC-135 EMP Assessment Program, Final Assessment Report, AFWL-TR-77-254, Rockwell International Autonetics Div., Anaheim, CA, November 4, 1977.

10. C. Ashley and J. V. Locasso, A brief Presentation and Discussion of the Algorithm Used to Determine EC-135 EMP Margin Reliability-Confidence, AFWL and Rockwell International Autonetics Div., Anaheim, CA, System Design and Assessment Note 23, September 27, 1977.

5. UNCERTAINTIES IN COUPLING ASSESSMENT

5.1 OVERVIEW

This section presents detailed information about the uncertainties which arise in the coupling assessment of systems to EMP. Such uncertainties may arise from many sources in testing or analysis or a combination of both.

In full-scale simulation tests, many factors contribute to uncertainty in the internal EMP response of interest.

- Differences between test and combat scenarios.
- Simulator field ambiguity.
- Instrumentation errors.
- Data processing of measurements to infer the EMP response.
- Extrapolation from test to threat conditions and for various possible points of entry (POE).
- Intra- and inter-system variations.

Computer simulation of external antenna or cable pickup involves modeling errors, as does integral equation or finite difference code determination of external surface current on the system envelope. Computer analysis of internal response from coupling through apertures or antennas and cables, external-internal transfer functions and current distribution by circuit theory is subject to large error.

Such model testing is subject to the same errors and uncertainties as full-scale testing, except that (1) additional modeling errors may be introduced, and (2) intra- and inter-system variations cannot be effectively

studied. The extrapolation function from test to threat conditions, which is used to convert full-scale simulation test response to threat level, is subject to error in modeling of system geometry and perhaps environment (i.e., ground conditions). If the equivalent circuit antenna parameters are derived from measurement and scaled to obtain the EMP response at a point of the full-size system, this too is subject to error and uncertainty.

Errors in surface current simulation can occur if one uses a system current injection scheme to excite the system of interest with localized current so as to replicate the spectral content of the EMP-induced surface current. Such a scheme might be called a sub-EMP simulation test.

Finally one may estimate the EMP response of a particular system by the response, computed and/or from scale model tests, of a similar generic system. EMP response deduced this way is subject to the coupling uncertainties in the generic system response plus a certain amount due to modeling error.

All these uncertainties determine the net uncertainties in the qualities of interest, namely the internal wire currents flowing through sensitive components. The measured internal currents are extrapolataed to threat level by factors derived from (1) computer analysis of an electromagnetic model of the system exterior, which allows for ambiguity in the various possible points of entry (POE), or (2) scale model test data plus POE ambiguity. Intra-system uncertainty is allowed because of incomplete knowledge of the splitting of currents inside the system or power on-off differences. And inter-system variations are included if obtained from system samples. A measurement procedure for obtaining threat internal currents and their uncertainties is superior to a purely computational one, particularly because of the complexity of the internal circuitry in practical systems of interest.

Following a discussion of the nature of coupling uncertainties and a [illegible] of the coupling assessment approaches of various organizations, we [illegible] in tabular form the nonsystem-specific coupling errors and [illegible] in Sections 5.5 - 5.9. These sections will give the reader a [illegible] of the relative importance of various uncertainties in

the different assessment techniques--full-scale simulation tests, computer simulation, etc. References to the sources of these uncertainties are included.

Conclusions from the coupling assessment analysis appear in Section 5.10, followed by references. A number of appendices contain information about the measurement techniques and associated errors reported by various organizations, useful data processing relations, and a discussion of surface current response computed by finite difference computer code.

5.2 NATURE OF UNCERTAINTIES

Coupling assessment includes the evaluation of EMP-induced currents on conductors which might direct the energy to susceptible circuitry. Various approaches are used in order to evaluate such currents, the most popular of which are:

- Full-scale simulation tests.
- Computer simulation.
- Scale model tests supplemented with analysis.

Another alternative to full-scale testing is the technique of "current-injection" at certain points of the system. A fifth method of assessment is by the EMP response of a similar, often simplier system. The Lawrence Livermore Laboratory has published a set of data on external coupling of EMP to generic structures,[1] which provides one with approximate estimates of EMP-induced current levels. In several assessment efforts, more than one technique has been employed.

In the absence of coupling data from actual high altitude nuclear bursts, heavy reliance is placed on data generated from full-scale simulation tests. Such tests have also been used to validate other simulation techniques.

However, full-scale simulation tests are in themselves prone to uncertainties, and this section has some review and discussion of these uncertainties. There are a large amount of data on simulators and the taking and processing of data in them.

The nature and the source of interaction and coupling uncertainties is closely connected to the type of system. For example, Army communciation equipment can be tested in a high altitude EMP environment similar to that anticipated in field use, with the possible exception of simulation tests on very long lines connected to the equipment. In contrast, the majority of aircraft and missile tests involve tests on the ground while attempting to simulate the vehicle in a flight condition. Problems of extrapolation of the test data to the desired operational case will be less severe when the system is more closely simulated in both its physical configuration and general operating environment.

Important coupling paths for Army ground communication equipment are from the external field to cables and antennas and then from these to the internal equipment. For aircraft and missiles, the EMP-induced effects enter the system through various points-of-entry such as apertures and external antenna systems. The aircraft, however, is still a localized system, whereas cables of communication systems may run for kilometers.

Various analytical and computer simulation techniques have not been very successful in providing the necessary data for making predictions of internal cable current levels, particularly the EMP induced levels on individual wires. Therefore, the coupling assessment of aircraft has relied more heavily on system level simulation test. The computer simulation approach, however, has been more successful for Army communication equipment. Various codes have been developed and validated with simulation testing in well-controlled configurations and then used to predict currents on long cable runs where simulator tests are not feasible. It is not implied here that one and only one coupling technique has been used for a particular system. This discussion refers only to the more common methodology used. Coupling data for aircraft have been generated with the use of computer simulation when such data

were not available or were difficult to obtain with system simulation tests. An example is an aircraft with a long trailing wire antenna.

The Navy has also performed a considerable number of coupling assessments on various ships through use of the EMPRESS EMP simulation facility. The EMP fields couple to the various antenna systems and cables on board the ships, which in turn propagate the energy conductively through aperatures to susceptible circuitry within the hull of the ship. The coupling of the EMP fields to internal cables directly is minimal, in contrast to aircraft coupling modes. This property of ships makes scale model testing for evaluation of coupling an attractive alternative to full scale ship simulation tests.

Solution of the coupling problem by computer methods is also attractive because of the availability of many efficient numerical techniques and computer programs. However, the greatest accuracy has been obtained in the prediction of external coupling levels, such as to external antennas (free space and lossy ground) and to the external conducting surface of an aircraft or missile. There has been apparently only limited success in the prediction of internal cable currents. Very extensive and complete descriptive information is needed, unless the configurations are quite simple. For external coupling, much validation work has been performed, so that the numerical modeling techniques can be used with high confidence. Internal coupling estimations have been attempted for complicated systems (aircraft, ships). The aircraft predictions have been validated.

Scale model tests have been used quite extensively for external coupling predictions and this technique has been validated. Recently, the scale model approach has also been used for making some internal coupling predictions for a ship, and the results indicate much promise for this approach in the future. Such scale model tests should be quite successful and accurate as long as geometrically small details in the full-scale system can be neglected. This implies that the very small apertures cannot be allowed to become major points-of-entry of energy into the interior of the ship. For this reason, the technique should be quite useful for ships but less useful

for aircraft. However, scale model tests are useful to predict external coupling to the aircraft.

5.3 COUPLING ASSESSMENT APPROACHES

The following sections summarize the procedures of the various organizations whose assessment data was examined in the course of writing this report.

5.3.1 Air Force Weapons Laboratory (AFWL)

The Air Force Weapons Laboratory has been concerned for years with estimating the internal EMP response of aircraft in various spatial modes. In order to extrapolate from simulator-environment level to threat-environment level, it has sponsored many analytical and some scale models for deducing extrapolation functions from external surface response. These have included L-, cross-wire, and stick analytic (computer) models, wire mesh and wing-root POE models, and a scale model B-1 and EC-135. External-internal coupling via penetrations such as exposed cables and apertures have been analyzed, and transfer functions have been evaluated for different POE on the B-1 model (major POE can usually be identified, according to J. P. Castillo of AFWL in a classified document). Better models of aircraft are needed and statistical methods must yield confidence levels for probability statements about EMP response.

5.3.2 Boeing Aerospace

Boeing's coupling assessment technique uses an electrical model of the system under EMP analysis. From computation and measurements numerical values

of the model parameters are chosen. Then EMP is applied, waveforms are computed at the inputs of critical components, and comparison with upset/damage threshold data yields probabilities of component disruption.

In the PREMPT program, EMP coupling into the system via antennas and cables connected to internal circuitry is computed from the WIRANT and PRESTO codes, respectively. Structure and shielding of the building are accounted for. A flow of internal current through various coupling paths to sensitive components is computed by PRESTO with transmission line and network analysis.

This methodology applied to communication facility EMP assessment is described in Ref. 2.

5.3.3 Harry Diamond Laboratories (HDL)

The Harry Diamond Laboratories approach to EMP coupling analysis (perfected for the Army's Multiple System Evaluation Program, MSEP) requires validation of an electromagnetic model of the system. Three computer codes are used for the task: TEMPO for antennas, NLINE for multiconductor transmission lines, and FREFLD for transmission line cable response. The model parameters for a system are adjusted until the frequency-domain, internal measured response to a simulator agrees essentially with the response computed from the measured incident field. The measured response contains negligible data processing error.

The model, validated for worst-case response, is then scaled in the frequency domain if necessary to represent a larger system, and the response of sensitive elements to the incident threat field is computed. Device data information for tolerabale peak current, energy absorbed, etc., then indicates the degree of hardening required.

A description of HDL's data processing and reduction technique is in Appendix A.

5.3.4 Mission Research Corporation (MRC)

Mission Research Corporation has been concerned with aircraft cable, penetration studies, extrapolation from simulator to threat field, finite difference solutions to external aircraft response, and alternate aircraft simulation (SCIT). A description of the external surface current and charge measurements in the F-111 simulator tests and the data compared to predictions by the finite differences THREDE code are in Appendix B. This appendix also outlines the MRC deterministic error analysis of measurement errors in simulator tests.

5.3.5 Rockwell International

The objective of Rockwell's assessment technique is to obtain confidence intervals (*namely reliability as the minimum* probability of non-failure of a given system and confidence level for that reliability) for internal pin (i.e., component) safety margins. Margin is the dB excess of threshold excitation over threat current induced.

The full-scale simulation test is performed and various internal pin-wire currents are measured. Thus measurement errors occur due to simulator variability, raw data errors, and digitizing and computer processing. The internal currents are extrapolated to threat level, introducing extrapolation error. Since the POE are unknown, that uncertainty is obtained by computing the geometric mean of surface current response at a number of likely POE and defining POE uncertainity by the deviation of the surface currents from the mean. Intra-system variation is accounted for by uncertainties associated with impedance ratio calculations of wire currents from the bulk ones and power on-off variations.

The so-called "analytic" wire current uncertainty due to coupling assessment error is computed as an rss of all the above mentioned errors considered independent of each other.

In assessment method 1, the error in extrapolation to threat was assessed by comparing computed and measured area under the f-domain amplitude curve for surface current since this area corresponds well to the inverse transform peak temporal value. The POE error was computed by extrapolating certain wire currents to threat at each of many POE, the geometric mean of the t-domain peaks was taken as reference for each wire current and the maximum variations about the mean defined the POE error. In assessment method 1, the "simulation error" was defined by the maximum deviation of "threat" pin current derived from scale model extrapolation from its geometric mean as both the POE and failure ports were varied.

More information about the Rockwell assessment technique is contained in Appendix C.

5.3.6 TRW

TRW considered four basic extrapolation methods of obtaining the EMP response at internal threshold reference points (sensitive wire currents), namely (1) direct scalar extrapolation from simulator field to threat field, (2) by a hybrid analytical-empirical model, (3) an analytical model prediction, and (4) by subthreat level excitation followed by threat level (i.e., free-field simulator) direct drive. For (1), one chooses the extrapolation parameter according to the mode of operation; for the ground-alert or in flight-TWA* mode of an aircraft, one chooses incident field; for an inflight-non-TWA mode or if non-localized or distributed coupling exists, one chooses skin current. In method (2), if surface current J_S were the extrapolation parameter, the internal wire response I_W would be $I_W^{threat}(f) = J_S^{threat} \times (I_W/J_S)^{sim}$, J_S^{threat} being the analytically derived quantity and the ratio being the empirically derived ratio. The analytical model (3) means a model chosen to predict the measured simulator response at an internal point, then used to obtain the threat response at that point.

*Traveling wire antenna.

Method (4) is employed to discover the major sources of EMP penetration, after which they are excited individually at high level to deduce the EMP response. This method is superior for evaluating nonlinear external coupling, for which superposition cannot be employed. One must consider the relative effect of each POE nonlinearity on the EMP internal response due to another POE and make a reasonable calculation of the response due to all these POE.

Along coupling assessment lines, Research and Development Associates, (RDA) proposed a methodology which involves a combination of system testing and model analysis to predict threat EMP response at internal pins (ports) with estimated uncertainty. In the testing, the transfer functions through the various POE's are obtained with known uncertainties so the pin responses have known uncertainties. In the analysis, the coupling paths are identified and modeled and the transfer functions computed--with unknown uncertainties. Involved statistical analysis is employed to predict the threat responses at all critical pins.

Because there is some philosophical objection to the use of a coupling model with unknown uncertainty in the pin threat responses and because the RDA work is primarily methodological,[3] it will not be discussed in more detail.

Besides the organizations listed above, both BDM and EG&G have been involved in bounding uncertainties in the measurement areas. BDM studied the digitization, transform, and other errors in recording systems, such as ADSET and DASET, and compared their performance.

Further discussion of their variables analysis study is in Appendix D. EG&G has been involved with error analysis of the upgrade test program of the HDP simulator and special analytical studies of instrumentation and data processing error. The objective was to establish error estimates on test data of 90% confidence limits at the 90% confidence level. Error analysis was performed on screenbox systems, a single-channel microwave screenbox system, and a five-channel microwave DASET measuring system. The determinantal error analysis of MRC was applied to the error analysis of instrumentation. Further details about the EG&G work appears in Appendix E.

5.4 SYSTEM SIMULATION TESTS

The full-scale system simulation tests considered in writing this section are tabulated below. The simulators are further described in the glossary.

	Simulator	System tests
Air Force	Achilles I, II	Large aircraft
	Athamas I, II	F-111, 707, 747, B-1, C-5A, EC-135
	Alecs, Ares	Large aircraft
	Atlas I, II	Large aircraft
	HPD	HPD upgrade program
	SRF, VPD	E-4, EC-135, AGM-28
Army	AESOP	-
	HEMPS	-
	REPS	Safeguard
	TEFS	-
	TEMPS (at HDL), VEMPS	MSEP: AN/PRC-77, AS-1729/VRC, TRC-145
Navy	EMPRESS	A-6, HMS Huron

5.5 COUPLING ASSESSMENT IN FULL-SCALE SIMULATION TESTS

Most of the information in this section was obtained from aircraft tests and analyses.

5.5.1 Measurement Error

Measurement error consists of environment (simulator) uncertainty and instrumentation and data processing error, all independent. Measurement error is smaller than the net extrapolation error and the intra- and inter-system variations encountered in full-scale simulation tests.

Environment

A reasonable and achievable uncertainty in simulator field is ±2 dB, due primarily to shot-to-shot variations.

Error type	Error/uncertainty ± dB about the mean, unless otherwise noted	Reference	Comments
Simulator magnitude variations	2.3	4	Worst of 8 HDL simulators excluding ACHILLES II.

	0.4	W. Petty*	One pulse every 5 s or so.
SRF simulator	0.85	5	90-90† confidence interval.
VDP simulator	1.4	5	90-90† confidence interval.
Environmental simulation	6	6	Simulator variations + nonprincipal components.
Simulator variability, calibration, and machine processing	5.3	5	90-90† confidence interval.

Instrumentation

Most of this information is from reports by EG&G and MRC, with ±3 dB overall being "reasonable and achievable" in a good quality controlled system.

Error type	Error/uncertainty	Reference	Comments
Test setups	0.8	G. Sower, EG&G	Prevents accuracy of calibration.

*For the TEMPS, AESOP, and VEMPS simulators E/U is ±0.6 dB for a single shot. Prepulses can be appreciable functions of the main peak on TEMPS and TRESTLE (private remarks to R. Bevensee, LLL, June, 1978).

†90% confidence (reliability) limit with 90% confidence level.

Error type	Error/uncertainty	Reference	Comments
q-probe	ampl(f)* ≤ -1 dB phase(f)* ≃ ±5	7-10	
I-probe	ampl(f) ≲ 0.5 dB phase(f) ≲ 1°	7-10	
	3	6	Includes sensors, cables and connectors, oscilloscopes, and photo-presentation.
Sensor	ampl†, 0.9; unbal, 0.09	1	Screenbox system in particular, unless otherwise noted.
Twinax cable	ampl, 0+; unbal, 0.023		
Power splitter	ampl, 0.26; unbal, 0.1		
RCI integrator	ampl, 0.64; unbal, 0.25		
TEK 485 oscilloscope	ampl 0.18; unbal, 0.09		

*Amplitude or phase in f-domain.

†Ampl = amplitude, unbal = unbalance. The net error due to both these is $\left[\epsilon^2_{ampl} + \epsilon^2_{unbal}(V_c/V_d+1)^2\right]^{1/2}$, where $V_c//V_d$ = common mode/differential mode ratio, < 0.1 in a good system[11].

Passive integrator	not specified
RCD-8 differentiator	ampl, 0 dB, $f \leq 1$ MHz
	$0.5 \log(f_{MHz})$ dB, $1 < f_{MHz} \leq 10$
	$\pm 0.5 \log(100/f_{MHz})$ dB, $10 \leq f_{MHz} < 100$ MHz
TEK 486 oscilloscope	Sweep speed error, 0.09
Oscilloscope (DASET)	Sweep speed error, 0.09
Ballun	Ampl $(0.25 + 3.18 \times 10^{-3} f_{MHz})$ dB
	Unbal $4.27 \times 10^{-3} f_{MHz}$ dB
Manual attenuator	ampl, 0.5
Active integrater	ampl, 0 dB, $f < 0.1$ MHz
	$0.33 \log (10^3 f_{MHz})$, $0.1 \leq f < 200$ MHz
Attenuator	ampl, 0-.2; unbal, 0.2
Microwave calibrator	ampl, 0.18
Power splitter	ampl, 0.26
Cable (DASET)	ampl, 0.07
Remote attenuator (DASET)	ampl, 0.13

AD-A096 696 CALIFORNIA UNIV LIVERMORE LAWRENCE LIVERMORE LAB F/G 12/1
CHARACTERIZATION OF ERRORS INHERENT IN SYSTEM EMP VULNERABILITY--ETC(U)
OCT 80 R M BEVENSEE, H S CABAYAN W-7405-ENG-48
UNCLASSIFIED UCRL-52954

2 OF 3
AD A 096696

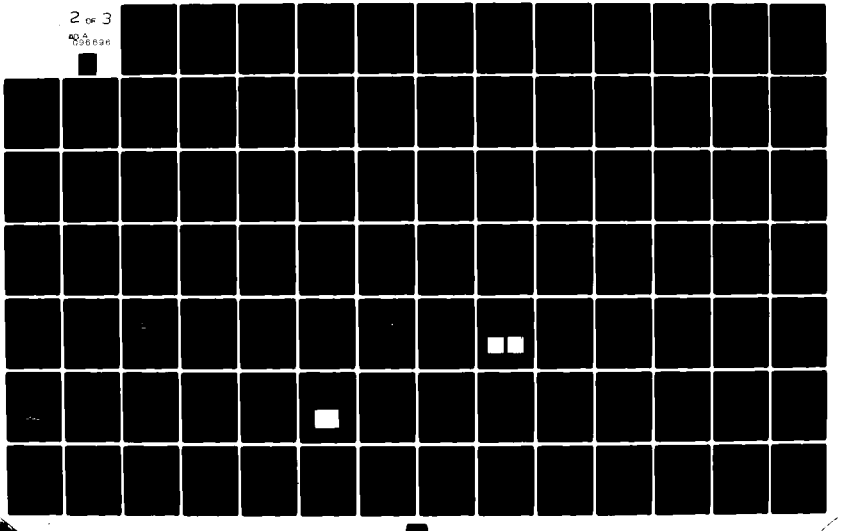

Network analyzer	ampl, 0.25		For calibrating transfer functions.
Microwave telemetry system	0.9, 2-50 MHz	12	dynamic range limitation.
Transmitter gain + dielectric waveguide Variations + oscilloscope	< 1	5	
Electric field		13	ADSET data acquisition on aircraft in ATHAMAS-I. Errors are in t-domain.
amplitude	0.9		
base line	< 0.2		
truncation	0.09		
Surface current density			
amplitude	0.5		
baseline error	0.9		
Truncation	1.25		
Noise/signal power	0.9		

x-y recorder	0.25	14	includes oscilloscope errors in net pen displacement.
Screenbox system	1.2 (integrated measurements) 0.35 (derivative measurements)	15	differential/common mode ratio 50/1; S/N ≥ 40 dB.
Improved screenbox (Video Digitization) System:		16	
amplitude	0.25		Errors are estimated from simulator data acquisition.
baseline shift	0.3		
Truncation	0.3		
Sweep speed	0.35		
Noise/signal power	0.15		
Transient Digitizer (with Autocal)			Autocal = computer-based calibration procedure. This transient digitizer system is better than a microwave system without autocal.

Amplitude	0.5		
Baseline shift	0.3		
Truncation	0.3		
Sweep speed	0.09		
Noise/signal power	0.15		
Time-base distortion	-0.4 +0.15	17	ADSET
Random amplitude fluctuations	0.35		Small fraction of total digitization error on ADSET, TELERECORDER, and DASET.
Amplitude nonlinearity	0.25 (f-domain)		

Data Processing

Most of the information below is obtained from EG&G and BDM reports, with ±3 dB being a "reasonable and achievable" overall data processing error.

Error type	Error/uncertainty	Reference	Comments
Processed film data	S/N ≃ 30 dB	1	

DASET 7912 processed data — S/N ≃ 50 dB

Data processing error estimates ϵ_{DP} (not in dB): — Based on regression analysis of data photographs or DASET recordings.

(A) f-domain, $\epsilon_{DP} = \frac{F(\omega)}{100} 10^{a} \left[F(\omega) / F_{max}\right]^{-20b}$,

where $a \simeq 0.838$, $b \simeq 0.037$ - Screenbox data

$a \simeq 0.733$, $b \simeq 0.027$ - DASET recordings

$\omega = 2 \pi f > 2.0/T_{trace}$

(B) t-domain, $\epsilon_{DP} = a' + b'x$

where $a' \simeq 0.108$, $b' \simeq 0.057$ - Screenbox data

$a' \simeq 0.062$, $b' \simeq 0.016$ - DASET recordings

$x = |$ slope of data trace in divisions/division $|$

Horizontal resolution of data	0.2		Error appears in f-domain as distortion of f-scale.
Digitization	0.2	17	Linear and additive errors.
Time offset in time tie	$S_{peak}/N_{eff} > 40$ dB		f-domain; N_{eff} is the effective noise power.

Interpolation in time tying	negligible		
Input word size	1/500 of peak amplitude		6- to 9- bit words, error in f-domain
Computer word size	<1/5000 of peak amplitude		15- and 25-bit mantissa, error in f-domain.
Sampling jitter	+2.3 -3.0		f-domain.
Linear error in	0.45		f-domain.
Time-base nonlinearity	+29 (f-domain) -4.4		5% maximum distortion.
Parallelogram effect, 2° skew	$\lesssim 6$		f-domain.
Keystone effect	6		f-domain.
Peak clipping	<1/400 of peak amplitude		f-domain.
Recorder:			
vertical calibration	0.26		
horizontal calibration	0.45		
Digital and machine processing errors	3	5	90-90 confidence interval

Data reduction	3	6	Digitization, Fourier transforms, etc.
Data processing errors:	neglibile out to 1 GHz	18	
transform			
digitization + transform			HDL technique. HDL says 85% of its data traces have no serious digitization errors.
Sampling			
Quantization			
Digitization + quantification + noise			

Useful data processing relations are summarized in Appendix F.

5.5.2 Extrapolation

Extrapolation refers to the multiplication of an internal current response from simulator environment to threat environment and has two error components. One is the simulator-to-threat conversion of a response quantity (such as surface current) by computer simulation with a model, ± 7 dB being "reasonable and achievable". The second is the variation among possible POE, 6-10 dB being typical. Both these error components are independent.

Error type	Error/uncertainty	Reference	Comments
Surface current	7.2	5	Extrapolation by computer code from test geometry to free space may correct only partially for the difference in geometry.
Incident field	9.5-14.0	12	Uncertainty relative to geometric mean.
POE	6-10	5	90-90 confidence level re geometrical mean of extrapolation functions at various surface points. External-internal transfer functions ignored.

(See also Sec. 5.6.2 for surface current extrapolation.)

5.5.3. Intrasystem Variations

These are due to variations in operating conditions (such as power on-off) or threat-deduced response at different sensitive points as a function of internal circuitry. The variation in measured internal current at various points gives an estimate of the error in approximating the threat current at a new internal point without detailed circuit analysis. This highly system dependent uncertainty could be $\pm$10 dB or more.

Error type	Error/uncertainty	Reference	Comments
Pin threshold current	13.3	5	Used to compute 95-90 margin given 90-90 error in wire current.
Power on-off	10	5	This error can lower thresholds and/or raise signal current. Error added in rss fashion.

5.6 COUPLING ASSESSMENT BY COMPUTER SIMULATION

This refers to computations by computer code of current induced in antennas or cables penetrating the system envelope or surface current on the envelope. The error is primarily due to modeling error resulting from approximation of the system by a simpler model amendable to computer analysis. Most of the errors and uncertainties reported below are for aircraft analyses.

5.6.1. Antennas and Cables

A "reasonable and achievable" uncertainty for both penetrating long-wire antennas* and cables is ± 3 dB.

Error type	Error/uncertainty	Reference	Comments
Log periodic antenna (forward incidence)	6.8	19	Multisegment thin wire model.

*For short antennas, to maintain a response error of $\lesssim 2$ dB it is necessary to measure their electrical parameters (i.e., input impedance and effective height).

Fan doublet, Hf-VHF	0.7	19	Multisegment thin wire model.
Cables over high conductivity ground	6	20	Measurements compared to classical analysis (no parameters fit by measurements).
HDL code (FREFELD)	2.3	R. Gray, HDL	Long cables above ground connected to radio equipment (parameters fit by measurements).
Aircraft cables: multi-conductor line parameters	negligible	21	Tedious to compute.
Output load voltage (short pulse)	+2.3 common mode +1.3 differential mode		Errors measured by difference between measured and computed
Output load voltage (long pulse)	+1.06 common mode +0.05 differential		

5.6.2 External Surface Current

The external surface current obtained by computer code based on an integral equation solution contains the modeling error introduced by the simpler computational model of the actual system. A "reasonable and achievable" error is $\pm$6 dB. This error is part of the extrapolation error mentioned in Section 3.5.2. The finite difference computer codes contain inherently less error when estimating surface current; $\pm$3 dB is reasonable.

Error type	Error/uncertainty	Reference	Comments
External surface current:		5	
VPD simulator (from 15 external points)	mean, -2.50; standard deviation, 2.35		Error = (I_{meas}/ I_{calc}) dB over f ≲ 100 MHz, I_{calc} by OSU on thin-wire stick model. These numbers varied widely over different frequency bands.
SRF simulator (from 19 external points)	mean, -2.50 standard deviation, 4.36		
(See also first entry in Section 5.5.2, Extrapolation.)			
External surface current on pipe models of aircraft	6	22 23	Computation compared to measurements of aircraft scale models: cylinder, miniature B-1 and miniature EC-135.
FD computer code*	≲ 3 dB high	24-28	t-domain J_s over 550-ns interval.

*Finite difference analysis of aircraft response is discussed in Appendix G.

5.6.3 Internal Response

Internal system response is computed from excitation on penetrating antennas and cables, apertures and other inadvertent POE, but rarely from diffusion of energy through the system envelope. These excitations are usually obtained from tests or computer simulation assuming no effect of the system interior upon the exterior response, except perhaps for equivalent loads on antennas or cables.

The estimates of intra-system variations of current from the measured variations at a few specified points have already been mentioned (Section 3.5.3). Uncertainties in internal currents are usually reduced by circuit analysis, even if approximate, due to the complexity of internal circuitry. Unfortunately, this complexity creates large uncertainties in internal current flow at unmeasured points or ports.

Error type	Error/uncertainty	Reference	Comments
Aperture fields	$\lesssim 6$	29	In f-domain, longest dimension $\lesssim \lambda$.
Typical internal cable currents		5 (Table 20)	Error = I_{meas}/I_{pred} in dB, where I_{pred} was computed from (1) external transfer function via OSU code, (2) penetration via Bethe theory, (3) distributed source single-wire transmission line to bulk current, (4) computer code or impedance ratio for wire current
average error among 13 bulk cable currents	-4.6		
spread of errors about bulk current (11.4 standard deviation)	-32. to + 17.		

average error among 14 currents	-9.2	
spread of errors about the average wire current	-15.7 to - 1.6	
Impedance ratio	13.5	Internal circuit computation of wire currents from bulk or other currents.

5.7 COUPLING ASSESSMENT OF SCALE MODEL TESTS

The purpose of scale model testing in a relatively low-level simulator environment may be to (1) obtain the extrapolation function F_s/E_{inc}, F_s being the surface response (current or charge density), and then scale it in frequency domain for a full-size system exposed to EMP or (2) measure the equivalent circuit antenna parameters for each external or internal response of interest, scale for the full-size system of interest, and then compute the EMP response at each point of interest. The University of Michigan, for example, has performed scale-model aircraft measurements for purpose (1) which have served in the Rockwell EC-135 assessment by method 2 (scale-model extrapolation). The Lawrence Livermore Laboratory, for example, has assessed both the external and internal response of generic structures (i.e., whips and loops on boxes and cylinders) and military systems such as an aircraft parked on a ground plane, tank, and ship.

See Section 3.2 for the numerical values of various uncertainties.

5.7.1 Measurement Error

This includes simulator field and the instrumentation and data processing errors similar to those for full-scale simulation testing.

Error type	Error/uncertainty	Reference	Comments
University of Michigan anechoic/chamber:		7	
Simulator	<1, $0 < f \leq 2$ GHz		
Model-chamber Interaction + Instrumentation	0.5-1 GHz, 3 dB ampl, $\pm 10^{\circ}$ phase 1-4 GHz, 1 dB ampl, $\pm 5^{\circ}$ phase 4-6 GHz, 3 dB ampl, $\pm 10^{\circ}$ phase		Model-chamber interaction predominant at low frequencies.
LLL Transient Range measurements:			
antenna external response	4	30	Due primarily to instrumentation (oscilloscope) noise.

5.7.2 EXTRAPOLATION BY SCALE MODEL PREDICTION

This has the same meaning as for full-scale simulator testing except that the simulator-to-threat conversion factor is derived from scale model testing rather than computer simulation of a model response.

Error type	Error/uncertainty	Reference	Comments
Internal cable currents	2-20	31	LLL Transient Range measurements on HMS Huron.

Surface current and charge	6	12	Geometrical average over many surface points of University of Michigan prediction vs simulator test measurement.

5.8 COUPLING ASSESSMENT BY SURFACE CURRENT INJECTION TESTS (SCIT)

This refers to simulation of the complete EMP response of a system, commonly an aircraft, by injecting currents at one or more points of the proper spectral content to excite properly the dominant modes of the system. In principle this is not too difficult, but in practice the temporal currents have not been sufficiently accurate to keep the error in peak surface current or charge less than 6 dB or so. SCIT is attractive though because it is only necessary to excite properly those few system modes with complex resonant frequencies in the range of the EMP spectrum.

Error type	Error/uncertainty	Reference	Comments
Surface current and charge in an aircraft	6	28	Comparison of SCIT-induced and measured current on A-6 aircraft in EMPRESS facility.*

*Data shows the difficulty of making a SCIT excitation equivalent to a simulator one over the narrow frequency bands near the dominant mode resonant frequencies.

5.9 COUPLING ASSESSMENT BY GENERIC SYSTEM RESPONSE

Below are compared the differences between the peak current responses of various systems and the corresponding responses of similar generic systems. The generic system data was generated at Lawrence Livermore Laboratory.[19]

System tested	Generic system response differences (dB)
Army horizontal dipole over ground	1.1
Army whip over shelter	2.5
Ex-USS Valcour (ship)	8.7
Spartan missile	3.6

5.10 CONCLUSIONS

The Lawrence Livermore Laboratory examinations of the literature on EMP coupling assessment indicates clearly that measurement errors in simulator field, instrumentation, and data processing are either minimal, or can be made so, compared to the following most serious errors:

(1) Extrapolation errors incurred in estimating threat internal response from simulation test response. For example,[5] estimates an error of $\pm$7.2 dB in extrapolating the external aircraft surface current by computer code so as to obtain free-flight response from simulated ground response. Modeling error is involved here also. In scale model testing,[5] quotes a "simulation error" in the range $\pm$6.7 - $\pm$12.4 dB for various aircraft orientations; this includes

error in extrapolation of external surface current by scale model testing and POE error, discussed next.

(2) POE error, as another kind of extrapolation error, is extremely variable ($\pm$6 - $\pm$10 dB quoted for aircraft) because of ignorance about the relative importance of various possible points of entry in EMP penetrations. There is no simple method of isolating the various POE.

(3) Intra-system variations of internal response due to power on-off($\pm$10 dB uncertainty) or variation in circuitry ($\pm$13.7 dB uncertainty quoted by Ref. 5).

(4) Computer simulation to obtain internal wire current estimates. For example[5] quotes a standard deviation of 11.4 dB among the 13 errors (in dB) of 13 bulk cable currents. Such a figure does not imply a confidence interval for a given current, but it suggests a large error in its computation.

All these errors can be reduced by obtaining more information from measurements. Extrapolation from test to threat conditions is improved if based on measurements of accurate scale model response; POE extrapolation uncertainty is reduced by tests of the system with more parameter variations (incident wave and ground parameters). Intra- and inter-system variations are both reduced by test measurements at more internal points and for more systems samples. And computer simulation of internal wire response, so difficult to do well and prone to error, can be largely supplanted by direct subthreat measurements of a real system to obtain the external-internal transfer functions.

For accurate EMP assessment of a realistic system, one should make as many measurements as possible, for a wide range of operating conditions, on as many samples or realistic models as possible. Only then will the worst-case EMP response in a threat situation become apparent, with the minimum overall error and uncertainty.

5.11 REFERENCES

1. Horizontally Polarized Dipole, Electromagnetic Pulse Simulator Upgrade Test Program. Characterization Report Vol. IV Error Analysis Report, EG&G, Alburquerque, NM, Al-1295 (April 1978).

2. W. W. Cooley, et al., DNA Prempt Program Communication Facility for EMP Response--Prediction Techniques," IEEE Intern. Symp. Electromagnetics Compatibility, August 2-4, 1977, Seattle, WA.

3. Statistical Relationship between Testing and Prediction of EMP Interaction, AFWL-TR-77-176, R&D Assoc., Marina Del Rey, CA (June 1978).

4. Misc. Sim. Memos, Memo 8, Some Performance Parameters for Various EMP Simulators, AFWL, Kirtland AFB, Albuquerquem, NM (November 1976).

5. EC-135 EMP Assessment Program Final Assessment Report, Vol. III Assessment Error Analysis, Rockwell Intern., Anaheim, CA (November 1977).

6. Measurement Note 21, Instrumentation Guidelines for EMP Testing, Rockwell Intern., Anaheim, CA (August 1974).

7. Sensor and Simulation Note 210, Sweep Frequency Surface Field Measurements, Final Report, Univ. Mich. Rad. Lab., Ann Arbor, MI, AFWL-TR-75-217 (December 1974-July 1975).

8. Surface Field Measurements on Scale Model F-111 Aircraft, Univ. Mich. Rad. Lab., Ann Arbor, MI, 014449-1-T (September 1977).

9. Surface Field Measurements on Scale Model EC-135 Aircraft for VPD and SRF Data Interpretation, Univ. Mich. Rad. Lab., Ann Arbor, MI, 015414-1-T (July 1977).

10. Surface Field Measurements on Scale Model EC-135 Aircraft, Final Report, Univ. Mich. Rad. Lab, Ann Arbor, MI, 014182-1-F (January 1978).

11. J. Yu, C-L Chen, and J. P. Castillo, "Responses of a Conducting Pipe," Athamas Memo 14, AFWL (April 1977).

12. Sensor and Simulation Note 232, Characterization of Errors in the Extrapolation of Data from an EMP Simulator to an EMP Criterion, Mission Research Corp., Albuquerque, NM (October 1977).

13. Measurement Note 25, Deterministic Error Analysis Applied to EMP Simulator Data Acquisition II, Application to Aircraft Test Data, Mission Research Corp., Albuquerque, NM (March 1978).

14. Measurement Technique for Determining the Time Domain Voltage Response of UHF Antennas to EMP Excitation, HDL, HDL-TR-1778 (August 1976).

15. K. Kunz and J. Prewitt, "Field Asymmetry in the Athamas I Facility: Causes and Possible Cures," Athamas Memo 17, AFWL, Kirtland AFB, Albuquerque, NM (October 1977).

16. Measurement Note 24, Deterministic Error Analysis Applied to EMP Simulator Data Acquisition, Mission Research Corp., Albuquerque, NM (June 1977).

17. EMP Data Reduction Variables Analysis Study, Braddock, Dunn & McDonald, Alburquerque, NM (May 1977).

18. Numerical Fourier Transform, Harry Diamond Laboratories, Woodbridge, VA, HDL-TR-1748 (September 1976).

19. R. M. Bevensee, et al., External Coupling of EMP to Generic System Structures, Lawrence Livermore Laboratory, Livermore, CA, M-090, (1978), (Table 10-1, pp. 10.5).

20. W. J. Stark, An analytical and Experimental Investigation of Cable Responses to a Pulsed Electromagnetic Field, HDL, Woodbridge, VA, HDL-TR-1618 (December 1972).

21. Aircraft Cable Parameter Study, AFWL, AFWL-TR-77-107, Mission Research Corp., Albuquerque, NM (October 1977).

22. C. Taylor, K. Chen, and J. Crow, "Study of Charge and Current Induced on an Aircraft in EMP Simulator Facility. Part III: Numerical Results," Athamas Memo 20, AFWL, Kirtland AFB, Albuquerque, NM (January 1977).

23. EMP-VPD Pipe Experiment Analytic Predictions, Mission Research Corp., Albuquerque, NM, AFWL-TR-75-78, Mission Research Corp., Albuquerque, NM (December 1975).

24. K. S. Kunz and K-M Lee, "A Three-Dimensional Finite Difference Solution of the External Response of an Aircraft to a Complex Transient EM Environment: Part I - The Method and its Implementation," IEEE Trans. Electromagnetic Compability EMC-20 (May 1978).

25. K. S. Kunz and K-M Lee, "A Three-Dimensional Finite Difference Solution of the External Response of an Aircraft to a Complex Transient EM Environment: Part II - Comparisons of Predictions and Measurement," IEEE Trans. Electromagnetic Compability EMC-20 (May 1978).

26. Calculation of the Transient Currents Induced on an Aircraft by 3-D Finite Difference Method, Mission Research Corp., Albuquerque, NM, AMRC-N-45 (October 1976).

27. "THREDE: A Free-field EMP Coupling and Scattering Code," IEEE Trans. Nuclear Science NS-24 (December 1977).

28. Final Report, Alternate Aircraft Simulation Techniques, Mission Research Corp., Albuquerque, NM (February 1978).

29. EMP Penetration Handbook on Apertures/Cables/Shields/Connectors/Skin Panels, AFWL, AFWL-TR-77-149, Dikewood Corp., Albuquerque, NM (December 1977).

30. R. M. Bevensee, et al., Validation and Calibration of the LLNL Transient Electromagnetic Measurement Facility, Lawrence Livermore Laboratory, Livermore, CA, UCRL-52225 (1977).

31. K. Kunz, LuTech, Inc., Albuquerque, NM, private communication to H. S. Cabayan, Lawrence Livermore Laboratory, Livermore, CA (1979).

6. SUBSYSTEMS AND COMPONENTS SUSCEPTIBILITY

6.1 INTRODUCTION

More attention is given to components than to subsystems in this section. A major reason for this is the scope of this task. Also, the assessment of subsystems (primarily meaning here separate pieces of equipment or modules inserted into a system) must necessarily be geared to a particular interfacing requirement. An interface requirement may be such an item as the specification of the range of allowable pin-pin or pin-ground voltages for different time signatures. The work presented in this section, however, does consider the uncertainty of the susceptibility threshold levels and failure damage models as might be employed in a subsystm or system assessment problem.

All of the work is based on current activity in the field, so that information contacts are essential for surveying purposes. The goal was to contact key facilities and individuals in order to get some expert opinion and obtain some key reports. An attempt is made to provide a general review of uncertainties as seen in conjunction with assessment methodology. As a certain amount of quantification of statistical properties is evident in the field, a sampling of the nature of this is also provided in Section 6.4 and in Appendix H. Some aspects of computer programs and modeling are also discussed in Section 6.4. (General and selected references are included at the end of this report.)

6.2 INFORMATION CONTACTS AND ONGOING WORK IN SUSCEPTIBILITY

A large portion of this work has been oriented to the survey for information on uncertainties. Several personal contacts have been made and several recent reports have been obtained. Thus, for sources of information, the following are included:

6.2.1 Contacts of Organizations

- Service Lead Laboratories: Harry Diamond Laboratories, Woodbridge, VA and Adelphi, MD; Naval Surface Weapons Center, White Oaks, MD and Dahlgren, VA; Air Force Weapons Laboratory, Albuquerque, NM.
- IIT Research Institute, Chicago, IL.
- The Boeing Co., Seattle, WA.
- TRW Systems Group, Redondo Beach, CA.
- The BDM Corporation, Albuquerque, NM.
- Rockwell International, Anaheim, CA.
- Corps of Engineers, Huntsville, AL.
- GE Space Center, Valley Forge, PA.

The first three organizations listed are, of course, the Service Lead Laboratories, and each has performed or contracted a significant amount of work in the components area. AFWL in particular has had a large test and modeling program in effect for several years. AFWL has done extensive subsystem testing on B-1, AABNCP, and EC-135 airborne subsystems. TRW and Rockwell have been principals in these efforts. Both BDM and GE have had active semiconductor and other component programs for years.

HDL has evaluated protective devices for DNA. HDL also has done a lot of work in conjunction with the Army's MSEP (Multiple Systems Evaluation Program). NSWC has done work on failure modes and modeling in the past and is currently evaluating some integrated circuits. The Corps of Engineers has had to look at broad classes of components as may be found in ground support facilities. The Boeing Co. has done modeling and testing. Although the Martin Co. was not contacted specifically during this task, it is also active

in component testing and failure analysis.[1] Lockheed has also done integrated circuit testing and modeling as part of various Navy programs. McDonnell Douglas has done a great amount of integrated circuit electromagnetic susceptibility (RF) investigation in the higher frequency end of the spectrum. IITRI has recently looked at long term reliability aspects for DNA.

6.2.2 Ongoing Work

A number of reports have been recommended by individuals contacted in the above organizations. Several of these have been obtained and reviewed. The contents of a few of the significant ones will be reviewed in Section 6.4. In general, there is a noticeable trend for component failure investigators to look at the statistical nature of the problem. Information on failure levels or failure models tends to be given with regard to grouping or statistical measure in conventional terms.

Component evaluation exercises are stimulated or driven primarily by specific assessment or hardening programs demands and thus may be less than ideal from the component investigator's viewpoint. Nearly every, if not all major programs, have used component failure information based on actual tests on devices. Therefore, the major uncertainties lie in either the use of such information, the errors related to test, or the lack of completeness of test coverage for all possible failure modes.

Information inputs for subsystems are found in the following sources:

- TRW/AFWL AABNCP Assessment Plan.[2]
- HDL - Lance program reports.
- HDL - MSEP program reports.
- AFWL AABNCP Reports.[3]

- Defense Civil Preparedness Agency studies.
- Corps of Engineers--Safeguard facilities reports.
- Sprint/Spartan Missiles.
- EC-135 Reports.

Information inputs for components are found in the following sources:

1. Chapter 13 DNA EMP Handbook.[4]
2. R. L. Williams/HDL 1978.[5]
3. TASCA/GE - HDL 1976.[6]
4. AFWL/Boeing/BDM 1974.[7]
5. Tasca/O'Donnell GE 1977.[8]
6. Egelkrout/Boeing 1978.[9]
7. Kalab/HDL 1978 (draft).[10]
8. Miletta/HDL 1977.[11]
9. Lockheed 1976.[12]

6.2.3 Comments on Information Sources

In addition to the special EMP-oriented sources, there are several, indeed hundreds, of papers and reports dealing with the subject of failure modes and processes in components. Two recent bibliographies contain most of the references to this material (DNA Reports 4146T and 4285T).[13,14] Subsystem

reports are quite numerous also, particularly those connected with the Air Force AABNCP and EC-135 programs. These will not be listed and no attempt was made to survey them. However, the system reports for the EC-135 allude to results from the subsystem reports, and that aspect is reviewed. From previous experience, it is known that the AABNCP subsystem reports contain a great amount of information an analysis and testing.

6.3 REVIEW OF UNCERTAINTIES

In susceptibility work, uncertainty areas in general will naturally occur in some of the conventional phases of the work. Below are listed some of these phases of activity for subsystems and components.

Subsystems	Components
Methodology	Failure modes
Analysis	Modeling
Testing	Testing
Data handling	Failure analysis
Configuration	Prediction techniques

6.3.1 Discussion of Subsystems Uncertainty

Subsystem assessment work may be faced with different uncertainties, depending on the requirements. There is no standard practice in subsystems work. There are at least three different ways of approaching the problem.

1. Assessment relative to a specification placed on the interface of the subsystem. (For example, the B-1 aircraft or Airborne Command Post Pin Specification.)

2. Assessment which employs a replica or extrapolation of the actual signal present in the system (as might be obtained from tests on a missile program).

3. The use of "representation" whereby the number of subsystems is quite large so as to preclude detailed analysis or investigation of all of them.

After scanning briefly the phases of activity in subsystems assessment, we feel that the following are likely areas of uncertainty.

Methodology Development. By definition, the methodology should be a precise and orderly procedure. In practice it could be highly adaptive and ad hoc to fit the situation. The compromises which are made in developing a methodology for a particular program are usually recognized, but their full significance on errors may not be realized. The methodology would place emphasis on those phases of activity which are important to the project at hand. Thus, a decision not to do any testing because of costs or other reasons would create a different set of uncertainties than if some combination of tests and analyses were performed. The Boeing AABNCP Assessment Program[3,15] is an example of a strong methodology, heavily based on existing data, but backed up with test on selected subsystems for verification of predicted failure levels. Figures 6-1 and 6-2 show a flow diagram for circuit assessment (Ref. 3, Chapter 13).

Analysis. At the subsystems level, analysis could mean anything from that of doing a simple screening of susceptible components on a penetration interface to performing a detailed circuit analysis from the interface through several critical components.

Uncertainties in this work appear in the lack of suitable high-signal-level models for components, in the lack of information on parameters, and in the inability to handle large problems. Judgement is employed to simplify the circuit. This circuit is not always checked by experiment.

Testing. One of the largest uncertainties in testing may occur from not being able to inject signals simultaneously to all pins concurrently. This is a good argument for doing a systems test. Ground loops and other problems unique to the type of interconnection may not show up at the subsystem or unit tests.

Another uncertainty is, of course, in the simulation of the actual interface EMP signal. It is interesting to compare the set of test signals and how they affect the subsystem or unit with a set of possible EMP signals. The executive summary report[3] of the Boeing AABNCP program has information on the relative accuracy of subsystem assessment analysis as compared to certain test results. A later report[16] on the EC-135 program uses AABNCP data for comparisons and uncertainty statements.

Data Handling. The handling and processing of data in the bandwidths and quantities required for EMP appears to be of more economic than of error-uncertainty concern. Reference 15 discusses the handling of subsystem functional description data.

Configuration. A specification may or may not be closely tied to the expected actual operating environment from EMP-induced signals. Uncertainty exists in the basic concept of using an interface specification to permit subsystems design of assessment to uniform criteria. Even after accepting the specification as correct, a major uncertainty in the analysis of a subsystem appears in the knowledge of the basic configuration of the subsystem. Such an uncertainty cannot be easily resolved and can cause large errors in assessment. An example is assuming a lack of direct path where in fact there

is one. "Ordinary" circuit analysis by computer plays a significant role in subsystem assessment, and relies heavily on prior determination of configuration.

6.3.2 Discussion of Components Uncertainties

There has been a great deal of investigation of physics of failure, of various failure modes, and of failure thresholds for many different devices. Given essentially unlimited opportunity to examine a device, to control its manufacture, and to understand how it is used in actual practice, there appears to be little problem in coming up with a suitable failure model and using it for predictions of failure. Given the large number of devices, particularly the sensitive solid-state components, it is seldom that a single device can be controlled and studied in detail; rather, attempts were made using small samples to derive general models which could be used with prediction techniques. Such a model is the familiar $P=kt^{-1/2}$ model for prediction of semiconductor device junction failure, and its empirical extensions to the case of integrated circuits in the form of $P=At^{-B}$, where A and B are the empirically determined constants.

The following list of uncertainties in the components and circuits areas are typical of those experienced by workers in the field.

- Circuits:

  a. Parameters.

  b. Nonlinear effects of transformer core.

  c. High-signal-level solid-state device models,

  d. Nonlinear models in general.

  e. Stray circuit elements.

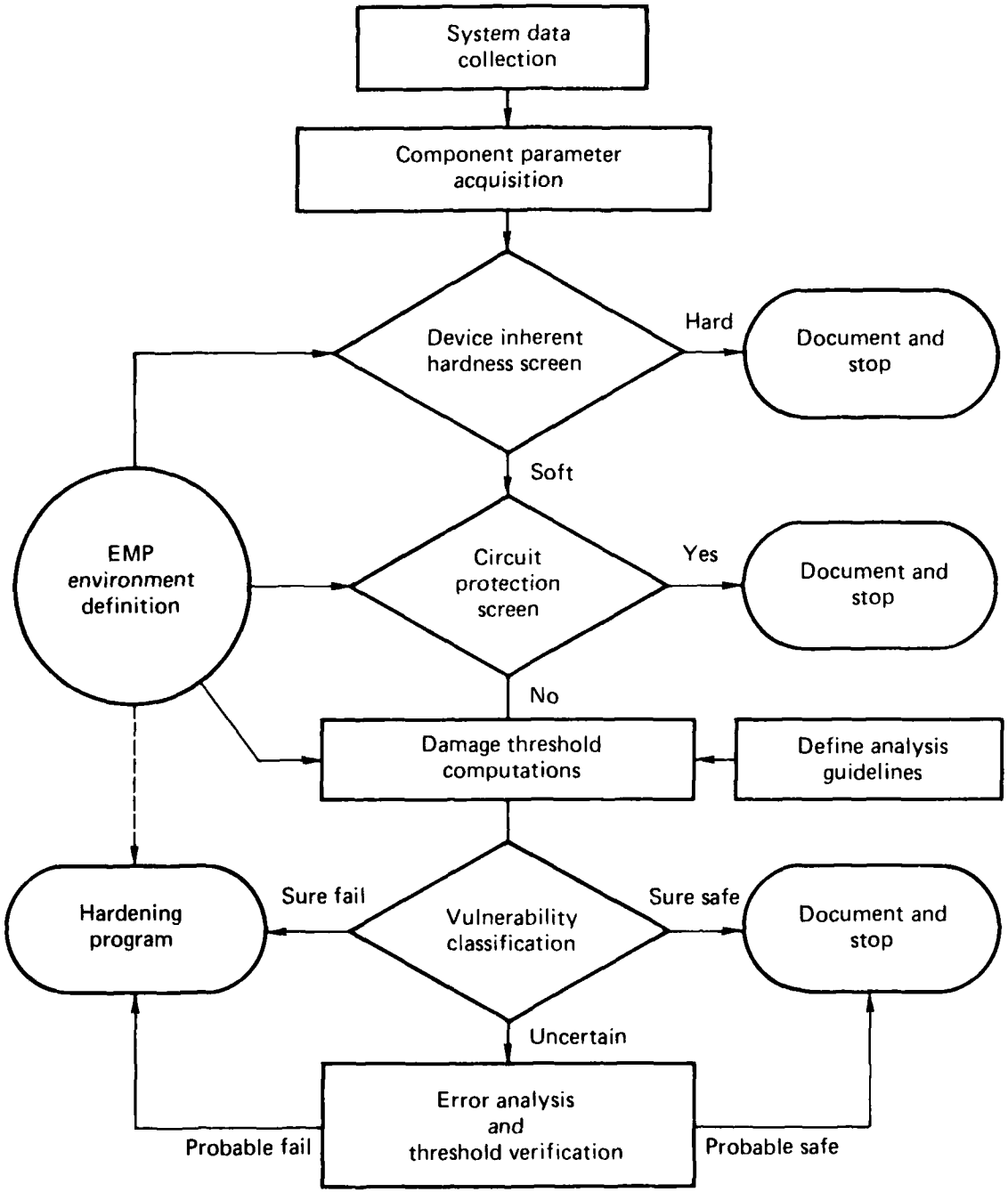

FIG. 6.1. Flow diagram of a generic EMP damage assessment methodology (Ref. 4).

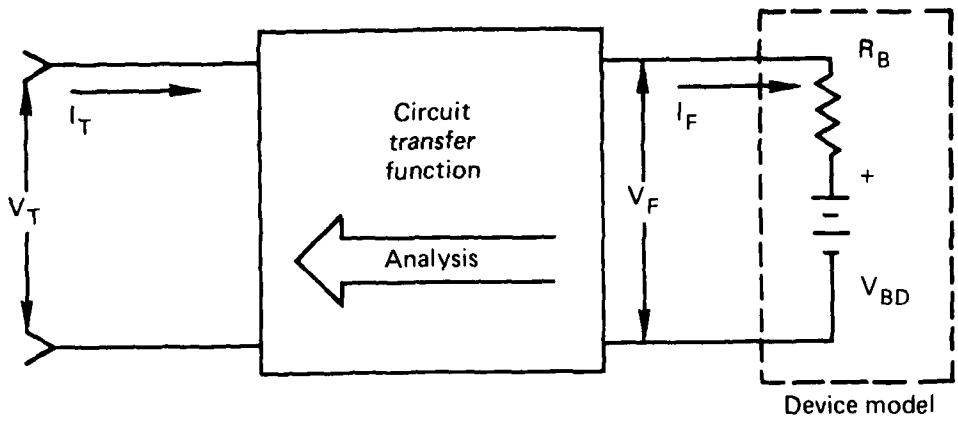

(a) Circuit inherent hardness estimate

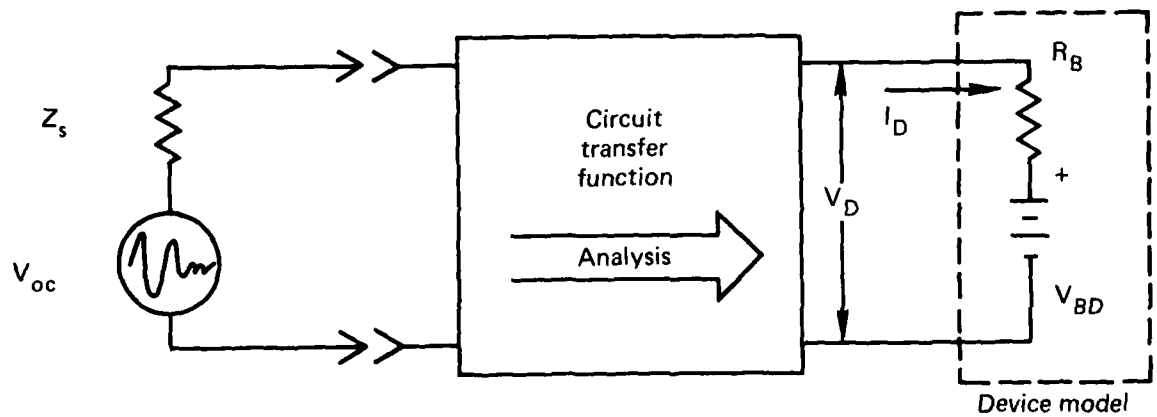

(b) Circuit vulnerability estimate

V_{BD} – Device breakdown voltage
R_B – Device bulk resistance
Z_s – Source impedance
V_{oc} – EMP-induced open-circuit voltage

FIG. 6.2. Generic approach for determining circuit specification vulnerability inherent hardness (Ref. 4).

- Components:

  a. In the use of theoretical models for damage prediction.

  b. Waveform differences (actual system vs component testing).

  c. Ranges of distribution of failure threshold values.

  d. Definitions of integrated circuit damage.

In the components area, items a, b, c, and d are all-important sources of uncertainty. Theoretical models must resort to published device parameter data, usually based on junction capacitance. Waveform differences are significant whenever a device exhibits either a lower failure level for one polarity than the other or the failure level is affected by repeated pulses of varying polarity. There is a quantization error associated with the finite steps. Sometimes it is actually quite difficult to determine when an integrated circuit has failed.

Experimental Uncertainties in Component Testing.

- Environment Simulation:

Very little testing of components is performed with a simulation of the actual in-place or in-circuit environment. Testing of components is performed primarily with a unipolar type of pulse waveform for practical reasons of economy and ease of generation. A high degree of automation is employed in much of the testing. Actual environment waveforms (as observed from system EMP simulation tests) are nearly always some variation of a damped sinusoid with frequency content which depends on the system configuration.

- Instrumentation:

Sensing of voltage and current is not a source of major uncertainty. Step-stressing is commonly used as a technique, so that large errors are unlikely. However, determination of exact time of failure can be a source of error. Pretest instrumentation normally involves an automated parameter-measuring test set; post-test determination of possibly degraded parameters can be evaluated by the same test set, thereby removing an uncertainty through standardization. Absolute errors or uncertainties in component use for a particular application are then only as good as the completeness of coverage of the original parameter test set.

Test methodology and error analysis are discussed in Appendices A and B of Ref. 7. Errors are summarized in Tables 6-1 and 6-2.

Uncertainties in Analysis. Chapter 13 on "Component EMP Sensitivity and System Upset" of the DNA EMP Handbook[4] contains some general information of uncertainties or accuracy factors of variables as used in analysis. The three phases of damage analysis methodology (Fig. 6-1) are:

I. Data Acquisition

II. Susceptibility Screen Development

III. Detailed Theoretical Analysis.

Uncertainties in Data Acquisition. The detail and quality of data on subsystems, circuits, and components available for analysis varies considerably. Inference of circuit parameters from schematics is often necessary. Some circuit details may not be available. The availability and accuracy of failure parameters for devices are two of the most significant constraints in doing an EMP assessment. Some methods for obtaining component failure parameters, in addition to doing actual testing, are use of data in the Air Force Weapon Laboratory code SUPERSAP, use of existing equations

TABLE 6.1. Measurement and digitizer errors - discrete device testing (Ref. 7).

Quantity	Worst-case error %	rms error %
$V_{oscilloscope}$ $I_{oscilloscope}$	7.1	5.4
$V_{digitized}$ $I_{digitized}$	11.1	6.6
$\bar{P}_{calculated}$	23.	9.3

TABLE 6.2. Measurement and digitizer errors - integrated circuit device testing (Ref. 7).

	Worst-case error %		rms error %	
Quantity	t_p = 10 μs	t_p = 1.0 or 0.1 μs	t_p = 10 μs	t_p = 1.0 or 0.1 μs
$V_{oscilloscope}$	6	6	4.2	4.2
$I_{oscilloscope}$	10	6	5.8	4.2
$V_{digitized}$	10	10	5.7	5.7
$I_{digitized}$	14	10	6.9	5.7
$\bar{P}_{calculated}$	25	21	8.9	8.0

(supplemented by measurement), use of equations and certain published data, and general estimates of damage thresholds in various categories of devices.

Detailed Theoretical Analysis Uncertainties. Detailed theoretical analysis at the circuit level requires several types of information and tools, each of which can involve a large amount of uncertainty.

The principal types of tools, for complex circuits, are the large and general purpose circuit and system codes such as CIRCUS, NET2, SCEPTRE. Complete circuit simulation is possible in principle, but may be prohibitively costly. A simplification of circuit in order to reduce the order of complexity may omit certain responses which are important. A preliminary analysis by an engineer familiar with the design basis for the circuit will eliminate certain sections or components, but there is apparently no good way to account for the possibility of damaging a "buried" circuit component. Such circuits are those having no direct or apparent connection, and thus the components may not be visible or apparent to a circuit analyst dealing with one separate functional section or circuit.

Uncertainties in Screening for Susceptibility. Screening of subsystems or components for EMP hardness makes use of some method of ranking components for inherent hardness. This can be quite simple, with little uncertainty, such as screening out all semiconductor circuits as being inherently soft. A more sophisticated screen makes use of values of failure threshold parameters for devices, usually a "K" value. Lack of properly acquired data concerning circuit description can cause a great amount of uncertainty in all cases. For instance, an assumption that a circuit must be solid state, when in fact it is not actually required to be for function, could create serious susceptibility uncertainties regardless of method of screening.

6.4 AVAILABLE RESULTS

Results are available which express in quantitative manners some of the uncertainties which have been identified. In the components area, there are several reports which do have composite data, figures, tables, etc. Very briefly, some of that information is presented in this section. In Appendix H, there are included separate reviews of each report and typical information. No attempt is made to reproduce this extensive body of results on component failure models and susceptibility levels, as this information is quite readily available from the reports referenced or in the data base associated with the AFWL code SUPERSAP.

6.4.1 Ranges of Susceptibility Levels

First, it is pointed out that the DNA EMP Handbook, Chapter 13 revised (Ref. 4), has quantitative information on component sensitivity and factors of uncertainty related to prediction of failure thresholds. This includes data for transistors, diodes, integrated circuits, and some resistors and capacitors as well. Figure 6.3 shows uncertainty as expressed in observed ranges of failure. The handbook expresses other aspects of uncertainty, including:

- Factors in analysis:

  a. Transient waveform effects.

  b. Reactive elements.

  c. Source impedances.

- Accuracy factors: Largest sources of uncertainty are associated with component damage thresholds. There may be a voltage-sensitive failure mode when one is anticipating only a thermal failure regime.

- Confidence statements (95%) are provided for the following:

  1. "K-factor" estimates.

  2. Integrated circuits by category.

Tables 6.3 and 6.4 contain uncertainty information regarding device damage-constant estimation based solely on a generic type classification of device. The 95% confidence limits are shown for several categories. Sample sizes are given. The data assumes that the thermal damage model applies. Values given in Table 6.4 represent average values for this nonlinear parameter. R_S is the so-called surge resistance of the junction as considered for high level currents. In the forward bias region, R_S represents the bulk resistance R_B and an effect due to high level injection. In Table 6.5, integrated circuits (ICs) are also summarized by category, with confidence limits provided for the parameter A. The failure model in this case is $P_f = At^{-B}$. Average values are given for the other parameters.

6.4.2 Component Damage--Conversion of Waveform Effects for Equivalent Damage Effects

Actual waveform effects on component damage threshold levels remain a source of uncertainty in the field. Common practice for EMP has been to make assumptions, such as reverse bias failure mode and failure on the first pulse of a multiple pulse waveform. A conversion factor is given in the DNA EMP Handbook (Ref. 4, Chapter 13, p. 13-7). This simple conversion factor relates the rectangular pulse failure model to the resonant frequency of a damped sinusoid: $t = \frac{1}{5f}$, where f is the resonant frequency and t is the equivalent rectangular pulse duration. This conversion is based on circuit considerations rather than a detailed junction model. It also is based on the $P = Kt^{-1/2}$ damage model. Another source[15] gives the square-pulse

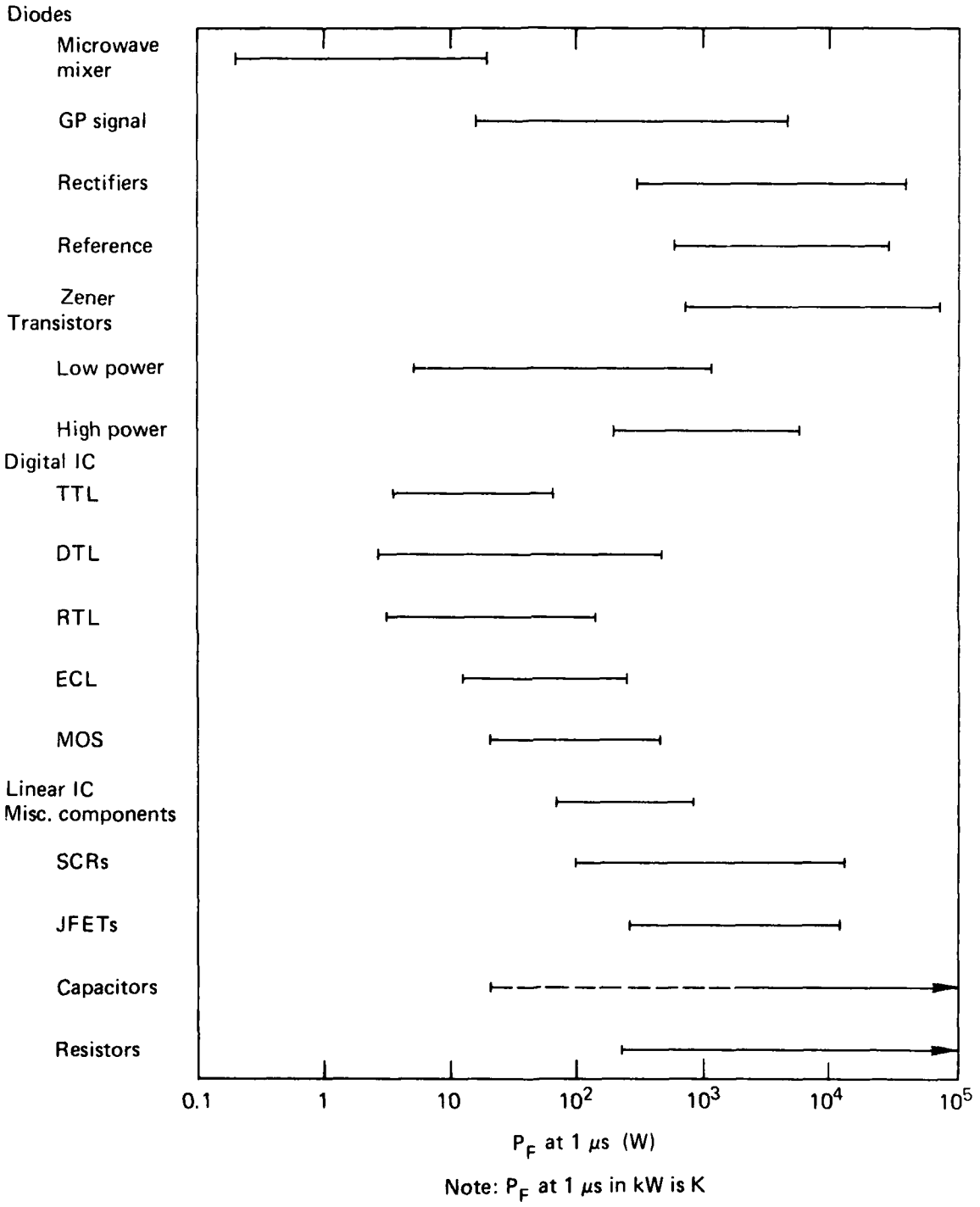

FIG. 6.3 Relative damage susceptibility of electronic components (Ref. 4).

TABLE 6.3. Damage-constant estimation based on device category.

Category of device	K_{min}	K_{max}	K_{mean}	K_{lower} 95%	K_{upper} 95%	Sample size
			($W.s^{1/2}$)			
Diodes						
Zener	0.73	87.9	10.1	1.05	96.5	52
Reference	0.60	27.9	4.9	0.12	199	4
Hi-voltage rectifier	0.30	40	2.94	0.19	46.5	56
General purpose signal (Ge)	0.014	0.23	0.040	0.005	0.30	7
General purpose signal (Si)	0.12	5.2	0.67	0.11	4.18	13
Microwave mixer	0.00029	0.026	0.00194	0.00028	0.0138	22
Switching	0.00717	0.92	0.13	0.0088	1.83	21
Transistors						
NPN low power (Ge)	0.01	0.1	-	-.	-	3
PNP low power (Ge)	0.01	1.1	0.30	0.01	6.7	7
PNP high power (Ge)	0.88	5.7	1.31	0.38	4.49	8
NPN low power (Si)	.0075	1.14	0.11	0.01	1.96	47
NPN med power (Si)	0.2	2.1	0.63	0.12	3.3	7
NPN high power (Si)	1.56	3.43	2.13	1.11	4.06	5
PNP low power (Si)	0.005	0.65	0.15	0.01	1.8	25
PNP med power (Si)	0.442	1.0	-	-	-	2
Miscellaneous						
JFET	0.11	15	-	-	-	2
SCR	0.40	11.7	2.33	0.15	37.4	7
UJT	0.16	0.16	-	-	-	1

TABLE 6.4. Surge resistance data for discrete semiconductor devices.

Category of device	R_S - Reverse bias (ohms)	R_S - Forward bias (ohms)
Zener diodes	1.0	0.1
Signal diodes	25	0.25
Rectifier diode	150	0.05
Low power transistor (e-b)	10	1.0
High power transistor (e-b)	2	0.2

TABLE 6.5. Summary of IC thresholds by category.

Category				V_{BD}	R_S	Lower 95%	Upper 95%
Family	Terminal	A	B	(V)	(ohms)	A	A
TTL	Input	0.00216	0.689	7	16	0.00052	0.00896
	Output	0.00359	0.722	15	2.4	0.00098	0.013
RTL	Input	0.554	0.384	6	40	0.12	2.6
	Output	0.0594	0.508	5	18.9	0.0096	0.39
	Power	0.0875	0.555	5	20.8	0.026	0.70
DTL	Input	0.0137	0.580	7	25.2	0.0046	0.041
	Output	0.0040	0.706	1	15.8	0.0012	0.0136
	Power	0.0393	0.576	1	30.6	0.009	0.17
ECL	Input	0.152	0.441	20	15.7	0.045	0.51
	Output	0.0348	0.558	0.7	7.8	0.0031	0.397
	Power	0.456	0.493	0.7	8.9	0.22	0.935
MOS	Input	0.0546	0.483	30	9.2	0.0063	0.47
	Output	0.0014	0.819	0.6	11.6	0.00042	0.0046
	Power	0.105	0.543	3	10.4	0.038	0.29
Linear	Input	0.0743	0.509	7	13.2	0.0054	1.01
	Output	0.0139	0.714	7	5.5	0.0045	0.043

approximation for the damped sine wave with Q = 24, at t = $\frac{1}{2.25f}$.
Still another source[17] does not give an equivalent, but suggests that if both voltage and current are obtained by some means and instaneous power is calculated, then an equivalent square pulse is constructed from the dominant peak in the instantaneous power response. The maximum amplitude of this peak and the width of the peak at the half-amplitude points are then compared to a conventional damage threshold power vs pulse width. (An equavalence of this type was also need for an experiment performed on the LLL Transient Range for nanosecond pulse widths. Refer to Appendix I.)

6.5 CONCLUSIONS AND RECOMMENDATIONS

6.5.1 Conclusions

There are considerable data on the variations in failure constants of collective semiconductor devices. The grouping, display, and analysis of such data are provided in the published work surveyed. Ongoing work is paying more attention to statistical properties of failure levels, particularly in variations from manufacturers.

With one or two exceptions, there is little statistical data on the failure variation of individual device types. Small samples are typical; and there is expressed concern about variations when safety margins are as low as 10 dB.

Test methods seem to preclude any surprises or anomalies due to automated step-stressing procedures and decisions on lower threshold directions. Considerable engineering judgement is necessary. Integrated circuit failures are not obvious. Parameters are not measured by test sets before and after testing.

6.5.2 Recommendations

Examine subsystem assessment methodology with view to application of statistically based failure models and data for components.

Relate the methods of circuit analysis, as the capability exists in modern network and system codes, to the failure level assessment of subsystems. Code NET2, Version 9.1 has potential for Monte Carlo simulation studies. Use existing subsystem assessment for comparative applications.

Continue a review of uncertainties and confidence methods as they pertain to component failure distributions and models. Spot check published failure data for a few selected components to see if other failure modes exhibit lower than expected levels.

Examine the problem of subsystem specification development and its effect on subsystem assessment uncertainties.

6.6 REFERENCES

1. R. L. Huffman and D. W. Coleman, Final Report, EMP Characterization of Sprint Autopilot Components, Martin Marietta Corp., CREG 69-2 (September 1969).

2. Vulnerability Assessment and Hardening of AABNCP Electronic System Detailed Program Plan, TRW Systems Group, Air Force Weapons Laboratory, Contract F29601-74-C-5 (July 1974) (Appendix B).

3. Advanced Airborne Command Post GFE Assessment Program Executive Summary Report ,TRW Systems Group, Redondo Beach, CA, Air Force Weapons Laboratory Contract F29601-74-C-0035 (December 15, 1975).

4. DNA EMP (Electromagnetic Pulse) Handbook (U), Defense Nuclear Agency, Washington, D.C., DNA 2114H (1974) (title U, report CRD).

5. R. L. Williams, Semiconductor Device Damage Assessment for the INCA Program--A Probabilistic Approach, Harry Diamond Laboratories, Adelphi, MD, HDL-TR-1833 (March 1978).

6. D. M. Tasca and S. J. Stokes, III, EMP Response and Damage Modeling of Diodes, Junction Field Effect Transistor Testing and Semiconductor Device Failure Analysis, General Electric Co., Space Division, Philadelphia, PA, Harry Diamond Laboratories Contract DAA G39-74-C-0090, Defense Nuclear Agency Subtask R99AQXEB097, HDL-CR-86-090-1 (April 1976).

7. EMP Susceptibility of Semiconductor Components, The Boeing Aerospace Company (in cooperation with Braddock, Dunn, and McDonald, Inc.) (September 1974), Air Force Weapons Laboratory, AFWL-TR-74-280; also, Addendum, 1978.

8. Hugh B. O'Donnell and Dante M. Tasca, Development of High Level Electrical Stress Failure Threshold and Prediction Model for Small Scale Junction Integrated Circuits, General Electric Co., Department of the Army, Harry Diamond Laboratories Contract No. DAAG39-76-C (September, 1977).

9. D. W. Egelkrout, Component Burnout Hardness Assurance Safety Margins and Failure Probability Distribution Models, IEEE Annual Conf. on Nuclear and Space Radiation Effects, Albuquerque, NM (July 18-21, 1978).

10. B. M. Kalab, Damage Characterization of Semiconductor Devices for the AN/TRC-145 EMP Study, Harry Diamond Laboratories, Adelphia, MD, (Draft Report - 1978).

11. J. R. Miletta, Component Damage from Electromagnetic Pulse (EMP) Induced Transient, Harry Diamond Laboratories, Adelphi, MD, HDL-TM-77-22 (October 1977).

12. N. Kusnezov and D. L. Crowther, Current Injection Testing of Selected Integrated Circuits, Lockheed Palo Alto Research Laboratory, Palo Alto, CA. LMSC-D506527, U.S. Navy Contract N00030-74-C-0100 (August 1976).

13. Bibliography for Electrical Overstress Review, BDM Corp., Albuquerque, NM, DNA 4146T (October 10, 1976).

14. Bibliography of Breakdown Effects in Semiconductors, BDM Corp., Alburquerque, NM, DNA 4285T (August 8, 1977).

15. Vulnerability Assessment and Hardening of Advanced Airborne Command Post (AABNCP) Electronic System, Detailed Program Plan, TRW document No. 25715.00, CRDL A018 (July 1974).

16. EC-135 EMP Assessment Program Final Assessment Report, Vol. III, Assessment Error Analysis, Rockwell International Autonetics Div., Anaheim, CA, C77-1022.3/201, Air Force Weapons Laboratory Contract F29601-75-C-0103 (November 4, 1977).

17. L. W. Ricketts, J. E. Bridges, and J. Miletta, EMP Radiation and Protective Techniques, (John Wiley and Sons, New York, 1976).

6.7 BIBLIOGRAPHY

1. Aeronautical Systems EMP Technology Review, The Boeing Co., Seattle, WA, April 1972, AFWL-TR-73-118 (AD 913 267L).

2. AFWL-TR-65-3 Add. 1, Vulnerability Assessment for UHF Communications Subsystem ARR-71/ART-47. Addendum 1, Detailed Upset Analysis. TRW Systems Group, Redondo Beach, CA, AD-C010 1266.

3. Clark, O. Melville, Development of Disc TranzZorb for TPD Applications in EMP Suppression, General Semiconductor Industries, Tempe, AZ, Final Report, Contract No. DAAG39-73-C-0143 (April 1974).

4. Design Guidelines for Hardening of Aeronautical Systems, Autonetics, Anaheim, CA, July 1973, AFWL-TR-73-117, (AD 912 389L).

5. DNA EMP Awareness Course Notes, Defense Nuclear Agency, DNA 2772T, August 1973 (AD 769 781).

6. Electromagnetic Pulse Handbook for Missiles and Aircraft in Flight, Sandia Laboratories, Albuquerque, NM, September 1972, AFWL-TR-73-68 (AD 919395L).

7. EMP Electronic Design Handbook, The Boeing Company, (in cooperation with Braddock, Dunn, and McDonald, Inc.), Seattle, WA, April 1973, AFWL-TR-74-58, (AD 918 227L).

8. EMP Hardening of GFE, The Boeing Company (in cooperation with Braddock, Dunn, and McDonald, Inc.), Seattle, WA, July 1973, AFWL-TR-74-61, (AD 918 275L).

9. EMP Preferred Test Procedures (Selected Electronic Parts,) IT Research Institute, Chicago, IL August 1974, (AD 787 482).

10. Engineering Design Guidelines for EMP Hardening of NAVAL Missiles and Airplanes, Mission Research Corporation, Albuquerque, NM, December 1973, (AD 917 958L).

11. Engineering Techniques for Electromagnetic Pulse Hardness Testing, SRI International, Menlo Park, CA, DNA 3332F, September 1974, (AD 786 7222).

12. Hampel, D. and R. G. Stewart, EMP Hardened CMOS Circuits, RCA Advanced Communications Laboratory, Somerville, NJ, Final Report, Contract No. DAAG39-73-C-0254 (January 1975).

13. Hart, W. C. and Daniel F. Higgins, A Guide to the Use of Spark Gaps for Electromagnetic Pulse (EMP) Protection, Joslyn Electronic Systems, Goleta, CA (1973).

14. Kreck, J. A., Actual Operating Characteristics of Three Terminal Protection Devices Applied to the AN/PRC-77 Field Radio, Harry Diamond Laboratories, Aldelphi, MD, HDL-TR-1826 (December 1977).

15. Lutzky, M., E. B. Dean, Jr., and M. C. Petree, "Modeling Second Breakdown in PN Junctions with ENT-2," IEEE Transactions on Nuclear Science, Vol. NS-22, No. 6, December 1975.

16. Olson, H. M., "DC Thermal Model of Semiconductor Device Produces Current Filaments as Stable Current Distributions," IEEE Transactions on Electron Devices, Vol. ED-24, No. 9, September 1977.

17. Pease, R. L., D. R. Alexander, and C. R. Jenkins, Electrical Overstress Program and Integrated Circuit Failure Mode Evaluation, the BDM Corp., Albuquerque, NM, Defense Nuclear Agency Report DNA 4467F (April 26, 1976).

18. Principles and Techniques of Radiation Harding, Vol. 3, Electromagnetic Pulse (EMP) and System Generated EMP, N. J. Rudie, Western Periodicals Co., No. Hollywood, CA (1976).

19. Randall, R. N., P. A. Young and D. R. Alexander, "HANAP2: An Important New Dimension in EMP Damage Assessment," Abstracts of Technical Papers, NEM 1978 Record, Nuclear EMP Meeting, Albuquerque, NM, June 6-8, 1978.

20. Smith, J. S., "Electrical Overstress Failure Analysis in Microcircuits," 16th Reliability Physics Proceedings, April 18-20 1978, San Diego, pp. 41-46.

21. Stark, W. J. and G. H. Baker, EMP Analysis of an FM Communications Radio with a Long-Wire Antenna, Harry Diamond Laboratories, Woodbridge, VA, HDL-TR-1846 (June 1978).

22. Survivability Design Guide for U.S. Army Aircraft Nuclear Hardening, Los Angeles Aircraft Division Rockwell International Corporation, August 1974, Eustis Directorate, U. S. Army Air Mobility Research and Development Center, USAAMRDL-TR-74-48A, (ADB000299L).

23. Susceptibility of Point-Contact Diodes to One Nanosecond X-Band Pulses, IKOR Inc., Burlington, MA, Naval Weapons Laboratory Contract N00173-71-M-1408, Report No. TR 0167 (January 1971).

24. Tasca, Dante M. and Joseph C. Penden, EMP Surge Suppression Connectors Utilizing Metal Oxide Varistors, Harry Diamond Laboratories, Adelphi, MD, TR-179-1 (August 1974).

25. Williams, Robert L. Jr., Test Procedures for Evaluating Terminal Protection Devices Used in EMP Applications, Harry Diamond Laboratories, Adelphi, MD, TR-1709 (June 1975).

7. PROTECTION AND HARDENING

7.1 INTRODUCTION

There are many general techniques to use in the protection or hardening of systems. These are well known in principle. It is in the details of specific systems and specific data that questions of uncertainty will arise. There appears to be very little discussion of quantitative uncertainties in the protection literature. Much of the protection design is oriented toward reducing the EMP-induced signal to such a value that it becomes (theoretically) insignificant. This cannot always be done. It would be of interest to associate the effect of protection designs with the necessary safety margins and considerations of variability throughout the life cycle of the system.

In this secton there is a brief review of the protection techniques in Section 7.2, a discussion of uncertainties in Section 7.3, a review of some past work with references in Section 7.4, and conclusions and recommendations in Section 7.5.

7.2 REVIEW OF PROTECTION OR HARDENING TECHNIQUES

The general objective in a protection scheme is to reflect, divert, or absorb somehow the interfering electromagnetic energy, induced in a system by the EMP, away from the vulnerable parts of the system. It is also possible to protect a system through a circumvention scheme and also by the use of components in the system which are not affected by EMP, such as optical signal transmission systems.

The following is a list of some general techniques.

- Shielding practices.

- Amplitude and spectrum limiting.
- Circumvention and disconnects.
- Coding of signals.
- Microwave or optical transmission.
- Component selection.
- System layout practices.
- Cabling and connecting practices.

Much protection design is frequently centered around taking advantage of and/or supplementing existing EMP practices as well as other inherent protective features, such as shielding.

As stated above, a protection approach usually deals with reflection, diversion, or absorption of energy from the EMP. The selection of out-of-band or non-hard-wired components such as fiber optics, microwave links, or other non-susceptible components may be attractive from the EMP viewpoint, but other factors may void their use. Circumvention is a somewhat specialized technique, but some variations may be possible in the operational sense. Thus, an operator/detector either live or robotic, can take effective action against EMP under suitable conditions. In certain situations it may be possible to perform coding of signals so as to ignore an EMP transient which may be present in the channel.

A protection approach can, and usually will include one or more of the above techniques either singly or in combination. Thus, the protection problem does not typically have a unique solution, but instead is one which does involve a great amount of trade-off and engineering decision making.

7.3 UNCERTAINTIES IN PROTECTION

7.3.1 Systems Viewpoint on Protection

Various approaches are possible. Techniques will vary with the matrices of possible designs of systems. Tradeoff factors such as weight, cost of retrofit, cost of materials (as shielding), complexity (reliability issues), testing, verification, and perhaps simple availability influence decisions.

It would appear best to discuss uncertainty as associated with different possible approaches to protection; then it could also be a tradeoff factor. Uncertainty in exactly what is the level of protection or the margin of protection will force design decisions to be more conservative. This may increase dollar cost significantly. Confidence in hardening should be increased also, but criteria for this evaluation may not be available.

Protection from the EMP involves little drastically new technology from the techniques standpoint. Shielding technology is old, but the transient response viewpoint is new. Large-scale performance measures of shielding effectiveness do not exist. The nearest thing is an EMP simulation test.

From the systems viewpoint, uncertainties in protection will occur at all levels. The assessment, system hardening or protection engineer who must incorporate a regime of protection will be faced with the following actions:

1. Understanding the mission and defining the threat and overall system survivability requirements. (All of these factors can drastically influence the system protection scheme.)

2. Defining the survivable elements of the system as a function of the threat to it.
   Example: Close-in threat and high-altitude threat on Army equipment.

3. Defining or establishing the type and extent of protection, the threat environment throughout, and associating or locating the survivable elements with respect to the protection elements (or vice-versa).
   Example: If enclosing shielding is used, its extent must be specified and the threat at the shield must be know.

4. Establishing the hardening requirements at various sublevels within the system.
   Example: Given the location of a shield, establish protection requirements in terms of voltage and current at electrical projections beyond this shield.

5. Developing the subsystem requirements.
   Examples: Given a set of voltages and currents at points within a system, develop an interface specification for an electronic subsystem.

Steps 3, 4, and 5 may require a great deal of iteration, particularly if the system protection scheme is not very easily established either by design or by other considerations. Thus, if an airplane has essentially an all-enclosing shield from the airframe, the majority of the work would be in taking advantage of this inherent protective feature to come up with hardening requirements to supplement this feature in the interior.

7.3.2 Shielding

Shields enclosing circuits will substantially reduce the EMP-induced signals. Thickness is not necessarily a limiting issue, but construction details and imperfections, defects, or necessary apertures are. Conductors which penetrate an all-enclosing shield must be treated such that, to be consistent, they will produce no more energy into the interior than a continuous shield would.

In practice all the imperfections, apertures, and penetrations cause shielding degradation below that of a uniform envelopes shield. It is in the methods of evaluating this degradation and relating to the transients in circuits that considerable uncertainty prevails.

The usual shielding calculations assume an infinitely large plane sheet and the incident EMP field has a reflected component and a transmitted component. Losses in the material are accounted for by an absorption coefficient. The application of planar theory to three-dimensional objects is a source of uncertainty.

Another source of error is in the use of loops and dipoles to create "plane waves" to measure shielding effectiveness. EMP is a plane wave which can incident in many directons to a three-dimensional object and excites the entire system.

It is also possible to introduce error by relating strictly the current on the exterior of a shield to the current on an interior conductor as a measure of shielding effectiveness ($20 \log(I_1/I_2)$)

Madle discusses many of the above problems in Ref. 1.

7.3.3 Shielding Uncertainties

- Overall shielding specification and testing.
- Effects of imperfections/defects within shield.
- Composite materials effects.
- Planar theory of shielding.
- Measurements based on dipoles and loops.
- Closures of apertures.

7.3.4 Amplitude and Spectrum Limiting

Uncertainties in prediction of EMP response levels are introduced when the simulation response levels are so high as to introduce limiting of the temporal signals and/or limiting in the spectrum analyzers. Either effect tends to reduce the predicted EMP response levels.

7.3.5 Terminal Protection Devices (TPD)

These are included in the entire class of inline devices which can reflect, absorb, and/or shunt the conducted EMP-induced transients. Included in this class are such devices as:

- Spark gaps.
- Zener diodes.
- Avalanche transient suppressors.
- Metal oxide varistors.
- Step-recovery diodes.
- Filters.

Within the limited extent of this task, very little information was obtained on the overall uncertainty of TPD protection levels. As used in assessment, one of the key ingredients is to have a model of the surrounding circuitry. The TPD must be compatible with the operation of the remainder of the circuitry. As the TPD is a device which is inserted inline at a terminal, and which can either reflect, absorb, or shunt a conducted EMP transient, there are several parameters at play: reaction time, switching time, threshold level, energy dissipation, and reflection coefficient are important. Insertion loss of the TPD in a standby condition is a factor in many applications. The inherent hardness of the TPD itself is important also.

A difficult modeling task is to represent a highly nonlinear gas gap in such a way that it can be used with models of the associated circuitry and

inputs for reponse calculations. Although the device characteristics seem to be well-controlled, the lack of adequate representation will create errors in assessment. The following is a review of a source of work which has presented comparisons of experimental and calculated outputs from models of three types of TPDs.

Three types of protective devices are modeled and analyzed in the referenced report by Kreck.[2] There appears to be reasonably good comparison of the computer predictions with the experimental results. The devices are step-recovery diode, spark gap, and zener diode. The models are used in conjunction with the TRAC computer code. Numerical or other problems were experienced with TRAC models without modifications such as dc bias in parallel diodes. The back-to-back zener diodes also presented a problem; it was necessary to use a biased zener diode model. The spark-gap model is one that was developed to be used with TRAC. This model is unique and involves a special subroutine, which includes the complex phenomena in the action of a gas gap responding to transient inputs. This is highly nonlinear phenomena.

The essential accuracy of the models as used in actual protection applications is presented with comparative plots. Quantitatively, the amplitudes agree to $\pm$20%, indicated to be the greatest reasonable accuracy for the type of work. Figures 7.1, 7.2, and 7.3 show the characteristics, and representative comparative outputs of models taken from the Kreck work.[2]

7.4 REVIEW OF PAST WORK

In review of the subject of hardening of systems, the following appear to have been addressed at one level or another.

- Pershing system.
- Minuteman system.
  - Missile.
  - Ground system.

- Civil defense systems.
- Patriot system.
- B-1 aircraft.
- E-3A airborne warning and control system aircraft.
- PRC-77 radio.
- Lance missile system.
- Safeguard ABM system.
  - Radar Buildings.
  - Facilities.
  - Missiles.
- AABNCP (Advanced Airborne Command Post Aircraft).
- XM-1 tank.
- Other Army, Navy, and Air Force Systems.

The above represents quite a bulk of work, even in the available literature. It is not possible to discuss uncertainties system by system. In Appendix J, some reports are reviewed which deal with two main protection methods, shielding and terminal protection devices. There appears to be almost no literature dealing with uncertainty in protection methods and devices, although safety margins are frequently given in the test reports.

7.5 CONCLUSIONS AND RECOMMENDATIONS

7.5.1 Conclusions

There was relatively limited attention given in this study to reviewing all areas of protection. Several reports were examined and very little discussion of errors and uncertainty was noted.

Shielding is a major protection method, yet little is known about the response of large- or full-scale, three-dimensional shielding systems which relate to practice in design. Imperfections seem to dominate and introduce uncertainties in the expected performance.

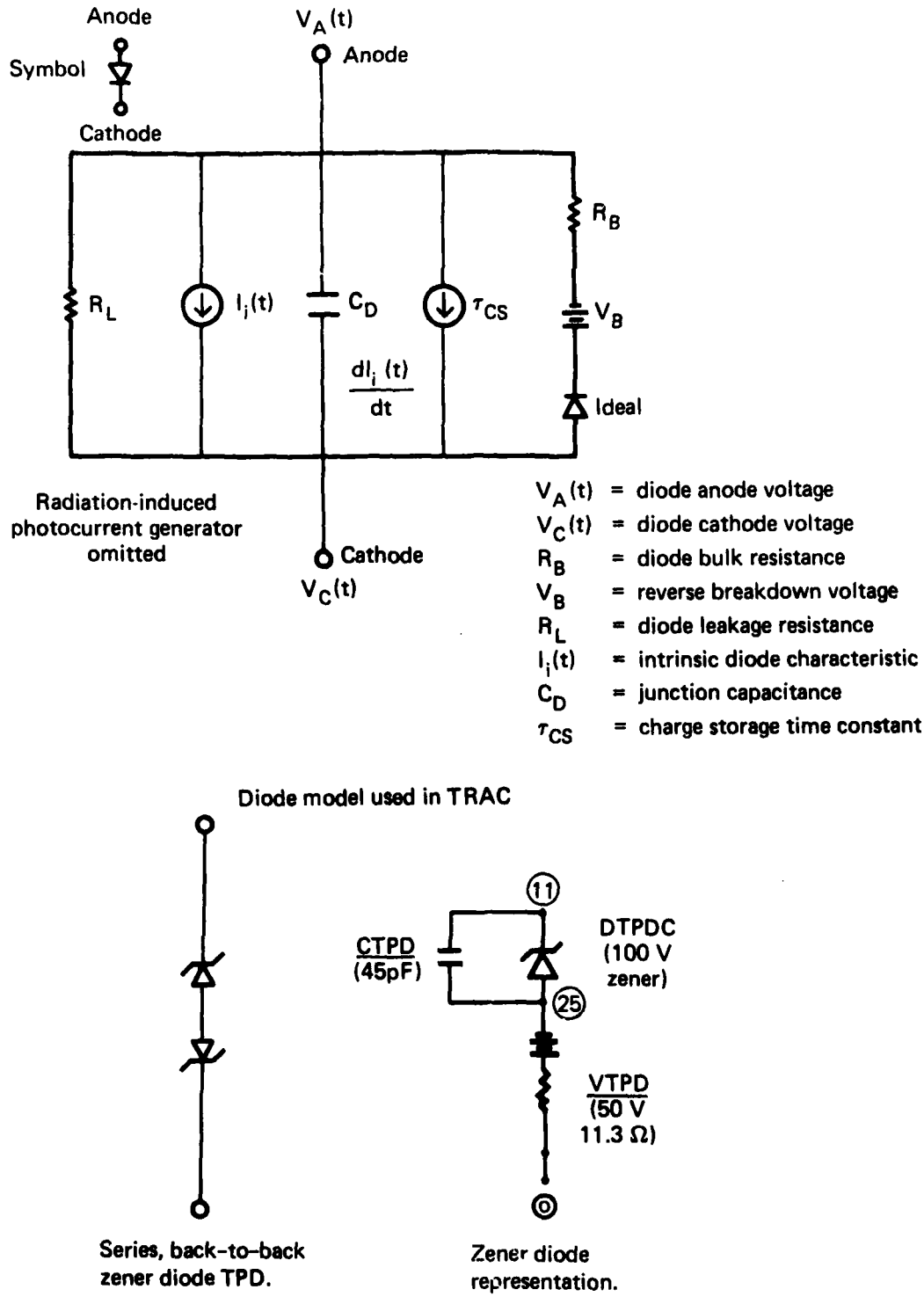

FIG. 7.1. Protection device models.

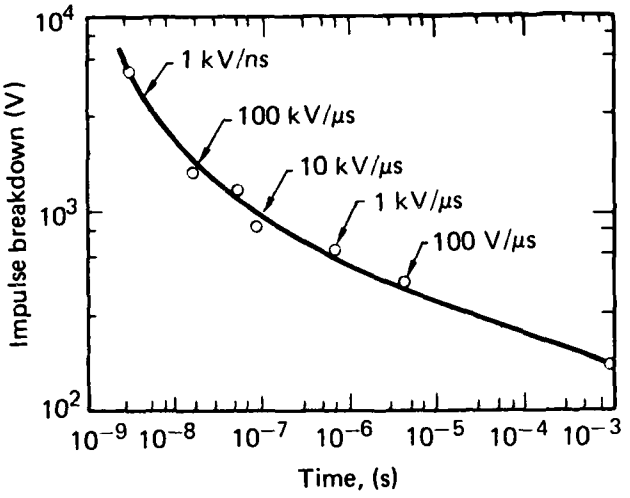

Rate of rise	Range of breakdown	Average breakdown
dc	170-190	180
100 V/μs	290-980	470
1 kV/μs	430-1100	652
10 kV/μs	690-1190	865
75 kV/μs	1100-1700	1419
100 kV/μs	1450-1800	1625
1.9 kV/ns	3.8 kV at 1 kV/ns 7.8 at 1.9	5200

(a) Volt-time curve of one type of spark gap. (Adapted from Hart and Higgins, Joslyn Electronic Systems, Goleta, CA, 1973.)

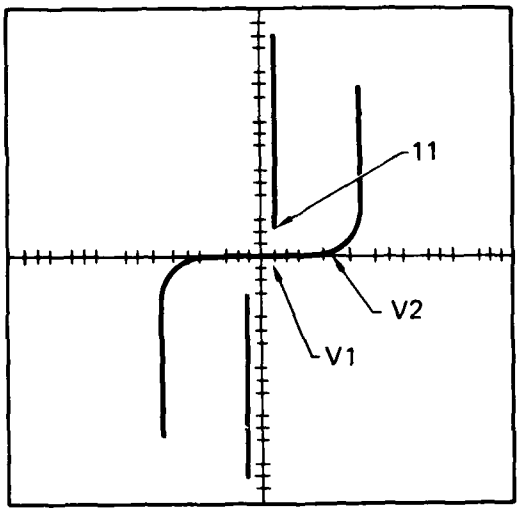

V = Maximum expected dc bias voltage
V1 = Arching voltage
V2 = Glow voltage
11 = Minimum clampinge current
500 mA/division vertical
500 Volts/division, horizontal

(b) Curve trace of spark gap.

FIG. 7.2. Characteristics of spark gaps.

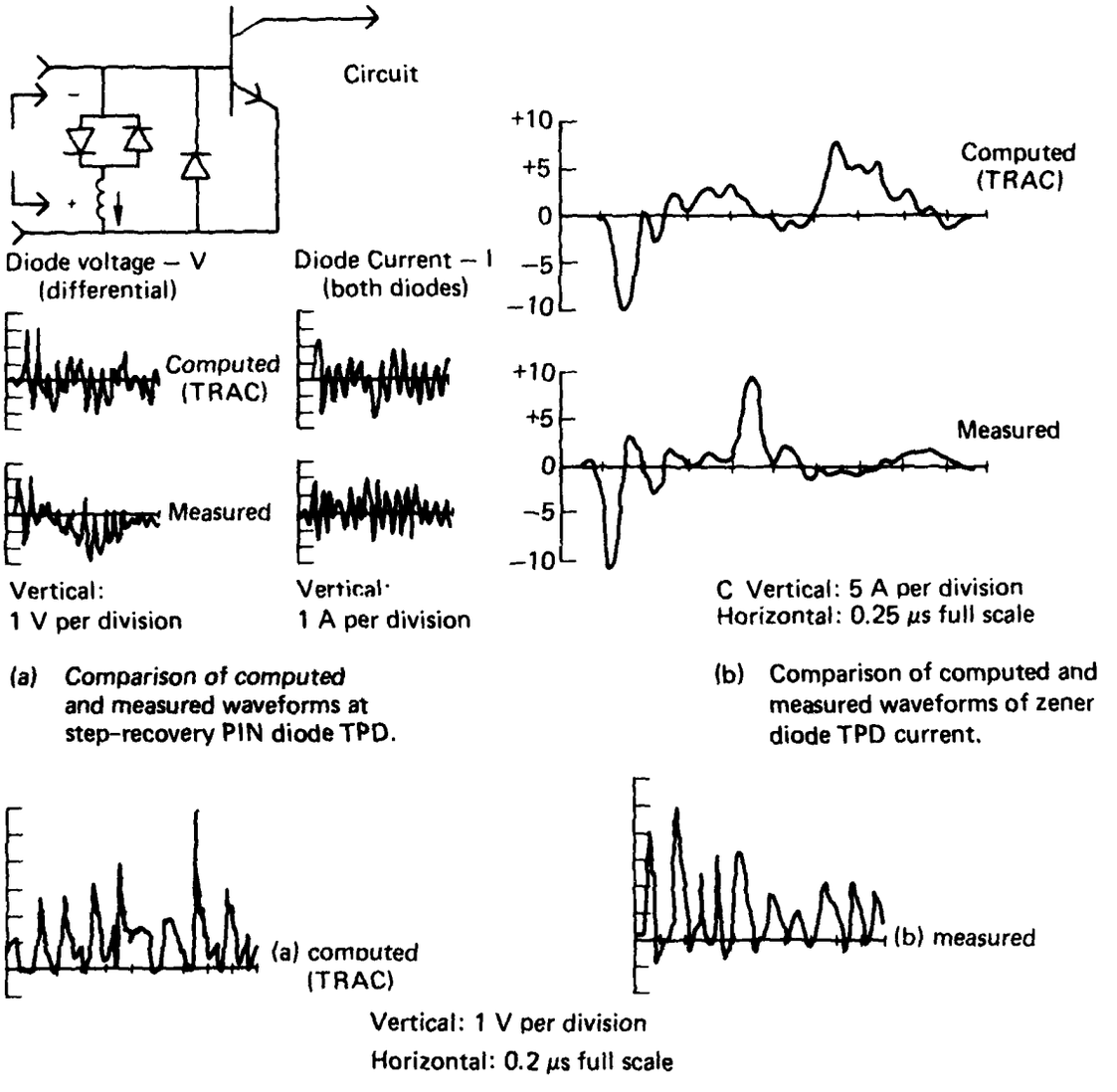

(a) Comparison of computed and measured waveforms at step-recovery PIN diode TPD.

(b) Comparison of computed and measured waveforms of zener diode TPD current.

(c) Comparison of computed and measured waveforms at base of first rf amplifier, spark gap TPD.

FIG. 7.3. Comparisons of computed and measured values.

Terminal protecton devices (TPD) are also a major protection method, yet only recently has a model been developed for the spark gap that appears suitable for computer application. Most semiconductor devices which are designed to handle transient overloads do have well-controlled clamping voltages for a range of input current; a zener regulating diode may not have. The greatest uncertainty would appear to be in how a device is used in conjunction with the surrounding circuitry. This relates to the general problem of knowledge of configuration, the model, and the inputs and terminations.

7.5.2 Recommendations

Examine several protection schemes, from existing systems if possible, to see if major uncertainties can be identified as reflected in those systems. This is the basic problem which demands continued attention in order to avoid poor system designs. Questions of adequacy and validation may not be answered to satisfaction and judgemental decisions are necessary. Life characteristics also enter in.

Terminal protection device characteristics: Do work on models of devices to demonstrate effect of model paramters on typical criteria that a TPD must meet. Uncertainties in protective features can then be related to device parameters which presumably can be controlled in design and manufacturing.

Additional review of specific protection methods is needed. Shielding is much too large a technological area for small uncertainties effort to review, but definitely work is needed in specifying and measuring properties of shields as used in systems.

7.6 REFERENCES

1. P. J. Madle, "Introduction to Field Penetration," in IEEE 1978 Intern. Symp. on Electromagnetic Compatibility (Atlanta, GA, 1958), pp. 82-85.

2. J. A. Kreck, Actual Operating Characteristics of Three Terminal Protection Devices Applied to the AN/PRC-77 Field Radio, Harry Diamond Laboratories, Woodbridge, VA, HDL-TR-1826 (December 1977).

8. VALIDATION OF PROBABILISTIC ANALYSIS

8.1 INTRODUCTION

The importance of incorporating errors and uncertainties into the vulnerability assessment analysis has been stressed throughout this study. Thus, it was considered essential that early in the study some limited demonstration of the capabilities of a method which includes errors be performed in conjunction with a real-world example. In particular, an experiment was performed to demonstrate the capabilities of the FAST code. The simple system selected for this experiment consisted basically of a 1N23B diode connected to a monopole antenna.

In principle, the experiment was designed to use statistical information available from previously derived sources as input into the FAST code. The results from the FAST code were to be compared with test results derived from testing the system on the Electromagnetic Transient Range at LLL. Thus, the system test would substantiate and demonstrate the capabilities of FAST.

In practice, damage statistics on the diode were not available and had to be obtained separately in the laboratory under similar operating conditions. Diodes from the same general group were used for evaluating damage statistics as well as for the system test.

8.2 TEST DESCRIPTION

To demonstrate the applicability of FAST to predict the failure of a "real life" circuit, we selected a very simple electrical network--a diode load connected to a monopole antenna, as shown in Fig. 8.1, and then tested this system at the LLL Transient Electromagnetics Range.[1]

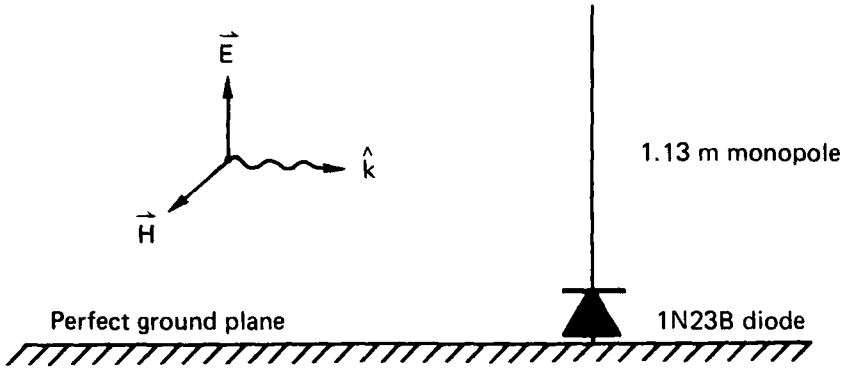

FIG. 8.1. Measurement configuration on the LLL Transient Electromagnetics Range.

This circuit, while admittedly simple in form, embodies all the elements of FAST. The device burnout is specified by the diode fragility curves, and the environment appears as the incident electric field, while the network transfer function is used to relate the incident field level to the energy collected by the monopole antenna and delivered to the diode load. The monopole/diode circuit was selected because it represents a network which could be tested to failure in the laboratory and analyzed with available tools.

The actual FAST tests were performed in two parts. First the input data for FAST were obtained through a combination of experiments in the laboratory and numerical calculations (details of which are given in Section 8.3 below). We then used FAST to predict the overall system probability of failure as a function of the environment stress.

Next, in order to validate these FAST predictions, we then performed an overall system test. The test configuration, shown in Fig. 8.2, is the way

the circuit was tested on the LLL Transient Electromagnetics Range. In this setup, a 5-ns pulse generated by the mercury pulser is sent to the monocone pulse antenna. The monocone is a very wide bandwidth antenna, and it radiates an electromagnetic (EM) pulse of much the same shape and form as the voltage pulse applied to its feed. The pulse radiates from the base of the cone and propagates out and away from the cone, reaching the 1.13-m monopole in 8 ns. The monopole in turn responds to the incident electromagnetic field, and sends a pulse down the 10-ns feed-line to the diode fixture containing the 1N23B diode. If the amplitude of the pulse sent to the diode load is sufficiently large, the diode will burn out; if not, the diode will survive. In each of the tests performed, only one pulse was sent to the diode load, and each of the diodes was used only once.

At each level of the environmental stress, the incident electromagnetic field in this case, FAST predicts the probability of system failure. Our experiment thus consisted of selecting a level of stress or EM field intensity which is obtainable by adjusting the amplitude of the mercury pulser. At this fixed field intensity, a sample lot of 26 diodes was tested for failure, with failure defined in this case as a factor of 12 increase in the diode reverse leakage current. The above experiment was repeated for three different levels of field intensity, and the comparisons between the FAST predictions and the actual measurements are presented in Section 8.5

8.3 DETERMINATION OF INPUT DATA FOR FAST

8.3.1 Device Failure Data

To establish a statistical data base to characterize the 1N23B point contact microwave diode, we purchased 400 single-lot devices from Kemtron Electron Products Incorporated in Newburyport, Massachusetts, (Lot #117-11-E EDCO 12/77). A typical V-I curve for the 1N23B is shown in Fig. 8.3 The failure mechanism observed for the diode occurs when the junction becomes reverse biased and goes into a reverse breakdown mode. When this happens,

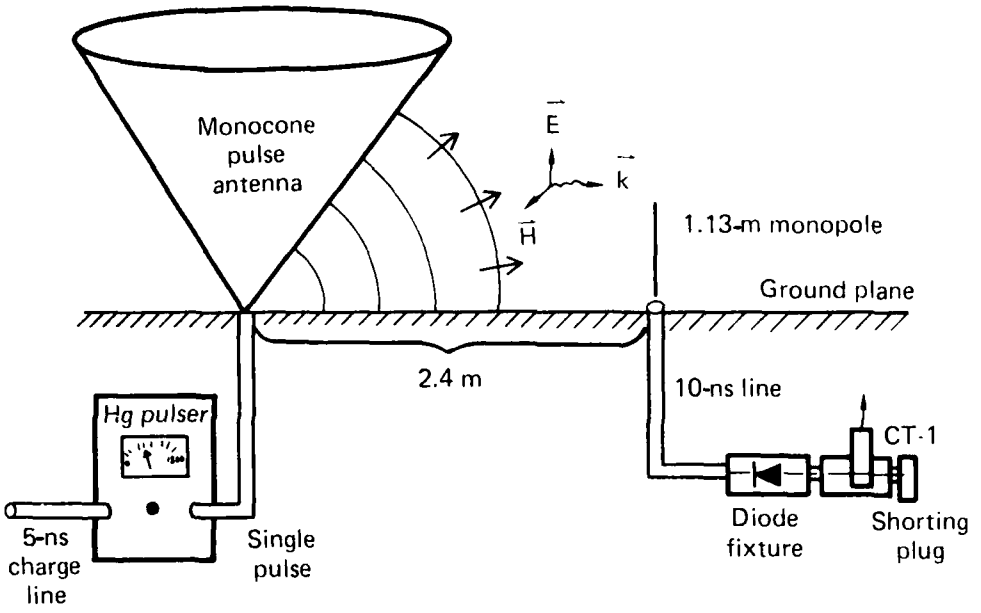

FIG. 8.2. Experimental setup for monopole/diode FAST tests.

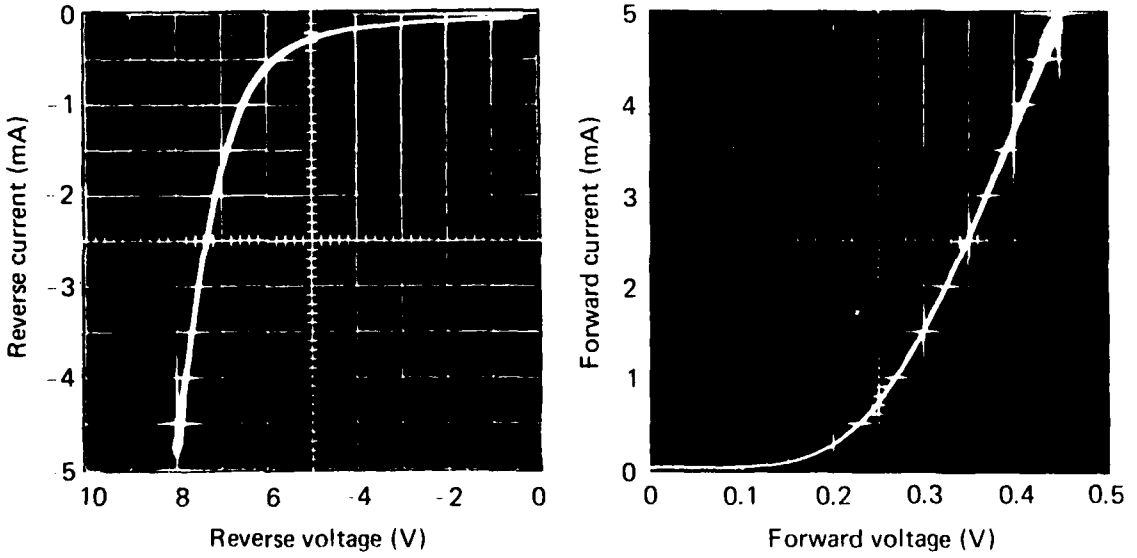

FIG. 8.3. Reverse and forward V-I characteristics of the 1N23B diode.

localized "hot-spots" appear, and the reverse leakage characteristics are permanently degraded. Thus our criterion for device failure is based upon the reverse leakage currents before and after stress.

To measure the reverse leakage currents, we built the standard measurement circuit shown in Fig. 8.4. Here a constant 1-V source is used to reverse bias the junction, and the resulting leakage current in microamperes is measured. All diodes were prescreened before stress testing, and the resulting distribution of leakage currents before testing is shown in Fig. 8.5 for a total sample of 234 devices. The mean leakage for this lot is 7.0 μA, with a standard deviation of 5.93 μA.

The burnout criterion we selected for our tests is based on the above measured statistics. If the diode reverse current exceeds by a factor of 12 the average leakage measured for the unstressed device, the device is considered to have failed, or in other words, if $I_{REV} > \mu 84$ A, then it has failed.

Because of the nature of the pulse durations and scale factors available on our Transient Range facility, we found it necessary to use short-pulse (5 ns) excitations for our FAST validation experiment. Unfortunately, little burnout data exists for the 1N23B diode in this short-pulse region, and thus we found it necessary to measure our own burnout data.

The techniques used to obtain the diode burnout data follow that of Stadler,[2] where the setup used is shown in Fig. 8.6. This circuit uses a mercury pulse generator with a 5-ns (2.5 ns long) charge line to generate a 5-ns-wide voltage pulse. The amplitude of the pulser is adjustable, and for each pulse amplitude, we can compute the energy delivered to the coaxial line leading to the diode load by the expression

$$E_{LINE} = \int_0^{T_P} \frac{V^2_P(t)}{Z_o} \, dt \quad ,$$

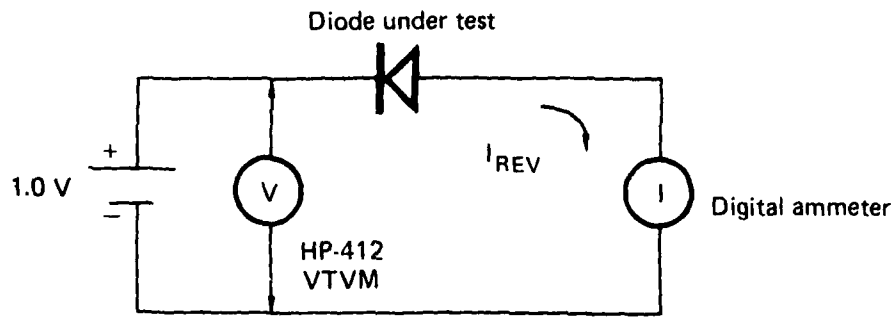

FIG. 8.4. Standard circuit for measuring diode reverse leakage currents.

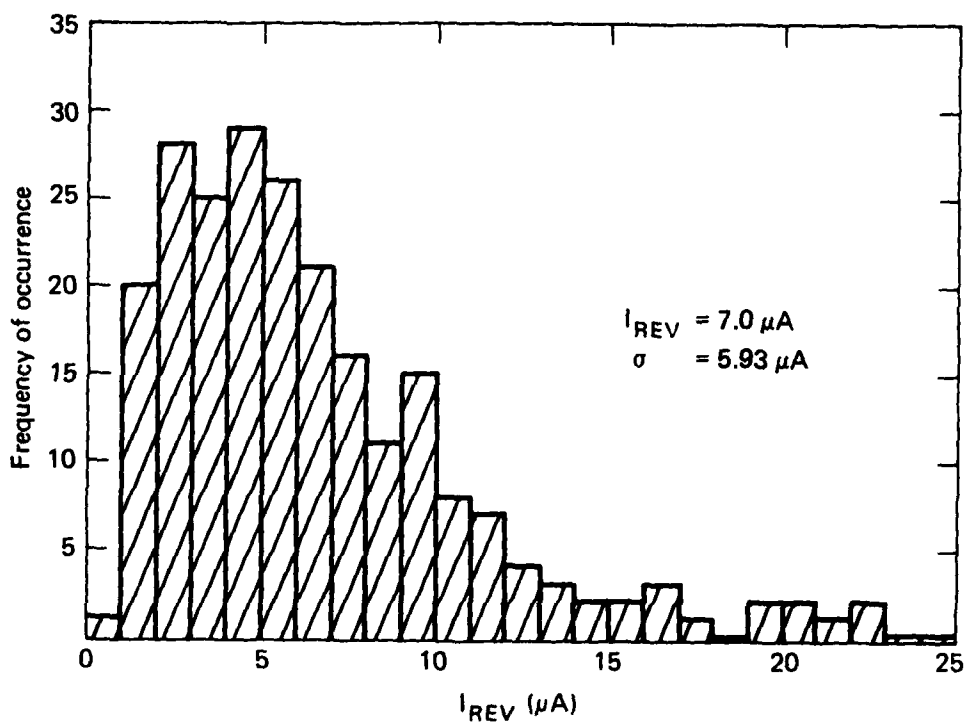

FIG. 8.5. Distribution of reverse leakage currents for 1N23B diode before stress testing (234 devices tested).

where T_p is the pulse width in seconds, V_p is the pulser voltage divided by 10 by the 10x attenuator, Z_0 is the transmission line impedance (50 Ω), and E_{LINE} is the energy delivered to the coaxial line, specified in joules. The CT-3 voltage pick off is used to monitor the voltage pulse going to the diode, and the CT-1 current probe was used to monitor the current through the diode, leading to the shorting plug. The diode itself also fits into a coaxial fixture to minimize stray capacitance and inductance. It should be noted that the 10x attenuator is used to diminish reflected pulses between the diode load and the pulse generator.

The experimental design used to develop the fragility curve (cumulative distribution function) for input into FAST was based on the assumption that the failure energy level is approximately a lognormal random variable. An attempt was made to make sure that the fragility curve was estimated at minimally, the 10th, 40th, 60th, and 90th percentiles (corresponding to the points $\mu \pm 0.25\sigma$ and $\mu \pm 1.25\sigma$). Based on the lognormal distribution and some design information, the pulse voltage levels chosen were: 15, 30, 40, 45, 50, 60, 80, and 100 V. These voltages corresponded to incident pulse energies at the diode of 2.25×10^{-8}J, 9.0×10^{-8}J, 2.025×10^{-7}J, 3.5×10^{-7}J, 6.4×10^{-7}J and 1×10^{-6}J, respectively. Twenty-six diodes were tested at each voltage, except 80 V, where a second set of 26 was tested. Each diode was subjected to a single pulse and then was checked for failure. None of the diodes were reused. A summary of the results of these tests is given in Table 8.1.

Point and 90% confidence interval estimates for the probability of failure, $\hat{p}_f$, based on the formulas (n is the number of diodes tested)

$$\hat{p}_f = \frac{\text{number of diodes failing}}{n} ,$$

$$(\hat{p}_{f,l}, \hat{p}_{f,u}) = (\hat{p}_f \pm 1.64 \sqrt{\hat{p}_f(1-\hat{p}_f)}$$

are given in the last two columns of Table 8.1. Empiracal cumulative distribution functions based on these estimates are given in Fig. 8.7.

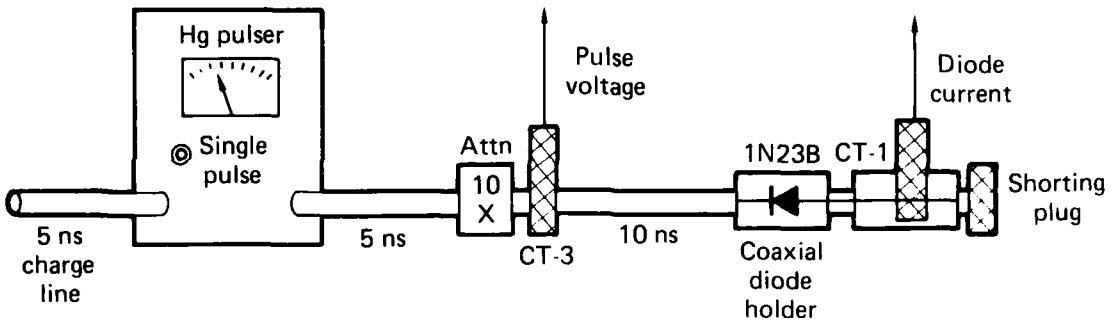

FIG. 8.6. Circuit used to obtain short-pulse diode burnout data.

TABLE 8.1. Summary of tests on the diodes.

Pulse voltage,[a] V	Energy, J	Number tested	Number failed[b]	Estimated probability of failure, p_f	90% confidence limits for probability of failure
15	2.25×10^{-8}	26	1	0.038	(0, 0.100)
30	9.0×10^{-8}	26	4	0.154	(0.038, 0.270)
40	1.6×10^{-7}	26	9	0.346	(0.195, 0.497)
45	2.025×10^{-7}	26	16	0.615	(0.459, 0.771
50	2.5×10^{-7}	26	18	0.692	(0.544, 0.849)
60	3.6×10^{-7}	26	19	0.731	(0.588, 0.874)
80	6.4×10^{-7}	52	44	0.827	(0.738, 0.916)
100	1.0×10^{-6}	26	25	0.962	(0.896, 1.0)

[a]Pulse voltage is the voltage into coaxial line leading to diode and is equal to the mercury pulser voltage divided by 10.

[b]Diode failure occurs if reverse leakage current exceeds 84 A.

Fragility curves to be used as input into FAST were developed to approximate the estimated cumulative distribution functions. These are given in Fig. 8.8 These represent the best estimate of the diode fragility based on the estimates p_f, and lower and upper limits on the fragility due to the systematic uncertainty of not knowing the true fragility curve but estimating it based on the test data.

8.3.2 Environment Data

The specification of the environment in the FAST calculations involves a description of the mercury pulser characteristics. Figure 8.9 shows a plot of 994 measurements of the amplitude of the nominal 600-V, 5-ns pulse used in this experiment. These amplitude measurements were made at a fixed point in time on the pulse, as shown in Fig. 8.10. Figure 8.11 shows the distribution of the amplitude of the pulse voltage. The plot of the measurements on

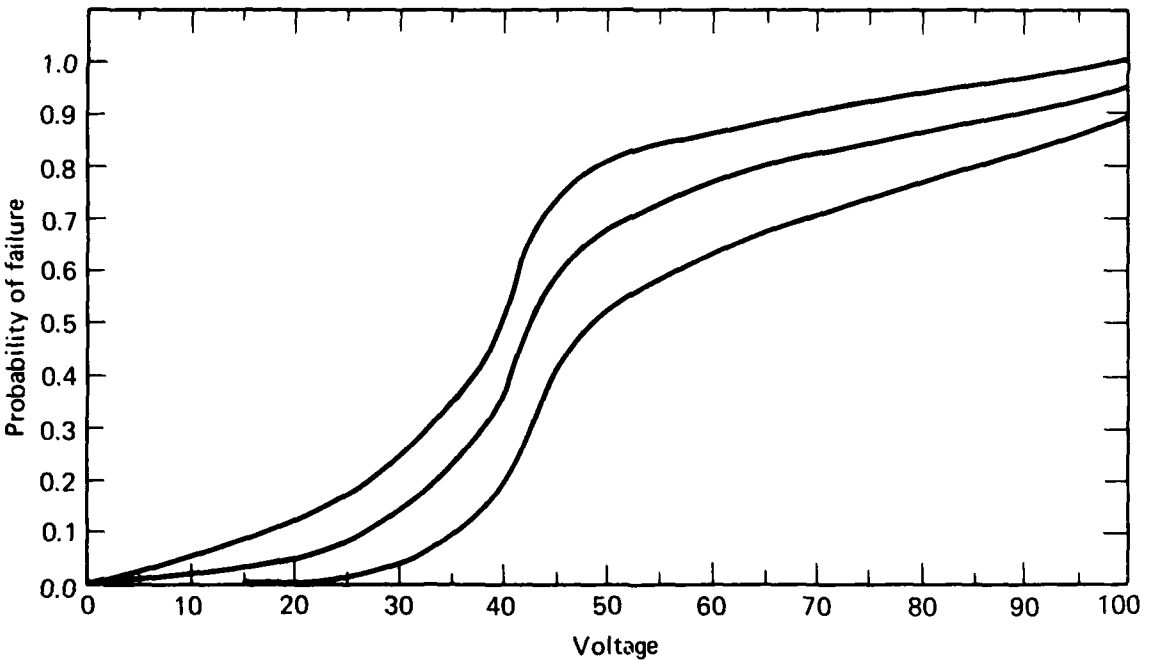

FIG. 8.7. Estimated failure distribution functions.

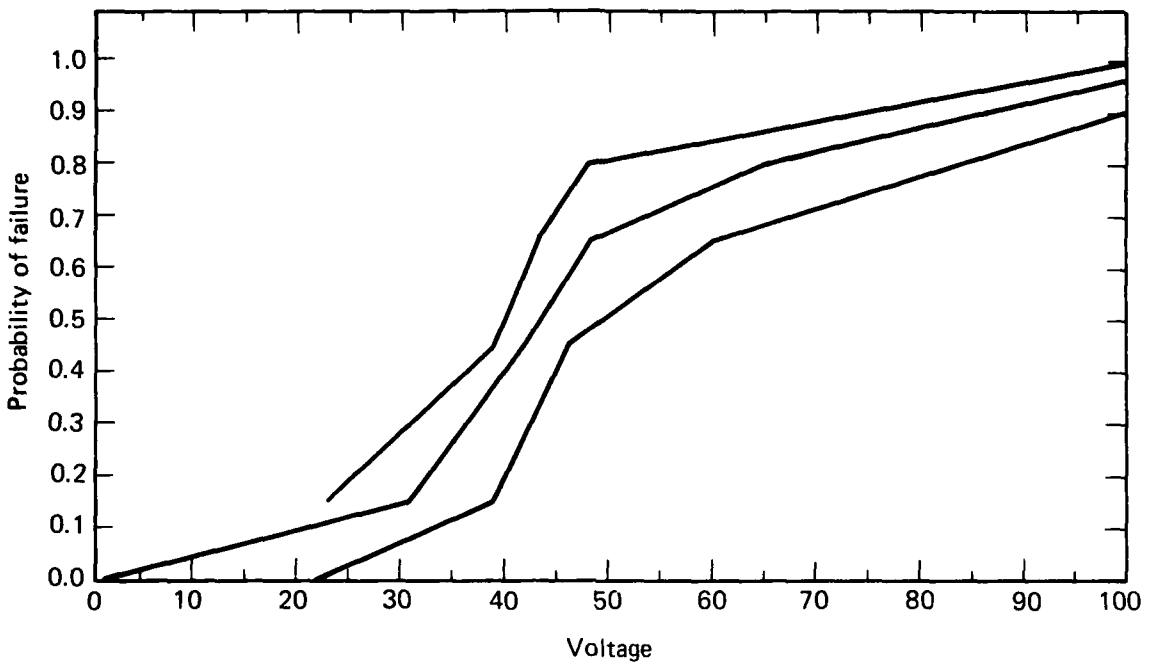

FIG. 8.8. FAST fragility curves.

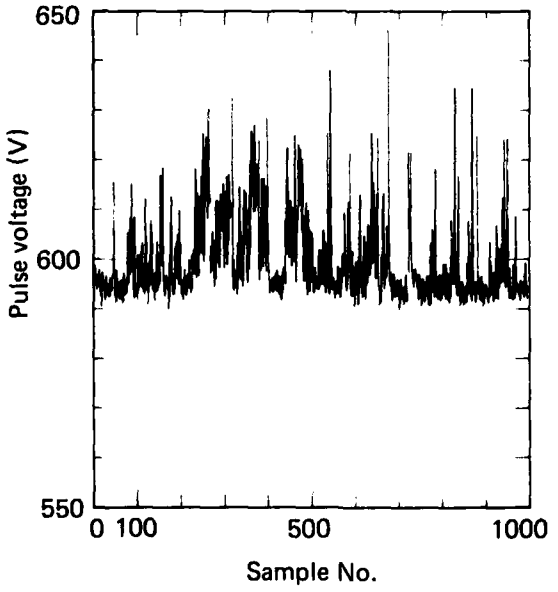

FIG. 8.9. Pulse amplitude variation for a nominal 600-V pulse; 994 sample points are shown.

lognormal probability paper, given in Fig. 8.12, suggests that the lognormal distribution is an appropriate model for the pulser voltage data.

The calculated standard deviation for the data is 10.95 V, and the coefficient of variation, c.v., is approximately

$$c.v. = \frac{10.95}{600} \times 100 = 1.82\% \quad .$$

Three incident electric fields, 256 V/m, 372 V/m, and 460 V/m were used to test the capability of FAST to estimate the probability of system failure. The corresponding pulser voltages were 517 V, 752 V, and 929 V, respectively. Using the estimated coefficient of variation, 1.82%, the estimated standard deviations for the distributions of pulser voltages used in the experiment were 9.41 V, 13.69 V, and 16.91 V, respectively. Thus, the environmental data used as input into the FAST code were modeled using the lognormal distribution with nominal values and standard deviations given above. The distribution of the environmental data was assumed known so no systematic error was included in the FAST input.

8.3.3 Transfer Function Determination

The transfer function used by FAST to relate the incident EM field levels at the monopole to the energy delivered to the diode load was obtained through numerical modeling techniques. The program used was WT-MBA/LLL1B,[3] which is a thin-wire, time-domain, electric-field integral equation solver for antennas and scatterers. This code, which has existed for several years, allows one to model wire structures such as the monopole used in this experiment by a series of short, interconnected segments. The numerical model of the monopole over ground actually resembles a dipole in free space, as shown in Fig. 8.13. The 50 Ω coax line presents a 50 Ω load to the monopole. (The length of the line is assumed sufficiently long to delay reflections from the diode load.) When the perfect ground image is included, the 1.3-m monopole antenna appears as a 2.26-m dipole with a total 100 Ω load at its center.

Plane-wave incidence theory was used for the calculations, and the incident field used was a rectangular pulse with 1-ns rise and fall times and 5-ns width at the 50% amplitude level. All calculations were performed for a 1 V/m incident field strength, since we were only interested in the energy delivered to the 50Ω coaxial line where linearity holds, and not directly interested in the energy dissipated in the nonlinear diode load.

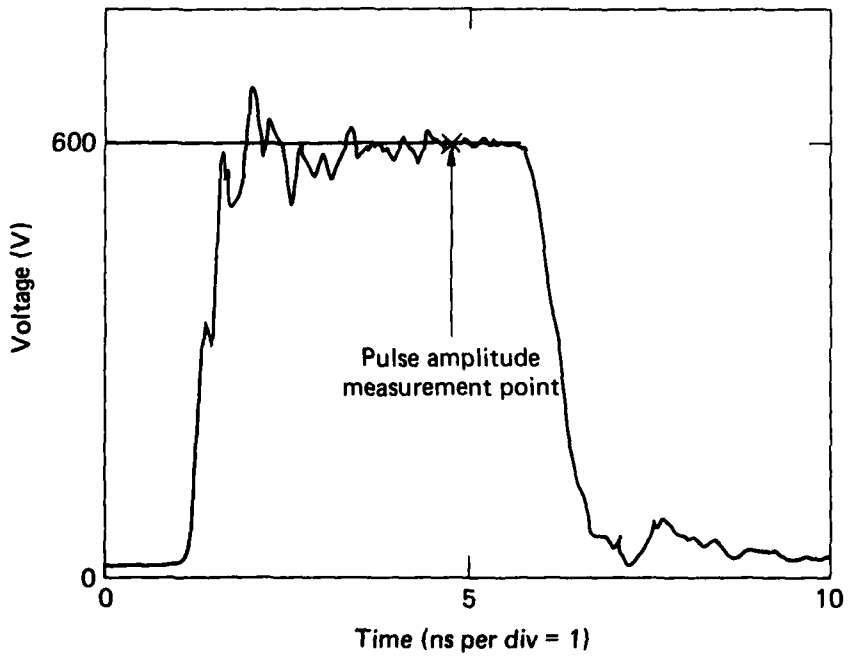

FIG. 8.10. LLL mercury pulser characteristics.

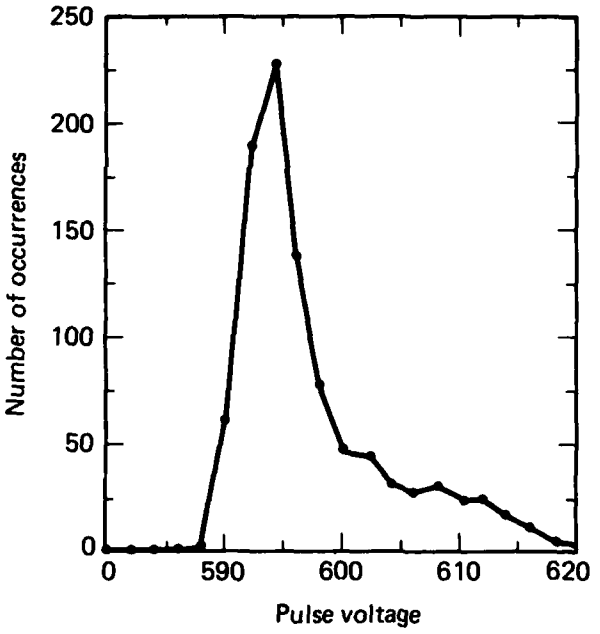

FIG. 8.11. Distribution of pulser voltage amplitude (standard deviation = 10.95 V).

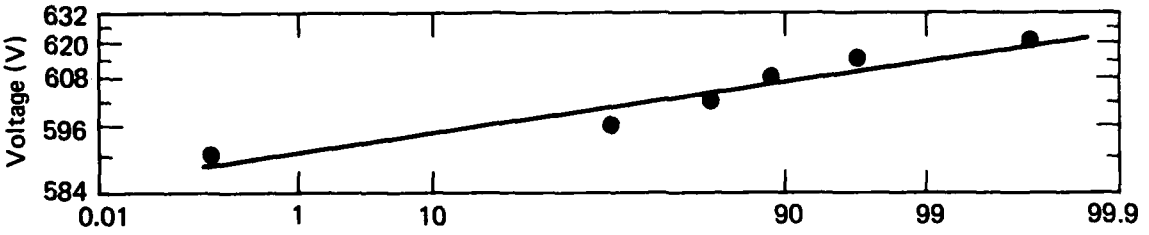

FIG. 8.12. Pulser voltage level distribution--lognormal.

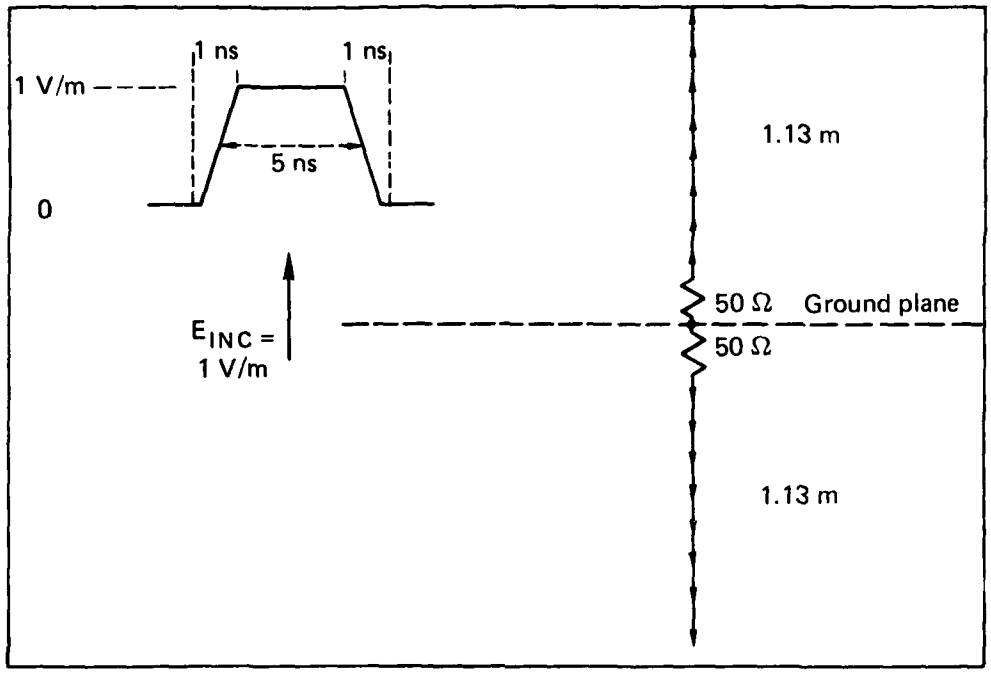

FIG. 8.13. *Numerical equivalent model of 1.13 m monopole with 50 Ω load.*

Figure 8.14 shows the calculated voltage across one-half of the 100 Ω load on the antenna. For comparison, Fig. 8.15 shows the transient waveform measured in the laboratory for a monopole with a 50 Ω load. As can be seen, the agreement between the calculation and measurement is good, and thus with confidence in the numerical model, we calculated the cumulative energy delivered to the 50 Ω load as a function of time. This is shown in Fig. 8.16 where each step increase corresponds to the cumulative energy dissipated in the load for each positive voltage cycle. It should be noted that only the positive cycles were included in cumulative energy calculation, since most of the diode damage occurs for this polarity of bias. We thus selected the asymptotic value of 1.35×10^{-12} J/(V/m)^2 as our transfer function value for FAST. We assumed that the transfer function is known exactly, and thus no systematic error for the transfer functon was included in the FAST input.

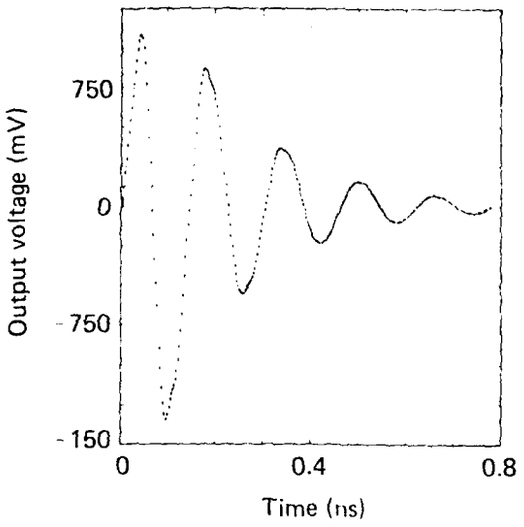

FIG. 8.14. Calculated voltage for a 5-ns pulse across 50 load.

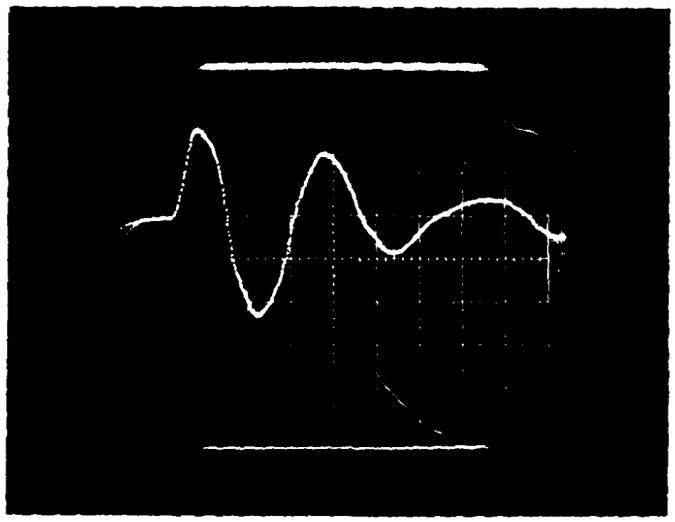

FIG. 8.15. Measured voltage across 50 load on monopole.

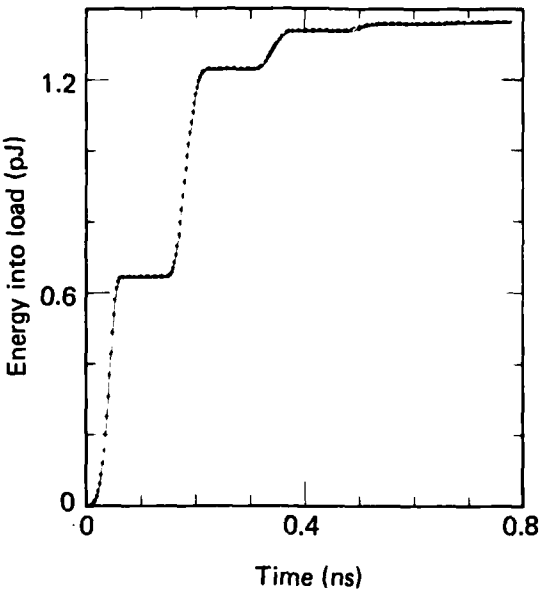

FIG. 8.16. Cumulative energy into a 50 Ω load on a 1.13-m momopole for a 5-ns, 1 V/m incident plane wave.

8.4 RESULTS OF FAST EXPERIMENTS

To have data to compare with the FAST output, an experiment with the sample electrical network consisting of a diode load connected to a monopole antenna, as shown in Fig. 8.2, was performed on the LLL Transient Range. The diode fixture and the cable attached to the monopole is the same as was used in establishing the diode burnout data. Three levels of incident electrical field, 256, 372, and 460 V/m, were used for the experiment. At each incident field level, 26 diodes were tested for failure. Each diode was only used once.

The value of the incident electromagnetic field at the monopole was measured with a calibrated ACD-1 Ḋ probe. The field intensity is directly proportional to the amplitude of the pulse sent to the monocone antenna, with a corresponding calibration factor of 0.495 V/m/V.

The results of these tests are summarized in Table 8.2. The point and 80% confidence interval estimates of the system probability of failure p_f are based on the formulas:

$$\hat{p}_f = \frac{\text{number of units failing,}}{n}$$

$$(\hat{p}_{f,l}, \hat{p}_{f,u}) = \left(\hat{p}_f \pm 1.28 \sqrt{\frac{\hat{p}_f(1-\hat{p}_f)}{n}}\right) ,$$

where n is the number of units tested.

TABLE 8.2. Measured failures for monopole/diode experiment.

Incident electric field, V/m	Pulser voltage	Number of diodes tested	Number of diodes which failed	Estimated probability of failure	80% confidence intervals for probability of failure
256	517	26	5	0.192	(0.093, 0.291)
372	752	26	15	0.58	(0.453, 0.701)
460	929	26	18	0.692	(0.576, 0.808)

It is interesting to note that in many cases, significant shifts in the diode reverse leakage currents occurred after stress testing. It was also observed that increased degradation occurred for multiple pulses widely separated in time. Typical increases observed in the leakage currents were three orders of magnitude after exposing the devices to the higher stress levels!

8.5 FAST OUTPUT AND COMPARISON WITH TEST DATA

Using the environment, transfer function, and fragility curve information described earlier as input, the FAST code was run at the three nominal

electrical field intensities, 256, 372, and 462 V/m. Selected percentiles of the outputed distribution of probability of system failure are summarized in Table 8.3. Also included in the table are the 80% confidence intervals based on the FAST computations and the experimental data from the LLL Transient Range tests. Histograms for the probability of system failure are given in Figs. 8.17 through 8.19 for 256, 372, and 460 V/m electric field, respectively.

Several comparisons of the FAST output and the experimental results were made to test the FAST capability to predict the failure probability for this simple system. The 80% confidence intervals for both the FAST output and the experimental data are included in Table 8.3. Note that a direct comparison of these confidence intervals may be questionable since the intervals using the experimental data are based on the input parameters being uncertain (i.e., are random variables with variation given by the systematic error). Even so, there is generally good agreement between the two sets of intervals. In general, the FAST inputs are narrower than the experimental intervals and intend to intersect with the lower ends of the experimental intervals.

In general it seems like the FAST output is comparable to the estimates of the failure probability based on the experimental data. It must be recognized that this comparison was made on a very simple system. There were several factors which affected the results and which may explain some of the discrepancies found between the FAST output and the experimental data. One such factor is the systematic uncertainty associated with the environment and the transfer function used as part of the FAST input. In both cases, the systematic uncertainty was considered negligible (i.e., the parameters of the electric field strength were assumed known and the transfer function used was considered to be exact), thus no systematic error was attributed to either input. Therefore, the only systematic error was that attributed to the uncertainty in the parameters of the fragility curves. As more experience is gained in this technique for system assessment, knowledge about appropriate systematic uncertainties will be developed. It is recommended that a study of the sensitivity of FAST to the value and type of systematic error be undertaken.

TABLE 8.3. Percentiles, P_o of probability distribution of p_f, probability of system failure.

Probability, $P(p_f \leq p_o)$	Incident field voltage, (V/m) 256	372	460
0.01	0.056	0.313	0.513
0.10	0.102	0.388	0.607
0.30	0.118	0.441	0.658
0.50	0.135	0.490	0.679
0.70	0.155	0.528	0.700
0.90	0.217	0.583	0.750
0.99	0.337	0.675	0.838
FAST 80% confidence interval:	(0.102, 0.217)	(0.388, 0.583)	(0.607, 0.750)
Experimental 80% confidence interval:	(0.093, 0.291)	(0.453, 0.701)	(0.576, 0.808)

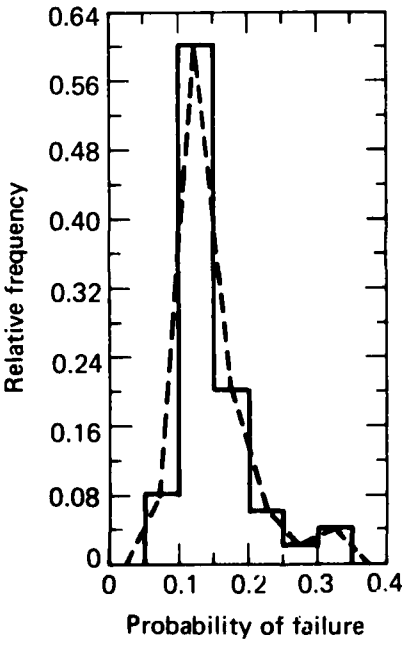

FIG. 8.17. Distribution of probability of system failure (256 V/m).

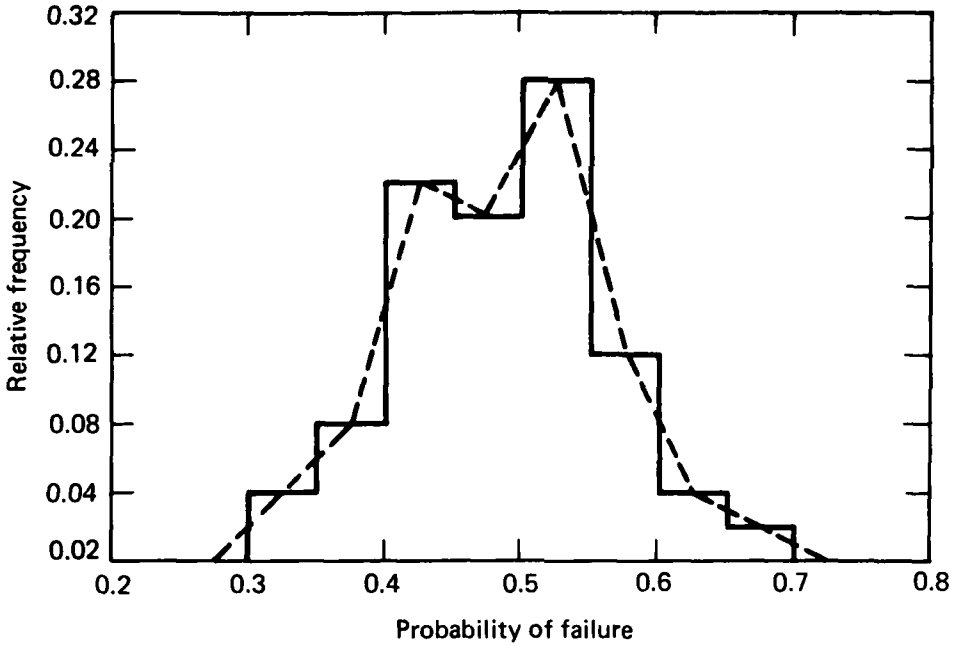

FIG. 8.18. Distribution of probability of system failure (372 V/m).

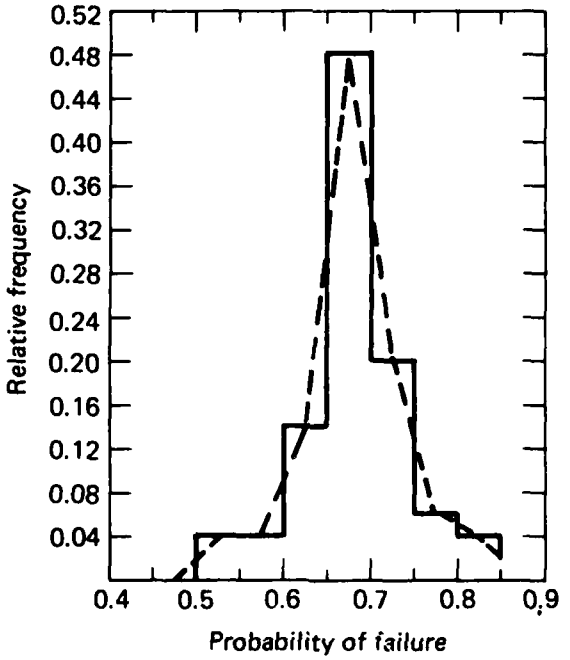

FIG. 8.19. Distribution of probability of system failure (460 V/m).

Another feature of FAST which we found restrictive was the requirement that the fragility curves be modeled by a distributon function described by at most five straight line segments. This forced us to approximate the apparent continuous fragility curve which we estimated from the burnout tests. It seems that certain continuous distribution functions could be included as possible models without too much difficulty. Of course, in our test case, we were only able to estimate the failure probability of the diode at a few energy levels. Better fragility curves would be developed with additional testing.

Certainly the fact that we were only able to use 26 diodes per test on both the burnout tests as well as the system failure tests contributed to the wide confidence intervals for the estimate of the system failure probability based on the experimental data. The width of the confidence interval is a function of $1/\sqrt{n}$, where n is the sample size. Hence, with additional testing the estimates of the two methods might be more comparable. Also a larger sample of experimental data would make the experimental results closer to the actual failure probability for the system. Then, of course, the comparison would be more meaningful.

For a second comparison, the probability of failure was computed analytically, based on the assumptions that (1) the diode threshold (energy level at which the diode fails) and (2) the stress (energy in joules) applied to the system are both lognormal random variables. The assumption that the stress applied to the diode is approximately lognormal is based on the lognormal probability plot of the voltage data given in Fig. 8.12. A lognormal probability plot of the experimental failure data is presented in Fig. 8.20. The probability failure was evaluated based on the following analysis:

If diode threshold, T, and applied stress, S, are each lognormal random variables, the probability of failure, P(fail), is given by

$$\begin{aligned} P(\text{fail}) &= P(S > T) \\ &= P(S/T > 1) \\ &= P(\ln S - \ln T > 0) \end{aligned}$$

Since T has a lognormal distribution with parameters (μ_T, σ_T), the density function for the distribution of T is $f(t; \mu_T, \sigma_T)$,

$$f(t; \mu_T, \sigma_T) = \frac{1}{\sqrt{2\pi}} \quad \frac{1}{\sigma_T} \exp \left[\frac{-1}{2} \left(\frac{\ln t - \mu_T}{\sigma_T} \right)^2 \right] , \quad t \quad 0$$

Based on the probability plot in Fig. 8.20,

$$\mu_T = \ln(2.05 \times 10^{-7}), \quad \sigma_T = \ln(5 \times 10^{-7}) - \ln(2.05 \times 10^{-7}) = 0.892.$$

Similarly, for the applied stress (energy), since

$$S = 1.35 \times 10^{-12} \ (V/m) \quad ,$$

where 1.35×10^{-12} is the transfer function developed for this system, it follows that S has a lognormal distribution with parameters μ_S, σ_S:

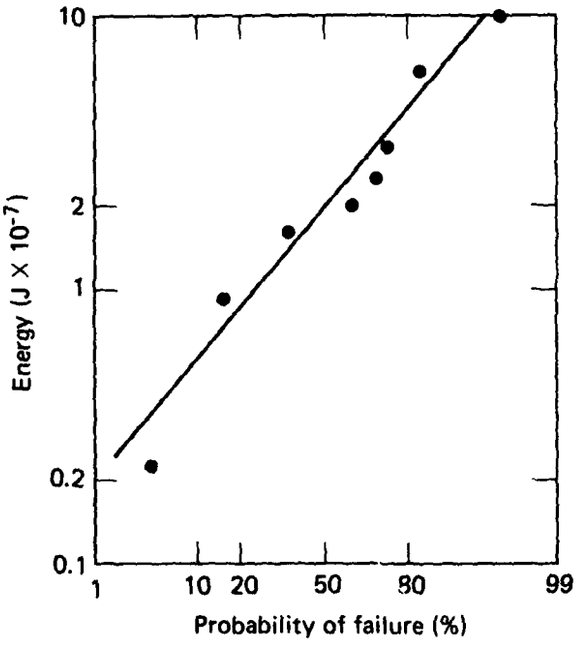

FIG. 8.20. Lognormal probability plot of diode failure data.

Voltage level, V/m	μ_S	σ_S
256	$\ln 1.35\times10^{-12} + 11.09036$	0.0032
372	$\ln 1.35\times10^{-12} + 11.83778$	0.0032
460	$\ln 1.35\times10^{-12} + 12.26246$	0.0032

Further, if $W = \ln S - \ln T$, then W is a normal random variable with mean $\mu_W = \mu_S - \mu_T$ and standard deviation $\sigma_W = (\sigma_S^2 + \sigma_T^2)^{1/2}$. Thus, the probability of failure, P(fail), is

$$P(\text{fail}) = P(W > 0)$$

$$= P\left(Z > \frac{-(\mu_S - \mu_T)}{\left(\sigma_S^2 + \sigma_T^2\right)^{1/2}}\right),$$

where Z is a standard normal random variable. The results are summarized in Table 8.4 along with the experimental results and the probabilistic analysis results based on FAST.

Table 8.4 Comparison of analytic results with FAST and experimental results.

Electric field level, V/m	Probability of failure: Experimental	Analytical	FAST
256	0.192	0.172	0.135
372	0.580	0.460	0.490
460	0.692	0.645	0.679

In general, both the experimental data and the probabilistic analysis results agree quite well with the analytical results. Of course, it must be recognized that this comparison was made on a very simple system. There are several factors which affected the results and which may explain some of the

discrepancies found between the three analyses. With regard to the analytical approach, it was assumed that both the input (stress) and the component fragility (threshold) are lognormal random variables. It is likely that these are only approximations to the actual distributions, particularly for the fragility distribution (see Fig. 8.20). This certainly influences the analytical results. One factor that affected the probabilistic analysis results is the systematic uncertainty.

8.6 REFERENCES

1. R. M. Bevensee, et. al., Validation and Calibration of the LLL Transient Electromagnetic Measurement Facility, Lawrence Livermore Laboratory, UCRL-52225 (1977).

2. P. H. Stadler, Failure Threshold and Resistance of the Protected 2N22222 Transistor in the Short Pulse Width Regime, Lawrence Livermore Laboratory, *Protection Engineering and Management Note*, PEM-7, May 1972.

3. R. M. Bevensee, et. al., "Computer Codes for EMP Interaction and Coupling," IEEE Transactions on Antennas and Propagation, Vol. AP-26, No. 1, January 1978.

9. CONCLUSIONS

9.1 GENERAL

System EMP vulnerability assessment programs have included provisions for dealing with uncertainties. The methodologies of such programs have not handled the uncertainties in similar manners, however. Some assessment approaches emphasized analytically oriented modeling, and others were based on more extensive use of simulation tests. Uncertainties do exist in all areas: in the EMP environment, in assessing how this environment couples to and interacts with the system, and in assessing the susceptibility of subsystems to the resultant types of EMP-induced signals imposed upon them. The assessment of coupling, and consequently the relevance of the associated uncertainties, depends on system configuration and degree of inherent shielding. The assessment of subsystem susceptibility depends strongly on the types of circuitry involved and how it interfaces with other circuitry in the system. The susceptibility of components is less sensitive to the type of system in which they are used as variability is inherent in the components characteristics. This survey and the associated investigation of tools for uncertainties analyses have shown that much is to be gained from probabilistic approach to assessment.

9.2 UNCERTAINTIES

9.2.1 Environment

The high altitude EMP environment will vary in amplitude and in time signature. These variations will typically be much less than those encountered in coupling and susceptibility.

9.2.2 Coupling

Measurement errors, extrapolation of test data, intrasystem variations, and intersystem variations are present in system tests. Extrapolation errors are largest and approach ± 20 dB in attempts to predict the induced levels of internal coupling on individual wires. Power-off and power-on variations may be ± 10 dB in aircraft systems. Predictions of external coupling are possible by computer simulation and scale models, as well as by full scale tests. Errors can be less than 10 dB in the predictions of coupling levels on exterior conducting surfaces. Most of these errors can be reduced by obtaining more information from measurements. Extrapolation from test to threat conditions is improved if such extrapolation is based on measurements of a good scale model response. More parameter variations and measurements at internal points will reduce the uncertainty in extrapolation of internal coupling.

9.2.3 Susceptibility

The variation in susceptibility of both subsystems or circuits and components is quite important in performing vulnerability assessments. The fundamental variation in failure threshold levels of components is a significant uncertainty in determining the susceptibility of a subsystem. This variation has been expressed many ways, and failure models have been developed for several classes of component devices. Variations within a particular class of a device, such as a semiconductor diode, may reach ± 20 dB. Standard deviation factors vary from 1.4 to 4.8, for example, for integrated circuits of several types. Analytical predictions of subsystem susceptibility are usually performed by circuit analysis techniques and depend, therefore, strongly on knowledge of the configuration of the circuit and model parameters. When a component of high variation is imbedded in a circuit, other elements of the circuit many act to control the susceptibility and limit the influence of this particular component. Consequently the variation in susceptibility of a circuit may be less than that of the

components within it. Figures of ± 13 dB have been observed for the variation in susceptibility at the interface of a circuit.

9.2.4 Protection

Protection aspects also enter into the assessment picture. Common practices such as shielding, cabling, and grounding affect very much the uncertainties in coupling, while protection techniques such as filtering and the use of terminal protection devices have a stronger effect on the susceptibility of the circuit in which they are included. Uncertainties are introduced into shielding effectiveness factors through imperfections found in the manner of construction. The usual shielding calculations involving planar theory are a source of error when applied to three-dimensional objects. Shielding effectiveness is measured by use of loops and dipoles, whereas EMP is a plane wave which can incident in many directions. Shielding is thus a major protection method; yet little is known about the response of large or full scale three-dimensional shielding systems. Terminal protection devices are also a major protection method, and semiconductor devices have well-controlled clamping voltage levels for a range of input current. It is in the application of a transient protection device when inserted into associated circuitry that uncertainty many arise, as the device must be compatible with required circuit performance in the absence of the EMP signal.

9.3 ASSESSMENT METHODOLOGIES

9.3.1 Existing

This survey has shown that the existing assessment methodologies have approached the problem of uncertainties in different manners. A most prevalent approach is to use the worst-case viewpoint and a deterministic analysis. Uncertainties in the input, coupling, circuit paraments, and component descriptions are all considered in attempting to develop safety

margins which are realistic. Another approach is based on the use of tests in EMP simulators which are supported by strong analytical work which leads to a figure for probability of survival. Here it is necessary to extrapolate to obtain desired wire currents from measured values.

More realistic aasessment methods recognize the random nature of uncertainties and attempt to handle the uncertainties accordingly. Even so, there is no consistent manner of handling uncertainties among the several assessment methods surveyed. All of the existing methods make some simplifying assumptions about the uncertainties throughout the assessment analysis. (For example, errors are normal or lognormal random variables; linear terms of a Taylor series are adequate to propagate errors for complex functions.) This introduces further uncertainties which seldom are assessed. One complication in comparing different methods is the use of identical statistical terms for quite different concepts. This does not allow correlation of the results obtained from different methods.

9.3.2 Probabilistic Analysis

One method of vulnerability assessment which recognizes the random nature of uncertainties and which overcomes some of the difficulties associated with existing methods is based on a probabilistic analysis. In such an analysis, the variability in uncertainties (random, systematic, or epistemic) is described by a probability distribution. The uncertainties, as characterized by the appropriate probability distributions, are propagated throughout the assessment process. Because of the complexity of the coupling and/or interrelationships between subsystems, the methodology used by LLL propagated the uncertainties using Monte Carlo sampling techniques. The resulting distribution of the assessment parameter (probability of system failure) is based on propagating all of the recognized uncertainties throughout the analyses. This assessment method was tested using two simple systems. In the case of a single monopole/diode system, only the Monte Carlo code was necessary, and a comparison with a laboratory system test was quite favorable. For a more complex system in which both a network code as well as the Monte Carlo code was

necessary, the test results were not as comparable as the simpler system. Several factors contributed to this; in particular, the nature of the component failure data, the difficulties in modeling a nonlinear system in the network code, etc. It is necessary for all future or more extensive applications to be able to supply the component fragility curves as well as the transfer function which relates the incident EMP field level to the point of interest.

9.4 RECOMMENDATIONS

The subject of errors and uncertainties is a dynamic one, and it would be very useful to keep summaries of important uncertainties current and available to the EMP community. At the minimum it would be particularly useful to use common terminology and format in expression of uncertainties in different system studies.

Probabilistic methodology needs further work, particularly in the allocation and analysis of protection for various types of systems. Tools such as NET2 (version 9.1) and FAST are powerful, but they have limitations. NET2 suffers from lack of documentation. FAST could be extended to handle more complex systems. These are practical matters, but computer program development is a costly process.

APPENDIX A
RECORDING SYSTEM ERRORS REPORTED BY BDM

An intensive study was made in Ref. 1 of various digitization errors in different recording systems, both in the time and resultant frequency domains. The most significant input data errors on transform results (f-domain data) were, 1) nonlinear errors of time-base nonlinearities, parallelogram and keystone effects, and peak clipping--each of which can, in principle, be removed, 2) random noise, and 3) digitization errors of horizontal and vertical offset, and rotation, 4) sampling errors, and 5) of least-importance, word-size limitations and linear scale errors. The effects of truncating the input time waveform and of both time-tying and frequency-tying were studied.

Table 5.1 of Ref. 1 is a summary of the major errors, showing the effect of time-domain errors on the f-domain errors. The first entry, truncation, shows a relative error in the f-domain modulus of 100% at some frequencies. It has more effect on time-derivative data. Although windows can improve transform data obtained from truncated waveforms, time-tying is the most common and effective way to counter this effect. But time-tying must be done carefully or the offset will create large frequency domain error. Frequency-tying, too, can improve f-domain data.

Of the various recording sytems studied, the DASET gave the best results, with typical modulus errors of 100% at high frequences > 50 MHz and $\simeq 40\%$ at lower frequencies (as tested with a damped-sine waveform, which tends to have more data processing errors than exponentially decaying waveforms). In this system, the 7912 oscilloscopes required constant surveillance to maintain their calibration and small digitization error.

The primary error source in the ADSET recording system was found to be the digitizer, and a recommendation was made to improve it.

Significantly, most of the errors in Table 5.1 of Ref. 1 were either relatively small or only large in a 100 DFP (down from peak) bandwidth. Thus

it was concluded that time-domain predictions of EMP response based on transfer functions with the kinds of errors studied would have maximum standard deviation of 55%. In other words, peak EMP time response would be forecast within about ±50% with the quality of data processing in the ADSET, DASET, and other recording systems studied by BDM.

1. EMP Data Reduction Variables Analysis Study, Braddock, Dunn & McDonald, Alburquerque, NM, May 1977.

APPENDIX B
THE ERROR ANALYSIS REPORT OF EG&G

In 1978, an error analysis report was written about the HPD Upgrade test program for the horizontally polarized dipole, the objective of which was to establish error estimates applicable to all test data of 90% confidence limits at the 90% confidence level.[1] Factors <u>not</u> treated in the report were: pulser amplitude and rise time variations, dynamic range limitations, and antenna/test object interaction.

Figure 5.1 of Ref. 1 summarizes the various errors involved in different systems for recording and processing test data. Each of the four systems--screen box, improved screen box, single channel microwave screen box, and five-channel microwave DASET--is represented by a string of series and parallel connections of boxes. The total error ϵ_t^e for a given box is

$$\epsilon_t^e = \sqrt{\epsilon_{AMP}^2 + \left[\epsilon_{UNBAL} \quad (1+V_c/V_d)\right]^2} \quad ,$$

where ϵ_{AMP} is the residual error with no common mode contamination and is the channel gain error for a balanced system. ϵ_{UNBAL} is the worst-case deviation of one channel gain from the other channel gain. The quantity in brackets is the amplitude error due to unbalance, V_c/V_d being the common mode/differential mode ratio.

ϵ_I refers to instrumentation error (minimized by proper calibration technique) and ϵ_{DP}, to data processing error. ϵ_r is the total rss error in either the t- or f-domains, $\sqrt{\epsilon_I^2 + \epsilon_{DP}^2}$.

ϵ_{DP} is usually computed as a fractional <u>linear</u> error in this report, while ϵ_I is computed as a dB error. All errors were assumed to have zero means.

Data processing error estimates of ϵ_{DP} based on regression analyses of data photographs or DASET recordings indicated the following functional forms:

(a) in f-domain,

$$\epsilon_{DP}(\omega) = 10^{-2}F(\omega)10^{a}\left|F(\omega)/F_{max}\right|^{-20b} ,$$

where $F(\omega)$ = signal amplitude at frequency ω ,

$$F_{max} = \max_{\omega}\left|F(\omega)\right|, \quad \omega > 1/(\text{data trace duration}).$$

(b) in t-domain,

$$\epsilon_{DP}(t) = a' + b'x ,$$

where x = (slope of data trace in divisions/division).

The values of a, b, a', and b' were approximately

Screenbox data	DASET data
$a \simeq 0.838$	$\simeq 0.733$
$b \simeq 0.037$	$\simeq 0.027$
$a' \simeq 0.108$	$\simeq 0.062$
$b' \simeq 0.057$	$\simeq 0.016$

The total error estimate ϵ_t in the t-domain was: (1) based on statistical processing of multiple t-domain data traces, (2) obtained with instrument calibration functions converted to the t-domain, and (3) obtained from instrumentation error estimates in the f-domain without phase information

A linear relationship was found between the t-domain error and t-domain signal slope, verified by regression analysis with high ($\gtrsim$ 90%) correlation for both screenbox and DASET data. The final confidence limit C was functionally related to the signal slope S as

$$C(x) = A + BS(x) .$$

The f-domain analysis was similar and revealed a linear relation between relative error and amplitude relative to peak amplitude, both in dB. This

linear relation was established by regression analysis with high correlation for both screenbox and DASET data.

The 90%-90% confidence interval (CI) obtained from the regression model was compared to that obtained from the individual classes of screenbox or DASET data. It was found the former CI was sometimes greater and sometimes less than the latter. The comparisons showed good overall agreement beyond 10 MHz.

The report also discussed application of the deterministic error model, to be described later in our report in the section devoted to MRC work. Several advantages over the statistical approach are claimed: (1) it is directly related to quality control (QC) and instrumentation accuracies, (2) error estimates can be made before testing, and (3) it is cost, time, and effort efficient. The error model is briefly summarized as follows.

Assuming negligible errors in sensor placement, test item interaction and numerical processing, the six dominant errors are: (1) amplitude, (2) sweep speed, (3) baseline shift, (4) rotation, (5) noise, and (6) data truncation. A 30 dB S/N ratio is the vertical (amplitude) limitation, establishing a lower bound on contributions of (3) and (4), a floor on trace width noise and subsequent digitization noise, and lower bounds on (6). Horizontal resolution is 1 part in 40, or 2-1/2%, the f-domain error appearing as a distortion of the frequency scale. Time-tie errors too are bounded by the three errors: noise 30 dB below signal, baseline shift, and rotation.

The various relative error magnitudes with no filtering and strict QC are found to be as follows:

Error type	Screenbox	DASET
Amplitude	$\pm$0.24	$\pm$0.5
Baseline shift	$\leq$ 1/30	$\leq$ 1/30
Truncation	$\leq$ 1/30	$\leq$ 1/30
Sweep speed	$\leq$ 1/25	$\leq$ 1/100
Noise/signal	$\leq$ 1/30	$\leq$ 1/30

Conclusions about the deterministic error analysis are: (1) sweep speed errors, though causing huge amplitude errors at deep nulls or high peaks, are not important if the response f-domain envelope is important, (2) baseline shift error is more important at low frequencies, and (3) truncation error has a bounding envelope constraint with frequency.

This concludes the summary of the report on the EG&G work on the HPD Upgrade Test Program. An earlier report[2] described the same techniques applied to photographic data forwarded to EG&G by TRW.

REFERENCES

1. Horizontally Polarized Dipole, Electromagnetic Pulse Simulator Upgrade Test Program. Characterization Report Vol. IV Error Analysis Report, EG&G, Alburquerque, NM, Al-1295, April 1978.

2. Misc. Sim. Memos, Memo 8, Some Performance Parameters for Various EMP Simulators, AFWL, Kirtland AFB, Albuquerque NM, November 1976.

APPENDIX C
HDL DATA REDUCTION AND PROCESSING

Data reduction and processing errors have been assessed in Ref. 1, as they occur in the HDL numerical data processing with their computer codes for taking Fourier and inverse Fourier transforms. Analysis of errors introduced by the transform process, sampling, quantification, digitization, and noise is summarized graphically. The analysis is performed on a "Mimipulse" model of a general temporal waveform containing power series, exponential, and oscillating components with adjustable parameters. Since the power spectrum obtained from a digitized trace shows a strong ocillating noise component, a subroutine (SMUZ) is used to smooth it.

Digitization is performed with Science Accessories Corp. GP2 digitizer, with 0.01 in. definition. Recordings of an event normally consist of four or more traces at differing sweep speeds. Further processing (time-tying, sequence checking, etc.) is performed on a CDC-6600 computer.

Numerous numerical experiments were performed with Mimipulse treated as a data input. The graphs compare the analytic transforms for various waveform parameters to the corresponding:

- Transforms of equispaced samples of a truncated pulse--indicating transform errors.
- Transforms of the true pulse at equispaced time points--sampling errors.

---

1. Misc. Sim. Memos, Memo 8, Some Performance Parameters for Various EMP Simulators, AFWL, Kirtland AFB, Albuquerquem NM (November 1976).

This report contains a good succinct statement of Cooley's theorem regarding the finite Fourier transform, with required conditions for good representation.

- Transforms of digitized points--digitization bias.
- Transform errors.
- Transforms of the truncated analytic values at the equispaced time points--quantification errors.
- Transforms of the truncated analytic pulse with a random component added--digitization plus quantification with noise.

A major conclusion of the report is that for Mimipulse-like traces, all these errors are minor out to 1 GHz ($\gtrsim$ 40 dB down from peak) compared to inherent data-taking errors of 5% or so.

The inverse transforms were correspondingly accurate, but it was observed that if the data-processing time or frequency interval, or both, do not cover the (significant) domain of the function, the inverse transforms--actually reconstructed data traces--could be nonreliable. Error in the time domain is often indicated by the failure of an inverse transform to return to zero or be zero at t = 0. Convergence is often indicated by the agreement of two of the HDL inverse transform codes (FFT, FLIT). One may advantageously use another code (INUFT) for a waveform defined at unequal f-intervals in some situations.

AD-A096 696 CALIFORNIA UNIV LIVERMORE LAWRENCE LIVERMORE LAB F/6 12/1
CHARACTERIZATION OF ERRORS INHERENT IN SYSTEM EMP VULNERABILITY--ETC(U)
OCT 80 R M BEVENSEE, H S CABAYAN W-7405-ENG-48
UNCLASSIFIED UCRL-52954

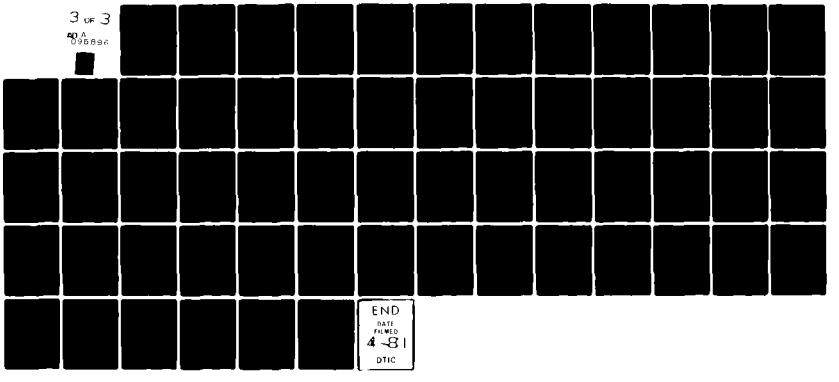

APPENDIX D
MEASUREMENT TECHNIQUES AND DETERMINATION ERROR ANALYZER OF MRC

MEASUREMENT TECHNIQUES

The measurement technique in the F-111 aircraft response and comparison reductions and measurements were described in another publication.[1] The sensors were MGL-5S and HSD-3S for J and q, respectively, mounted on the aircraft surface. They connected to double-shielded 50-ohm cables running inside the craft to a junction box that fed the outputs of five of the sensors to the 5-channel microwave transmitter. This last delivered the multiplexed sensor outputs to dielectric waveguide and to a receiver housed inside a remote recording station (mobile screen room). There, the signals were demodulated and passed through a power splitter for each channel to drive 10 Tektronix 7912 transient digitizers, where the signals were recorded. By splitting each channel, both slow-sweep and fast-sweep speed recordings were made of each sensor output, thus eliminating some sweep-speed limitations on data bandwidth. For data processing, the two traces were recalled from 7912 memory, time-tied, and passed through rigorous QC inspection.

From the component data, an overall recording-instrumentation response function was obtained and used to correct the data. The result was a high quality data base with error functions.[2]

It was found that recording derivative data significantly shifted the useful bandwidth upward in frequency: the overall system 30-dB dynamic range response increased from 47 MHz to 125 MHz.

The comparison of these measured $\dot{J}$- and $\dot{q}$-responses with the ones predicted by THREDE (see Appendix G) were good in both the t- and f-domains, at eight test points. Peak t-values were somewhat overbounded and the f-domain amplitude curves agreed well out to 50 MHz (set by the limit on measured HPD spectral output).

Both $\dot{J}$ and $\dot{q}$ with E^{inc} parallel to the fuselage agreed well with measurement:[3] On the dark side, the peak J values were almost the same, and the peak $\dot{q}$ computed was about 1.5 times the measured value. $\dot{J}_{peak}$ computed on the bright side was about 0.6 of the peak value measured (which was about the same as the peak on the dark side).

DETERMINISTIC ERROR ANALYSIS

In Measurement Note 24,[4] this analysis was applied to simulator data acquisition and six predominant error sources were identified. Assuming rigorous QC, the error types for various systems and typical values are listed in Table D.1.

TABLE D.1. Error types and magnitudes in data acquisition systems. For damped sine wave and doubly delayed double exponential type waves, the most significant error sources appear to be the first four in the table.

Error type	Screenbox[a] (Improved)	Screenbox[a] (Typical)	Transient digitizer[b]	Microwave[c] system
Amplitude	±0.24 dB	±0.46 dB	±0.50 dB	±0.50 dB
Baseline shift	≤ 1/30	≤ 1/15	≤ 1/30	≤ 1/15
Speed sweep	≤ 1/25	≤ 1/20	≤ 1/100	≤ 1/30
Noise/signal	≤ 1/30	≤ 1/15	≤ 1/30	≤ 1/15
Truncation	≤ 1/30	≤ 1/15	≤ 1/30	≤ 1/15

[a]Video digitization.
[b]With Autocal, a computer based calibration procedure.
[c]Without Autocal.

Analytic expressions for the noise error bounds are given in terms of the signal spectrum and σ_{noise}. The uncorrelated errors are added in rss fashion to get the f-domain absolute error $\epsilon_{abs}(f)$ of a response F(f). Then the overall relative error $\epsilon_{rel}(f) = \epsilon_{abs}(f) / |F(f)|$ was processed for a damped sinusoid (ds) and doubly delayed double exponential (ddde) (as shown in Fig. 5.2, a typical date acquisition and processing flow chart of Ref. 4).

Plots of $\epsilon_{rel}(f)$ for the systems in Table D.1 were characterized by: (1) high (> 100%) error for the ds and low ($\simeq$ 10%) error for the dde in the lower frequency range f $\lesssim$.3 MHz, (2) as ds error decreasing toward the nearly constant dde error and both about 10% at $\simeq$10 MHz, and (3) fluctuating rapidly rising errors above f $\simeq$ 10 MHz. The sweep speed and probably baseline errors caused huge amplitude errors, in the low frequency ds spectrum for example, when the signal contained deep nulls and/or high peaks.

Appendix 3 of Ref. 4 was devoted to estimating the noise transfer function from Fourier transform data processing. To get σ_{eff} for the noise, one: (1) truncates the (assumed) Gaussian noise (of instrumentation/digitization) at 2σ, (2) passes this noise through a processing system using the same Δt, T_{max}, and the FFT, DFT, or FIT algorithm (see Section 5 of Ref. 4) to be used on the actual data, and (3) repeats this procedure until the accumulated $\sigma_{eff}(f)$ of both the real and imaginary components of the f-domain noise are approximately equal. Then (4), one uses this σ_{eff} to predict the noise on a transformed noisy signal f(t) + n(t) having a specified S/N ratio, by scaling σ_{eff} to σ'_{eff} so as to have $(S/N)_t = |f_{max}(t)| / 2\sigma'_{eff}$ or $(S/N)_f = |f_{max}(\omega)| / 2\sigma'_{eff}$.

In measurement Note 25,[5] this same deterministic error model is described as implemented for ADSET. Analysis of measured responses on an aircraft at ATHAMAS-I is presented. Upper bandwidth limits to measured responses are determined by S/N ratios, while the lower limits are predominantly set by baseline error and the finite $\Delta f = 1/T_{max}$ resolution.

With good QC, t-domain amplitude errors of time-integrated measurements were 10.4%, and typically 6.0% for non-integrated measurements. Sweep speed errors with Autocal were $\lesssim$1%. Truncation and amplitude errors will bound the error envelope in the range $1 \lesssim f_{MHz} \lesssim 10$ when baseline shift is small and S/N large.

Five spectra were discarded because the error across the entire band of each was $\gtrsim$ 100%.

The time-domain error parameters and characterizations for different data records are summarized in Table 5.3 of Ref. 5.

More than half of the internal cable current data traces were unusable because of error $\gtrsim$ 100% of signal across the band. Transfer functions for cables derived from such data would be highly suspect.

REFERENCES

1. K. S. Kunz and K-M Lee, "A Three-Dimensional Finite Difference Solution of the External Response of an Aircraft to a Complex Transient EM Environment: Part II - Comparisons of Predictions and Measurement," IEEE Trans. Electromagnetic Capability EMC-20, May 1978.

2. D. Endsley, et al., HPD Upgrade Test Program, HPD Characterization Report Vol.II: Part 2--Response Test Report, EG&G, Al-1274 (draft) (August 1977).

3. "THREDE: A Free-field EMP Coupling and Scattering Code," IEEE Trans. Nuclear Science NS-24 (December 1977).

4. Measurement Note 24, Deterministic Error Analysis Applied to EMP Simulator Data Acquisition, Mission Research Corp., Albuquerque, NM (June 1977).

5. Measurement Note 25, Deterministic Error Analysis Applied to EMP Simulator Data Acquisition II, Application to Aircraft Test Data, Mission Research Corp., Albuquerque, NM (March 1978).

APPENDIX E
THE N. A. ROCKWELL ASSESSMENT ERROR ANALYSIS FOR THE EC-135 AIRCRAFT.[1]

The objective of this report was to obtain confidence intervals (confidence limits for reliability of at least R and confidence levels for those limits) for internal pin damage safety margins. The mathematical statement of an R-C reliability-confidence interval for a random variable $x = x_{true} + x_{error}$ is this: the confidence limits $-L_1$, L_2 are such that

$$P_r \left\{ P(-L_1 \leq x \leq L_2) \geq R \right\} = C \quad .$$

This states that x lies in the range $(-L_1, L_2)$ at least a fraction R of the time, and the confidence for this assertion is C. Note L_1 and L_2 are based on a sample of n(R,C) observations.

In assessment Method 1, simulator-measured wire currents are extrapolated to threat level via an OSU computer code; *in* Method 2, by extrapolation functions based on University of Michigan scale model data.

Assessment Method 1 is summarized as follows. A wire current I_w is extrapolated to threat level by the formula

$$I_w = I_w^{SIM} \left(E^{HAB}/E^{SIM}\right) \left[\frac{H^{AIR}/E^{INC}}{H^{SIM}/E^{INC}} \right] \qquad (E.1)$$

in which

I_w^{SIM} = measured simulator response, error $\pm X_1$ dB ,

E^{HAB}/E^{SIM} = simulator true response, error $\pm X_2$ dB ,

1. EC-135 EMP Assessment Program Final Assessment Report, Vol. III Assessment Error Analysis, Rockwell Intern., Anaheim, CA (November 1977).

H^{AIR}/E^{INC} = predicted external H-field transfer function, error $\pm X_3$ dB ,

H^{SIM}/E^{INC} = measured H-field transfer function error, $\pm X_4$ dB ,

the last ratio in brackets might have POE errors $\pm X_5$. All these errors are summarized in Table 5.5 of Ref. 1 for the R-C interval of 90%-90%. The errors $X_1,\ldots,X_4$ are treated independently.

The R-C interval $(I_w \pm X_i)$ in dB was defined to be a 90%-90% interval for the wire current I_w if $X_i = 1/2\ (I_{w\ max}/I_{w\ min})$ in dB. Defining the rss error $e_w = \sqrt{\sum_i X_i^2\ (dB)}$, the interval $(I_w \pm e_w)$ in dB was declared to be the net 90%-90% interval. This was checked by a 27-sample Monte Carlo run.

Based on Table 5.5 of the reference, $X_1 + X_2 = \pm 5.3$, $X_3 = \pm 7.2$, $X_4 = \pm 7.2$, and $X_5 = \pm 8.$ (typical) in dB, and $e_w = \pm 14.0$ dB. Then the impedance ratio, threshold, and power on-off errors are added to e_w in an rss sense (first column, Table 5.6 of Ref. 1). Then the median threshold current I_T is computed and its 90%-90% error interval is in the middle column of Table 5.3 of Ref. 1. The margins e_{mp} in dB appear in the last column; each entry is the rss of the two other numbers on that line. Safety margin M is measured by I_T/I_w, so $M(dB) = I_T(dB) - I_w(dB)$. Note the minimum margin $M_- = \hat{M} - e_{mp}$ in dB is not $(\hat{I}_T - e_T)/\hat{I}_w + e_w)$ in dB.

The simulation e_s for Assessment Method 2 is derived as follows: Let

$$g_1^{(c)}(f) = F^{-1}\left[f_1^{(B)}(f) g^S(f)\right] \text{ for each failure port} ,$$

where

$g_1^{(c)}$ = criterion current, 1 denoting the drive port ,

$f_1^{(B)}$ = extrapolation ratio ,

g^S = wire current measured from aircraft tests.

Then let

$$p_{\ell}^{(c)} = \max_{t} \left| g_{\ell}^{c}(t) \right|$$

and

$$p^{(E)} = \max_{t} \left| F^{-1}\left[f^{(B)}(f) g^{(S)}(f) \right] \right| ,$$

the extrapolated peak t-domain current for each failure port.

Then the simulation error is

$$e_s = \max \left| p^{(E)} - p_{\ell}^{(c)} \right| ,$$

maximized with respect to failure port, test criterion pair, and surface penetration modes.

The transfer function represented by the bracket in I_w in Eq. (E.1) is computed by the OSU computer code in Assessment 1 and contains significant errors.

The measure of error adapted for the H-field error analysis is the area under the f-domain amplitude curve because this corresponds well with the F^{-1} or t-domain peak value.

To compute the transfer function H^{OSU}/E^{OSU}, five frequency bands were distinguished:

$f < 1$ MHz , region of serious digitization error.

$1 < f < 6$, main fuselage and wing resonances.

$6 < f < 12$, higher order resonances.

$12 < f < 20$, higher order resonances.

$20 < f < 100$ MHz , response roll-off region.

The OSU code was not accurate in this last range; a 6 dB/octave roll-off was assumed.

Of the measured and predicted surface magnetic field H_s, typically the latter runs high in the 5-8 MHz region (SRF simulator). Digitization (offset) error renders measured values inaccurate for $f < 1$ MHz where the measured values are weak. The same general comments hold for the VPD simulator. The University of Michigan predictions of H_s show better agreement with measurement.

Sections III.3 and III.4 of the reference are devoted to the internal coupling subject of comparison of predicted and measured internal cable/wire currents. For lack of space these will not be commented upon.

Table 5.7 of Ref. 1 summarizes the external coupling errors, their means and standard deviations, from measurements at various test points and segments in the VPD and SRF simulators. It was found that the SRF and VPD simulators were so consistent shot-to-shot (ignoring "hang-fires") that their variations were very small relative to other assessment errors. For SRF-variations e/e_0 is lognormal and the 90%-90% interval in 20 log (e/e_0) is ± 0.85 dB. For VPD-variations the number is ± 1.4 dB. It was concluded simulator variability was ± 1 dB 90% of the time, with 90% confidence, and smaller over shorter test periods.

Errors in transmitter gain, dielectric waveguide variations and scope vertical calibrations were all lumped into an "error in calibration pulse accuracy" $< \pm 1$ dB. The remaining raw data error was $\simeq \pm 1$ dB worst-case in probe calibration. However, probe calibration was fixed for each test and no evidence exists for microwave transmitter calibration pulse-error changing during a test. The worst-case raw-data error seemed, therefore, to be ± 2 dB.

Digitization and computer processing errors were most significiant: t-domain digitization errors, f-domain amplitude and phase errors, or F^{-1} t-domain errors. Errors are relative to $I_{peak}(t)$. And ± 3 dB was taken as the 90%-90% error interval on the peaks of the inverse transforms to account for dititization and machine processing errors.

Summary of measurement errors; 90%-90% confidence intervals:

No.	Error source	VPD, dB	Simulator	SRF, dB
1	Simulator variation	± 1.4		± 0.85
2	Calibration errors	± 2.0		± 2.0
3	Processing errors	± 3.0		± 3.0
Total, $\sqrt{e_1^{\,2}+e_3^{\,2}+e_2}$		± 5.3		± 5.1

POE location errors were addressed for Assessment Method 1. Three measured f-domain wire currents were extrapolated as $(H_{threat}/H_{sum})_{OSU}$ code at 16 different POE locations. After getting $F^{-1}[\, I_{threat}(f)] = I_{threat}(t)_{peak}$, the area under the $\left| I_{threat}(f) \right|$ curve was compared to peak $I_{threat}(t)$. Each of the three currents was extrapolated, at location 2 (see Table 36 of Ref. 1) for the minimum peak value and location 3 for the maximum. The geometric mean current was found and variations about it represent error. The numbers were: $I_1 = 368$ A $\pm$ 7 dB, $I_2 = 4.55$ A $\pm$ 7.7 dB, and $I_3 = 0.066$ A $\pm$ 5.5 dB. These conservative estimates carry no R-C intervals.

Similar extrapolation to ground alert mode give dB errors for a dozen wires ranging from ± 2.9 dB to ± 11.8 dB.

Power on-off considerations: Several measurement points were chosen for worst-case, and another set was chosen for low threshold and large signal current. Of 32 samples, the 90%-90% interval was $\simeq$ (-11.8, +7.6) dB, or -2.1 ± 9.7 dB. More exactly, it was -2.1 + 10.0 dB. Thus, to represent this

effect the nominal wire current with the system on should be reduced 2.1 dB from its simulated-on value and an additional ±10-dB error added in rss fashion to the error interval.

It was found the nulls in the f-domain data do not alter the t-domain peaks very much, only 0-3 dB!

Extrapolation of the University of Michigan f-domain data (Assessment Method 2) from 20 to 50 MHz by two different functions gave a 3.7-dB difference for one of the wire current peaks and ≲ 2 dB for 109 out of 121 other wire currents.

A Monte Carlo validation of the rss error method was made, based on 27 measurements of three wires (this is a very small sample). Sixteen POE locations were selected randomly with replacement until 27 were obtained. Incidentally, the POE location error in a wire current was taken relative to the goemetric mean $|I_w|_{gm} = (|I_w|_{max}|I_w|_{min})^{1/2}$, where max and min refer to all POE. Then the POE error was $\pm 20 \log (|I_w|_{max}/|I_w|_{gm})$ about this mean. The details of the Monte Carlo procedure will not be described here. The errors represented were, from Table 5.5 of Ref. 1.

- Measurement error, including simulator variation, of ±5.3 dB.
- POE location error of ±6.1 dB (conservative).
- Calculated H-field error for numerator of Eq. (8.3.1), ±7.2 dB.
- Calculated H-field error for the denominator, also ±7.2 dB.

The predicted rss 90%-90% interval from all these is ±12.9 dB.

The Monte Carlo experiment showed ±15.6-dB variation among the $I_w(t)$ peak values. Is this compatible with the rss interval of ±12.9 dB? The report argues that there is a 0.737 confidence that this range of 27 Monte Carlo samples will bound 95.3% of the population, and the confidence is about

the same for the rss interval of +12.9-dB bounding 90% of the population. One feels the Monte Carlo-rss comparison should be analyzed further and should be based on a larger sample of the former.

REFERENCES

1. EMP Data Reduction Variables Analysis Study, Braddock, Dunn & McDonald, Alburquerque, NM (May 1977).

2. Horizontally Polarized Dipole, Electromagnetic Pulse Simulator Upgrade Test Program. Characterization Report Vol. IV Error Analysis Report, EG&G, Alburquerque, NM, Al-1295 (April 1978).

3. C. Ashley, Probability and System Statistics Note, PSN-1, Confidence and Reliability in a Finite Population, AFWL, Kirtland AFB, Alberquerque, NM (February 1971)

4. In-place EMP: A Discussion of Errors in Time Domain Inverses from the Frequency Domain, Rockwell Intern., Anaheim, CA (June 1971).

5. EC-135 EMP Assessment Program Final Assessment Report, Vol. III Assessment Error Analysis, Rockwell Intern., Anaheim, CA (November 1977).

6. Measurement Note 24, Deterministic Error Analysis Applied to EMP Simulator Data Acquisition, Mission Research Corp., Albuquerque, NM (June 1977).

APPENDIX F
USEFUL DATA PROCESSING RELATIONS

Some useful data processing relations were quoted in Ref. 1, relating standard deviations of f-domain data to their t-domain counterparts. For example,

$$\sigma_f \simeq \sqrt{N\Delta T}\,\sigma_t \ , \ T_{max} = N\Delta T \ , \qquad (F.1)$$

where

σ_f (σ_t) is the standard deviation of a signal in the f-(t-) domain,

N is the number of samples of width ΔT in the time window T_{max}.

The report[2] contains the observation that errors and error analysis depend on QC (quality control) which cannot be fully quantified. So one must prepare multiple data samples using the best QC available and a conduct regression analysis.

It was found by EG&G[2] that data in integrated form in the t-domain had virtually the same confidence limits as the data after F-transformation to the f-domain, and F^{-1} transformed back to the t-domain. But data in derivative form in the t-domain, F-transformed, then integrated in the f-domain, then F^{-1} transformed to the t-domain had final confidence limits which increased monotonically with time.

A strong correlation was observed between data f-domain magnitude credibility (where relative error remained < 100%) and associated phase stability.

For the oscilloscope/film data base six sets of data photographs were chosen, three of integrated data and three of derivative data. For the DASET data base, 40 data traces for each of the 5 microwave system channels were analyzed statistically. The statistical analysis* of the scope/film data base

*It is claimed, but is not obvious, that the EG&G method gives independent statistically varying representations of the same data trace.

alone for the 90%-90% confidence interval (CI) about the true data trace was determined by Ashley's distribution-free procedure in Note 3.[3]

After this t-domain statistical processing for the 90%-90% CI, the data sets were all transformed into the f-domain where the same statistical processing yielded the 90%-90% CI in that domain. Then the waveforms were F^{-1} transformed (derivative data were integrated in the f-domain prior to transformation) and the 90%-90% CI obtained in the t-domain again. Comparison of the earlier 90%-90% CI obtained directly in the t-domain with those obtained after the double Fourier transformation indicated the two 90%-90% CI were virtually identical for integrated data in either data base. Evidently, f-domain phase information is not necessary in such data processing situations for confidence intervals in the t-domain.

RELATIONSHIP OF ERRORS IN f- AND t-DOMAINS

In 1971, an internal memo[4] discussed the errors which occur when multiplying a transfer function T(f) by the criterion field $B_c(f)$ in the f-domain and then taking the inverse F-transform to obtain peak time response. It is implied that phase was neglected in the product TB_c. An empirical result found was that the upper (lower) confidence limit of the tranfer function multiplied by the criterion field and then inverse transformed yielded the upper (lower) confidence limit in the t-domain.

There is no analytic basis for the statement. Twenty-five Monte Carlo runs were taken, starting with randomly added digitization errors added to measured I(t) and B(t). Of the quantity $I_c(t) = F^{-1}\left[(I(f)/B(f))B_c(f)\right]$ it was stated "the errors to 90% confidence run about $\pm$6 dB about the nominal"--presumably, at the 90% confidence level.

It was stated that "Inverses of the f-domain confidence limits provide t-domain confidence limits which are both accurate in peak value and suggestive of potential wave shape variation."

Regarding the confidence intervals in the t- and f- domains, when the area $\int |I_w(f)|\, df$ and peak $|I_w(t)|$ are listed for each of the 27 Monte Carlo runs, it was found that the maximum variability in the f-domain is $\pm$15.5 dB, very nearly the maximum variabvility of $\pm$15.6 dB in the t-domain. (The run with maximum or minimum f-domain area was not necessarily the run with maximum or minimum t-domain peak). This information suggests that the C-confidence limits in the f- and t-domains do correspond in some situations, and that one should try to deduce general conditions for this correspondence.

ERROR AND UNCERTAINTY RELATIONSHIPS

Three references (Refs. 2, 4, 5) suggest a useful relationship between confidence interval CI in the t-domain and the same or nearly the same confidence interval in the f-domain. In Ref. 2, 40 time traces from a DASET representing integrated data indicated that a 90%-90% CI in the t-domain was nearly the same as the one obtained by inverse transform of the 90%-90% CI in the f-domain, neglecting phase. Reference 4 states the same thing more generally. In Ref. 5, Table 36, the dB difference between maximum and minimum t-domain wire currents, as determined by 16 POE locations, was quite close to the dB difference between their f-domain amplitude integrals. This was true of two or three internal wires examined.

Evidently in many situations one can expect a close relationship between an f-domain CI and a corresponding t-domain CI, although no strict analytic relationship is apparent.

A useful relation between the effective standard deviation σ_f in the frequency domain and its σ_t counterpart in the time domain is

$$\sigma_f = \sigma_t \Delta t \sqrt{n/2} \quad , \tag{F.2}$$

where n is the number of time samples at intervals Δt and the measurement time is $T_{max} = n\,\Delta t$ (Refs. 2 and 6).

APPENDIX G
FINITE DIFFERENCE (FD) ANALYSIS OF AIRCRAFT RESPONSE

Time-domain predictions from the code THREDE were compared with HPD measurements on an F-111 airplane sitting on an imperfectly conducting ground.[1] The craft was modeled by about 22,000 cells, each 1 by 1 m in the xz-plane by 1/2 m in the vertical y-direction from any extremity of the model to the computational radition boundary; ≥ 9 corresponding cells in the y-direction. A numerical upper limit of 75 MHz was imposed by the cell size ($\Delta \leq \lambda/4$).

The ground value of conductivity σ was set to 0.05 mho/m for best agreement of measured and computed axial current density on the aircraft belly (response was much less sensitive to μ, ϵ). The ground ϵ was taken as $7\epsilon_0$.

THREDE was driven by a modeled field with a reflected component based on a time-dependent reflection coefficient. This was justified by a very good agreement between computed and measured fields E_x and H_z at one point on the HPD Range, in an interval near the time peak.

It was necessary to compute over an interval ≤ 200 ns to obtain peak time response. The computer cost was about 1 s of CDC 7600 run time per ns of computed data. The accuracy in computed peak temporal surface current tended to be about ± 6 dB.

---

1. K. S. Kunz and K-M Lee, "A Three-Dimensional Finite Difference Solution of the External Response of an Aircraft to a Complex Transient EM Environment: Part I - The Method and its Implementation," IEEE Trans. Electromagnetic Capability EMC-20 (May 1978).

APPENDIX H
RESULTS IN SUSCEPTIBILITY

RESULTS OF SPECIFIC WORKS

1. Tasca and O'Donnell in work done for HDL in 1977[H.1] present work on 252 integrated circuits which were tested. There were 11 part types and five categories (TRL, DTL, TTL, ECL, and linear). This work is believed to be significant in regard to uncertainty investigations. It has:

   - Some evaluation of existing techniques for failure threshold prediction.
   - Modeling information.
   - Actual data on types that were tested from 10 ns to 10 μs pulse widths.
   - Confidence limits attached to presentation; all devices were tested with unipolar, step-stressed pulsing.

2. The Tasca and Stokes work (1976)[H.2] for HDL/DNA has damage models developed from multiple regression analysis of the large (existing at that time) experimental data base from HDL and AFWL. Separate models were developed for "classes" of devices, such as devices functionally classified as "rectifiers, diodes, and switches." Construction type diodes functionally classified or zener diodes are included also.

   Representative data from Ref. H.1 and H.2 are shown in Figs. H.1 through H.4 and in the section Tables of Specific Results at the end of this Appendix.

3. Kalab at HDL provided a draft report[H.3] of work he has recently completed on the damage characterization of semiconductor devices for specific equipment. He does make comparisons between experimental device

failure powers and the failure powers predicted by the theoretical models. The comparisons were made on diodes and transistors and use the junction capacitance model. Order-of-magnitude factors occur between K_{th} and K_{exp}. The problem of unipolar vs full-cycle waveform testing is discussed and a case for uncertainty in detail of failure due to transient excitation is raised. Prior work is cited regarding waveform differences (1N4148 diode). There is much data in tables presented.

4. Miletta (1977)[H.4] reports on pulsed transient tests on over fifty component types. About 1800 individual devices were damage tested. (The testing appeared to be done in the 1972 time period.) The report shows the model assumes log-normal distributions. However, no one type of distribution provided a consistently good fit to the experimental data, as was pointed out in the paper. This work substantiates to a certain degree the work presented in the EMP Handbook with respect to classes of devices. The work implies a need for better understanding of failure threshold distributions for refined estimates of such thresholds using empirical formulas.

5. Jenkins and Durgin (December, 1977) present statistics[H.5] associated with open-circuit failure voltages for seven IC types. The results of comparisons of measured data with predictions obtained from the Jenkins-Durgin model show that the model provides conservative predictions. The empirical model is, $P_F = At^{-B}$ where A and B are empirically determined constants.

6. Egelkrout (1978) has presented a paper[H.6] which includes analysis of data taken at Boeing over the past several years. The summary of the paper at the IEEE Annual Conference on Nuclear and Space Radiation Effects and communications with Egelkrout (see also Ref. H.7) indicate lot-to-lot or vendor-to-vendor variations must be considered in establishing safety margins. It is pointed out that insufficient data are available to summarize the lot-to-lot variation in low failure probability levels.

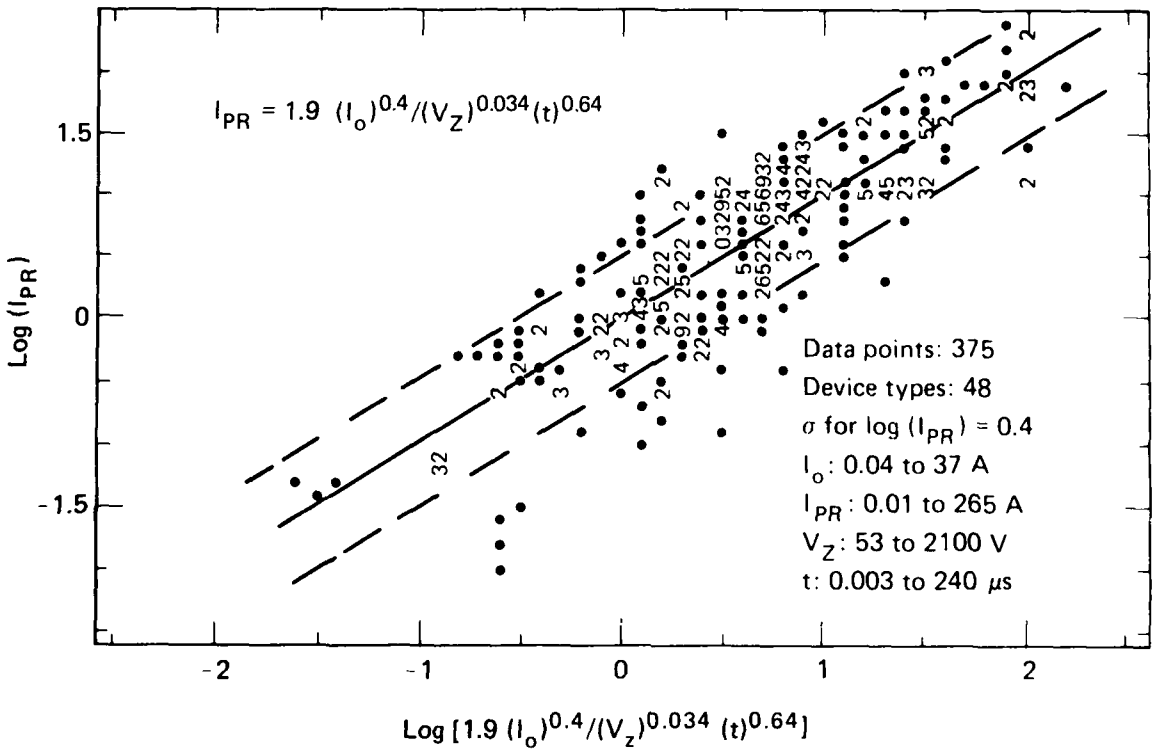

FIG. H.1. Example of the type of uncertainty data presented in Ref. H.2. Plot shows reverse pulse damage current characteristics for all contruction-type diodes functionally classified as rectifiers, diodes, and switches.

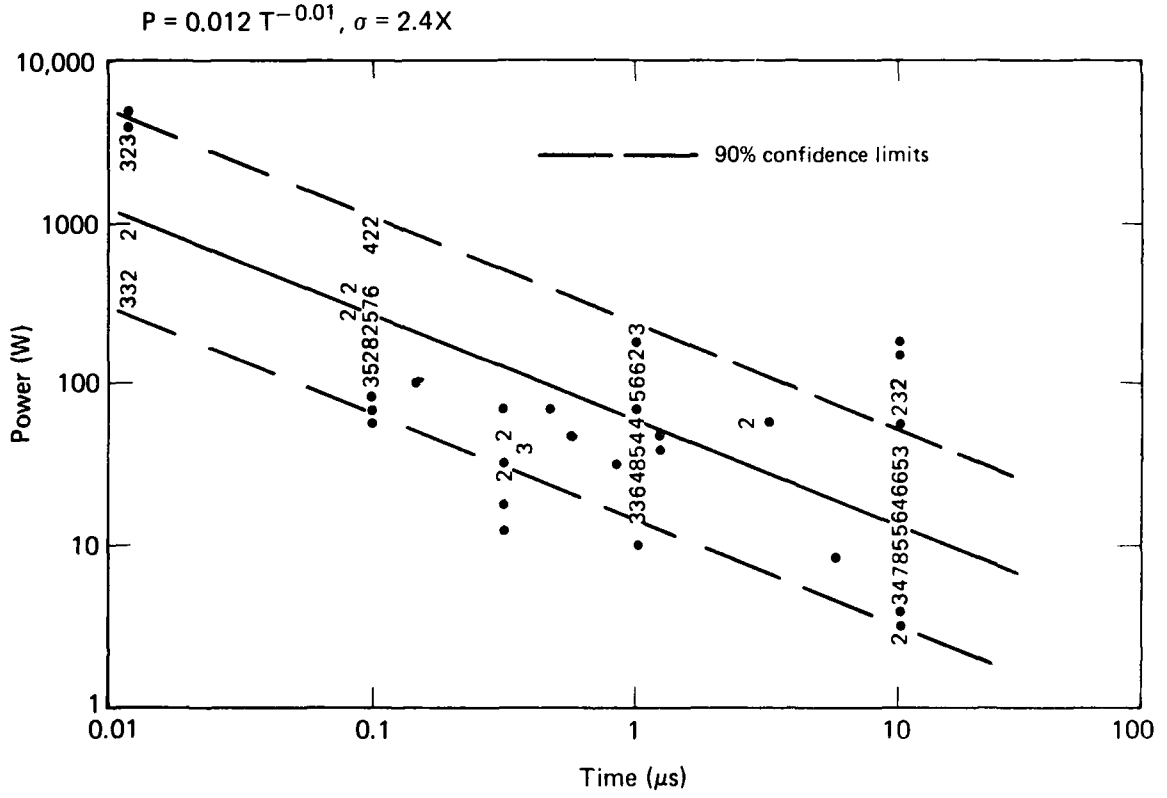

FIG. H.2. Example of uncertainty data taken from Ref. H.1. Input power failure model for standard TTL devices.

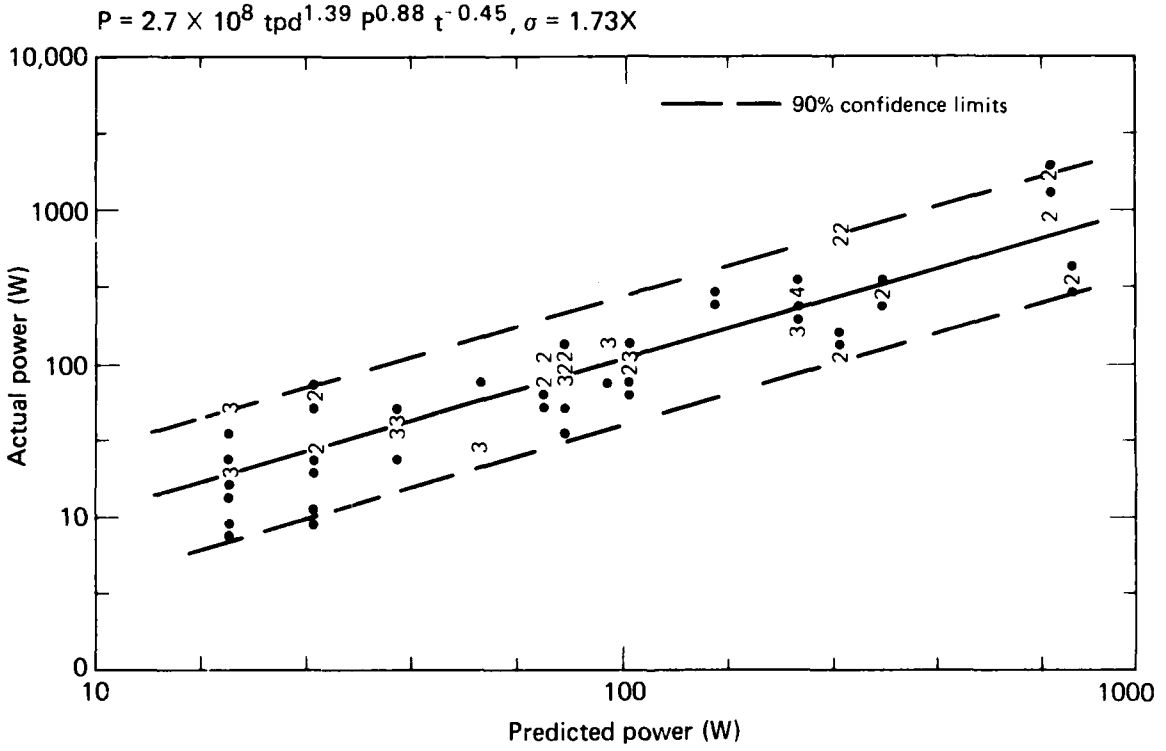

FIG. H.3. RTL input power failure model including electrical parameters (Ref. H.1).

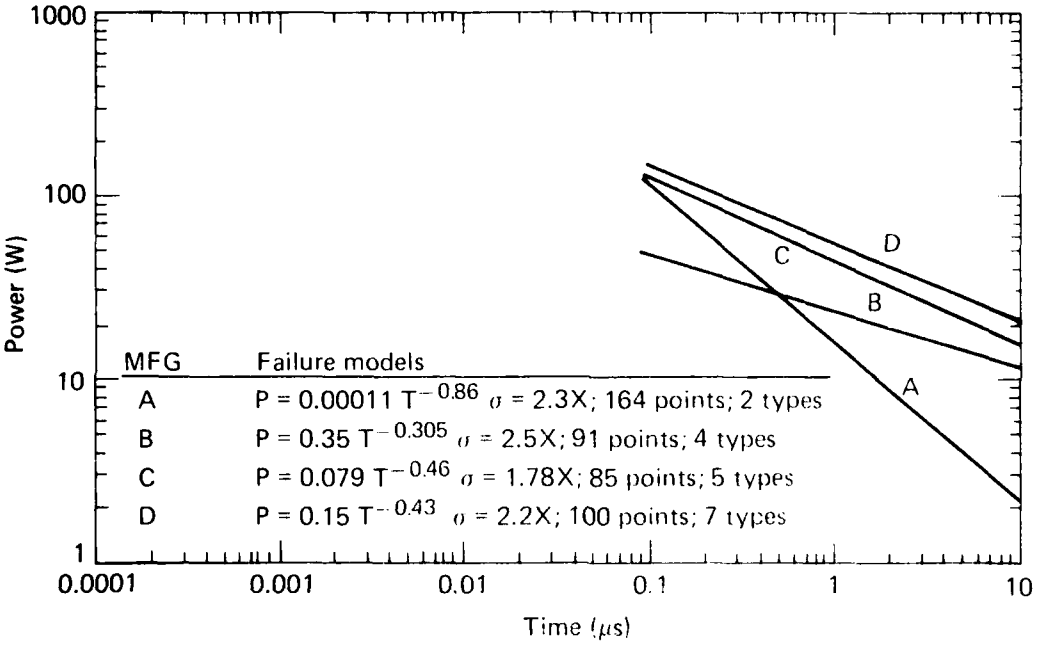

FIG. H.4. Example of uncertainty data taken from Ref. d.1. Comparison of input-ground power failure thresholds for different manufacturers of DI devices.

The actual damage points are plotted vs time delay for the devices. The plots are shown from 10^{-8} to 10^{-5} s. Spread in failure data was investigated for the 2N1132 transistor as 150 were tested to failure. Failure was arbitrarily defined as a 20% degradation in junction breakdown voltage or device gain. Histograms display the variation.

7. Navy-contracted Lockheed work (Kusnezov and Crowther 1976, Ref. H.5) involved current injection testing of some six types of integrated circuits (NAND gates, multiplexers, ROMs, RAMs, or OPAMPs). This work has the data on tests. It is not presented in a statistical format, but it does include the range of values encountered. It also includes the functional failure criteria and fits failure curves of the type,

$$P = At^{b+c(\ln t)} W \quad .$$

Simple equivalent circuits do not fit the data, which are presented in numerical form. There are also data on surge resistance and some discussion of the use of the data. The test configurations are discussed in detail. Examples from this work are shown in Figs. H.5 to H.9 and in Tables H.7 and H.8.

8. Williams at HDL[H.8] reviews and discusses device damage data and relates it to probability of device damage. The thermal response is obtained for nonrectangular waveforms by convolution, and effects such as a significantly lower probabilty of survival for multiple peaks close together are pointed out. Damage assessment is based on the assumption of approximately lognormal distributions for damage data.

9. The work by Le Poer and Behrens in 1977[H.10] is an example of a theoretical assessment of a small system (albeit foreign). It is performed theoretically with the aid of circuit analysis by computer. The antenna response is found separately, and the source is used in the receiver front-end equivalent circuit. The process is relatively straightforward, providing that the equivalent circuit can be derived from the equipment description or other information.

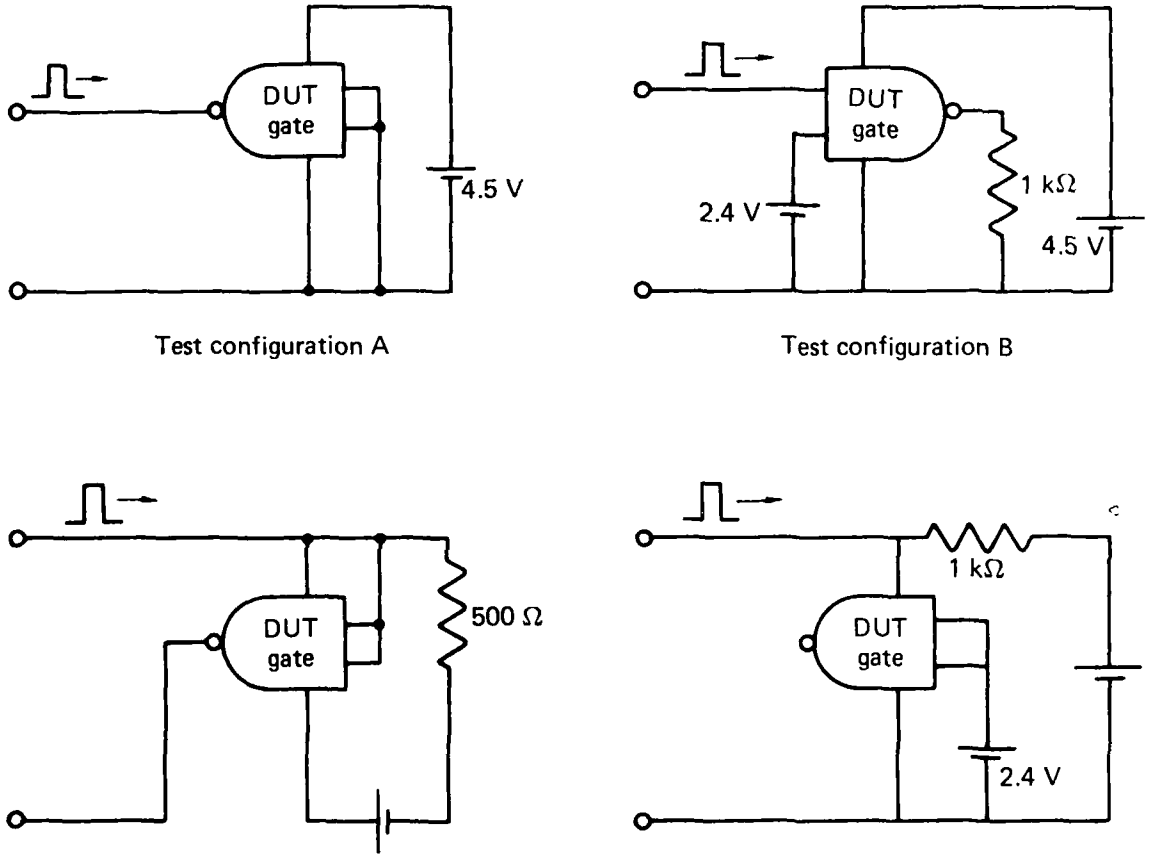

FIG. H.5 Test connections for the 306481] two-input NAND gates used in the current injection testing. In configurations C and D, supply voltage was adjusted so that 4.5 V appeared at the gate VCC terminal (Ref. H.9).

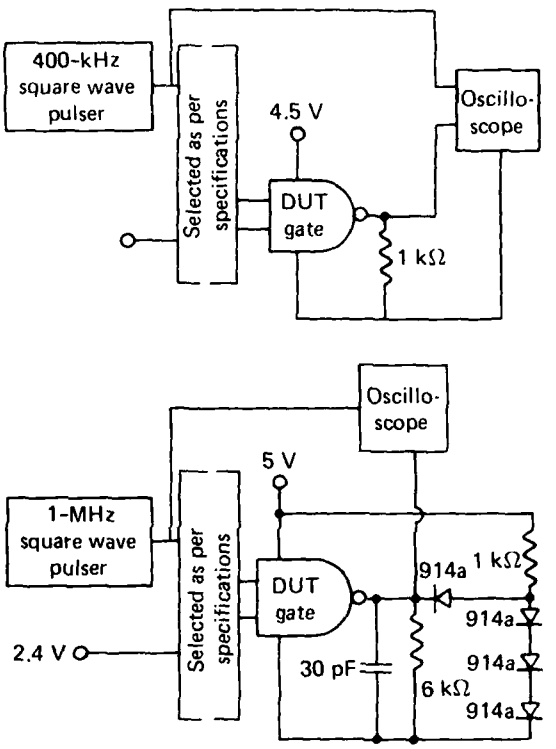

FIG. H.6. Connections of the 3064811 two-input NAND gate for the post-test checkout. At the top is the circuit used for the truth table content verification, on the bottom is the switching test circuit. Capacitance of 30 pF includes the scope input capacitance. The 914a diodes were held to be equivalent to 1N3064 diodes required by the specifications and were used in the test circuit instead of 1N3064's (Ref. H.9).

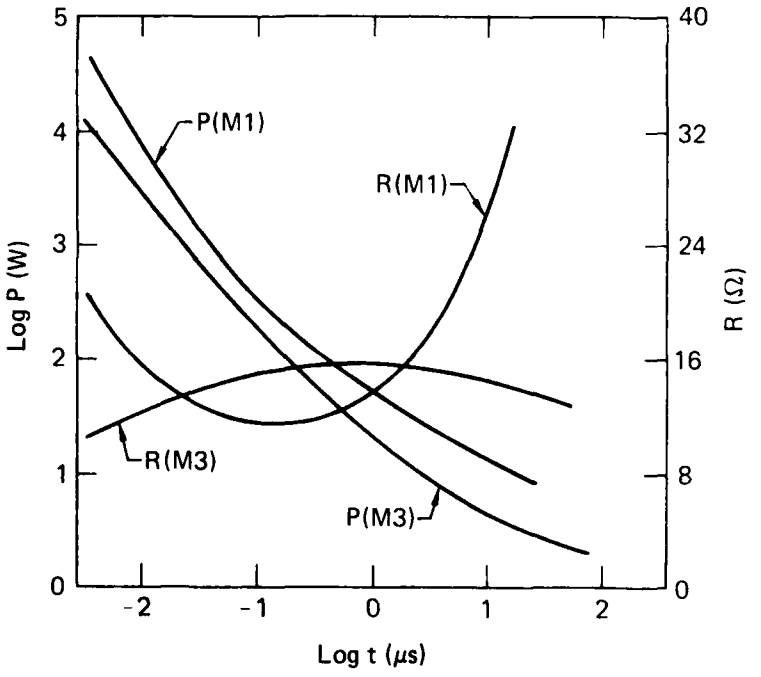

FIG. H.7. Summary of the experimental results for dielectrically isolated 3064811 two-input NAND gates. Failure powers and failure resistances for test configuration A, measured at 16 s, 1 s, and 4.5 ns are presented as least-square quadratics fitted through the data points. Curves connecting points measured for NAND gates of two different manufacturers are differentiated by indicies M1 and M3 (Ref. H.9).

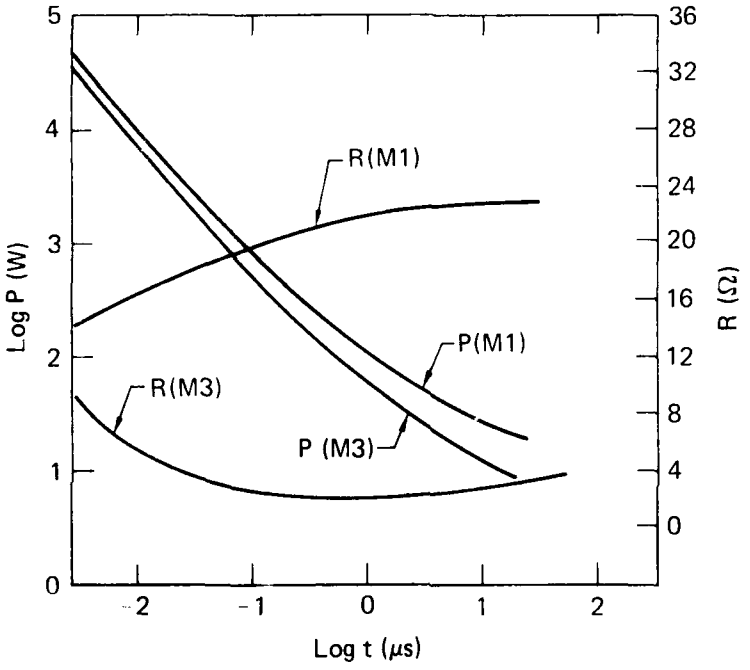

FIG. H.8. Summary of the experimental results for dielectrically isolated 3064811 two-input NAND gates. Curves are least-square quadratics fitted through the data (16 μs, 1 μs, and 4.5 ns) obtained for test configuration B. M1 and M3 denote different manufacturers (Ref. H.9).

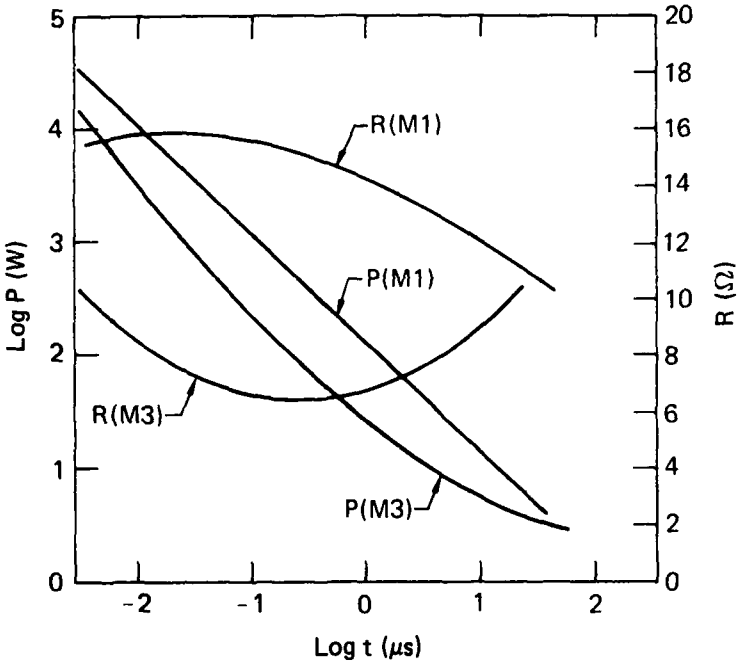

FIG. H.9. Summary of the experimental results for dielectrically isolated 3064811 two-input NAND gates. Curves are least-square quadratics fitted through the failure power and resistance data of configuration C. M1 and M3 denote different manufacturers (Ref. H.9).

10. The Safeguard program, Corps of Engineers 1975,[H.11] has employed a principle of "representation" for EMP assessment for many thousands of subsystems. Five-thousand six-hundred thirty-three items are represented by 26 subsystems. The technical uncertainties uncovered in the process are listed below.

- Internal environment - concrete rebar.
- Small metalic enclosure attenuation.
- Instrument pickup, conducted and field near device.
- Buried conduit pickup.
- Shielding of flexible joints.
- Additions to signals via induced signals (networks, multiple sources, and cross-coupling.
- Energy isolation devices (switches, shielded transformers, filters, peripheral welds, MG set, and DC power supply).
- General use of representation principle.
- "As-built" conditions (vs "as-designed").
- Equipment failure or upset thresholds.

No validation of the representation principle was performed in the Safeguard program. However, the technical uncertainties suggest difficulties in attempting such a task without very much engineering judgment included.

11. In the 1977 IITRI work,[H.12] the objective was to determine the effect of EMP stressing on the reliability of selected semiconductor devices. Screening at high levels of testing may possibly damage components in the

long run. Multiple pulsing of semiconductors apparently increases damage when levels approach the damage point for one pulse. The IITRI data for the 2N918 under carefully controlled conditions shows significantly more failures among the devices stressed at a small fraction of the damage threshold (0.1) than those stressed at a 0.93-fractional level. In conjunction with this work, 61 1N918 transistors were tested to failure to determine the distribution of the damage threshold. The data approximates a normal curve well, and also a lognormal distribution since the logarithmic standard deviation is small.

12. H. M. Olson, "DC Thermal Model of Semiconductor Device Produces Current Filaments as Stable Current Distributions, IEEE Transactions on Electron Devices, vol. ED-24, No. 9, September 1977.

The model demonstrates that conductance rises as temperature increases, current flow in the device becomes filamentary; at a critical level of power dissipation, the uniformly distributed current suddenly shrinks into a tight filament, thus creating an intense hot spot. The model simulates the avalanche diode burnout mechanism. It is device oriented. The use of such models at the device design level may help remove some of the uncertainties connected with burnout.

13. M. Lutzky, E. B. Dean, Jr., and M. C. Petree, "Modeling Second Breakdown in PN Junctions with NET-2," IEEE Transactions on Nuclear Science, vol. NS-22, No, 6, December 1975.

This paper provides an example of the complexity of modeling the large signal nonlinear breakdown behavior of a diode junction. Even this complexity, which has the diode equation

$$I_D = I_s(e^{q_V/K_T}-1) \quad ;$$

the saturation current

$$I_s = AT^3e^{\left[-qV_g/kT\right]} \quad ;$$

the avalanche breakdown,

$$I_z = \frac{V_J - V_{RB}}{R_{sc}} \quad ;$$

and the temperature computation (heat conduction PDE), does not have other effects. The paper recommends inclusion of forward effects, capacitance, and also the connection between second breakdown and burnout. The complexity would make system simulation somewhat unwieldly.

14. J. S. Smith, "Electrical Overstress Failure Analysis in Microcircuits," 16th Annual Proc., Reliability Physics, 1978, pp. 41-46.

This work is an example of working backward from a failed device in order to determine the dimensions of the electrical transient causing failure. Conditions which set this stage are well-defined features such as resistive open or short circuits, "softening" reverse characteristics, and gain degradation in transistors. Metallization burnout is related to pulse width of transients.

15. D. W. Egelkrout, "Component Burnout Hardness Assurance Safety Margins and Failure Probability Distribution Models," Paper submitted to IEEE Transactions on Nuclear Science for vol. NS-25, No. 6, December 1978.

A typical EMP program has three phases (1) assessment, (2) detailed analysis and design, and (3) hardware production and lot hardness verification. In phase 2, safety margin is based on acceptable component failure probability, deviations of failure levels from means, lot and vendor variations, and costs. For systems with large numbers of components N, system failure probability can be high even if device failure probability is low. Actual system failure probability is complex to determine. Previous data on failures are compared many ways with both log-normal and Weibull distributions. A demonstration of a need to use a failure model such as $P = At^{-B}$ is given; data shows B-variations between 0.2 and 1.2. The data indicates that typical existing component

burnout hardness assurance approaches may be inadequate. Instead of 10 dB, for instance, the recommended lot control point is 30 dB for safety margins of mean burnout level to expected stress level ratios.

16. W. J. Stark and G. H. Baker, EMP Analysis of an FM Communications Radio with a Long-Wire Antenna, Harry Diamond Laboratories, HDL-TR-1846 (June 1978).

Appendix A of this reference discusses errors in computed-aided system simulation. Errors are due to the following:

a. Incomplete models.

b. Simplified driving function representation.

c. Limited experimental data.

d. Variance in real system component characteristics.

e. Numerical differentiation/integration.

f. Nonlinear equation convergence check tolerances.

Error sources in categories (a) and (b) were minimized in this study through detailed modeling of the long wire antenna and circuit topology of the radio. The antenna as a component is modeled by a linear lumped parameter network, while other receiver components are represented by lumped parameter networks, some of which are nonlinear. A note on the error source in category (d) points out that the inherent uncertainty in the real system's response broadens the admissible range for the behavior of the modeled circuit.

Damage prediction is a goal of the assessment. The two main sources of uncertainty are:

Large spread in experimental values of power-to-damage.

Intractability of device behavior at the time of failure.

17. R. L. Pease, D. R. Alexander, and C. R. Jenkins, Electrical Overstress Program and Integrated Circuit Failure Mode Evaluation, the BDM Corporation, Defense Nuclear Agency Report DNA 4467F (April 26, 1976).

Device physical parameters which have been identified as influencing failure distributions:

- Junction Area.
- Background doping concentration.
- Epitaxial thickness.
- Junction radius of curvature.
- Metallization and Diffusion Spikes.

Failure modes for different categories of integrated circuits:

- DTL: Input - diode junction failure.

  Output - transistor junction damage.

- RTL: Input - transistor junction damage, and also adjacent transistor damage.

  Output - transistor short or degraded gain.

- TTL: Input - clamp diode.

  Output - transistor junction damage.

- ECL: Input - transistor junction failure.

  Output - transistor (metallization failure).

- Linear: Input - transistor junction damage.

  Output - several modes.

- MOS: Input - device type dependent metallization burnout, oxide punch through.

TABLES OF SPECIFIC RESULTS

Included here are several sets of tables which express the statistical nature of the large variety of semiconductor components and methods of failure modeling. Some of this reported work represents the results of much study of previous component testing in attempts to express the variability and to develop more accurate models. The work by the group at General Electric[H.1,H.2] is particularly complete in demonstrating this. Also, earlier work by Boeing/BDM is significant.[H.13] There is a large amount of data and it appears that much more is needed for detailed, accurate analyses and control of parts in production.

The following tabulations are not meant to be complete, as some of the referenced reports are already tabular in nature and should be consulted for applications. These tabulations permit the investigator to observe the many failure parameters involved along with some associated confidence factors.

Table H.1 shows subsystem test vs analysis uncertainty ranges for several airborne systems expressed on ratios of thresholds. The ranges are from 0.5 to 744 for current threshold prediction.

Table H.2 illustrates the problem of prediction of failure constrants from various models. The ranges are from 2 to 310 for small sample sizes indicated.

Table H.3 is illustrative of the type of uncertainty work and presentation currently being pursued in integrated circuit modeling and testing. Models are of the form At^{-B} for Power, Current, and Resistance. R varies with current. R_{AVG} is found from V_{AVG}/I_{AVG} during the pulse time. Note that the current failure model shows smaller variation than the power mode. Tables H.4 and H.5 show variations in polarity groupings. By comparison, Table H.6 shows failure models as presented in the DNA EMP Handbook (data from Jenkins and Durgin in 1975). Here values of breakdown voltage $\bar{V}_B$ and surge resistance $\bar{R}_B$ are given as required in the associated equivalent circuit consisting of R_B and V_B in series for different terminals. Also by comparison, another approach is illustrated by Tables H.7 and H.8 for one example, the 811 dielectrically isolated NAND gate integrated circuit of the TTL family. P for failure is expressed by $P = At^{b+c(\ell n\ t)}$. R has a similar expression. A value of minimum energy for failure is given.

Diode information from nearly all available sources was analyzed in Reference 17. The summary of damage models is presented here in Tables H.9 and H.10. These models use the familiar t^{-1}, $t^{-1/2}$ variations and correctly express the surge resistance as nonlinear.

In addition to these tables presented here for illustrations, there are many more such types of presentations in the References. There are many problems in attempting to represent a highly nonlinear process, as occurs in device failure, by a few simple parameters that can be used accurately and effectively in assessment problems.

TABLE H.1. Box test correlation summary (Ref. H.14).

Sys No.	Box Name	With Post-Test Thresholds I_F/V_T[a] Min	Max	V_F/V_T[a] Min	Max	With Pre-Test Thresholds I_F/I_T[a] Min	Max	V_F/V_T[a] Min	Max
1		7.88	8			1.2	8		
3		0.64	156	0.92	258	0.64	156	0.6	258
31		6.7	8.1	8.1	8.6	6.7	8.1	8.1	8.6
31		0.5	3	5	17	0.5	2.4	1.1	9.6
31		0.7	12	0.3	0.6	0.7	12	0.3	7.6
61		1.9	7.5	1.3	3.7	1.9	3.1	0.56	1.6
61		1.7	12	1.3	4.0	0.35	9	0.17	2.5
69						78.9	744	71.1	1.5
81		1.5	11.3	2.0	3.7	0.7	5.1	4.5	25
81		1.9	4.2	1.3	2.8	2.4	9.8	1.3	10.7
81		1.2	1.5	0.44	0.68	0.69	8.5	0.07	3.8
31		No Burnout Noted - Transmissibility Assumptions Verified							
61		No Burnout Thresholds Noted, Arc-Over Predictions Verified							
87		3.7	37	3	9	8	22	1.8	11
28		1.17	10.1	2.02	10.1	1.17	10.1	2.02	10.1

[a]Subscript F denotes Test failure threshold and subscript T denotes analytical threshold. Post Test implies new information for models.

TABLE H.2. Transistor and diode test correlation (Ref. H.14).

	Ratio of Test K Factors to Predicted K Factors								
	Collector Base			Base Emitter			Diodes		
	Min	Max	Range	Min	Max	Range	Min	Max	Range
Junction Capacity Model									
Power (K_D)	0.78	19	24	0.16	9.2	58	0.014	1.7	121
Current (K_I)	0.35	23	66	0.05	2.1	42	0.010	1.0	100
Sample Size			16			16			6
Thermal Resistance to Case Model									
Power (K_D)	0.085	5.0	59	0.09	2.4	27	0.18	0.50	2.7
Current (K_I)	0.02	2.8	140	0.02	1.0	50	0.06	0.12	2
Sample Size			14			14			3
Thermal Resistance to Case Model									
Power (K_D)	0.024	9.5	395	0.0085	4.2	494	0.021	6.5	310
Current (K_I)	0.024	3.9	162	0.006	3.4	567	0.018	4.0	220
Sample Size			14			14			2

TABLE H.3. Summary of TTL models (Ref. H.1).

Model	Input	σ	No. Points	No. Types	Output[a]	σ	No. Points	No. Types	Power	σ	No. Points	No. Types
ALL TTL												
P_{avg}	$P=0.00036\ t^{-0.87}$	3.3X	571	39	$P=0.0186\ t^{-0.61}$	2.6X	397	28	$P=0.0021\ t^{-0.87}$	2.8X	177	14
I_{avg}	$I=0.00134\ t^{-0.53}$	2.3X	532	32	$I=0.031\ t^{-0.35}$	1.9X	393	27	$I=0.0096\ t^{-0.48}$	2.1X	177	13
R_{avg}	$R=25.5\ I^{-0.5}$	2.0X	531	32	$R=10.7\ I^{-0.44}$	1.8X	393	27	$R=15.7\ I^{-0.37}$	1.7X	175	13
Standard TTL												
P_{avg}	$P=0.012\ t^{-0.61}$	2.4X	232	13	$P=0.0092\ t^{-0.69}$	2.4X	207	13	$P=0.00017\ t^{-1.0}$	2.1X	76	4
I_{avg}	$I=0.018\ t^{-0.32}$	2.0X	216	13	$I=0.0175\ t^{-0.41}$	2.0X	203	13	$I=0.0012\ t^{-0.64}$	1.8X	74	4
R_{avg}	$R=28.6\ I^{-0.45}$	1.7X	216	13	$R=12.7\ I^{-0.53}$	1.6X	203	13	$R=18\ I^{-0.44}$	1.5X	74	4
High Speed TTL												
P_{avg}	$P=0.02\ t^{-0.5}$	2.3X	66	4	$P=0.13\ t^{-0.43}$	1.4X	16	2	Insufficient Data			
I_{avg}	$I=0.013\ t^{-0.32}$	1.7X	66	4	$I=0.1\ t^{-0.23}$	1.5X	16	2	Insufficient Data			
	$R=17.7\ I^{-0.57}$	1.6X	66	4	$R=8$	2.0X	16	2				
Low Power TTL												
P_{avg}	$P=2.6\times10^{-4}t^{-0.9}$	3.5X	140	12	$P=0.013\ t^{-0.60}$	2.4X	43	5	$P=0.027\ t^{-0.73}$	2.5X	23	4
I_{avg}	$I=0.001\ t^{-0.55}$	2.0X	116	8	$I=0.02\ t^{-0.35}$	1.8X	43	5	$I=0.029\ t^{-0.42}$	1.8X	23	4
R_{avg}	$R=35.3\ I^{-0.48}$	1.4X	116	8	$R=15.5\ I^{-0.53}$	1.9X	43	5	$R=14.2\ I^{-0.3}$	1.8X	23	4
Schottky TTL												
P_{avg}	$P=0.1\times10^{-4}t^{-1.1}$	4.2X	39	2	$P=0.0029\ t^{-0.7}$	2.5X	43	2	$P=0.0021\ t^{-0.87}$	2.5X	32	2
I_{avg}	$I=0.00029\ t^{-0.66}$	3.5X	39	2	$I=0.019\ t^{-0.37}$	1.8X	43	2	$I=0.32\ t^{-0.28}$	1.7X	33	2
R_{avg}	$R=18.3\ I^{-0.51}$	2.2X	39	2	$R=7.1\ I^{-0.22}$	1.6X	43	2	$R=3.2$	1.6X	32	2
Low Power Schottky												
P_{avg}	$P=2.7\times10^{-5}t^{-1.0}$	2.7X	94	4	$P=1.1\times10^{-4}t^{-0.91}$	2.4X	88	4	$P=0.0026\ t^{-0.81}$	2.8X	44	2
I_{avg}	$I=0.0041\ t^{-0.5}$	1.5X	95	4	$I=0.0096\ t^{-0.42}$	1.44	88	4	$I=0.036\ t^{-0.37}$	1.7X	45	2
R_{avg}	$R=3.6$	2.2X	94	4	$R=2.9$	1.8X	88	4	$R=7.5$	1.8X	44	
ALL TTL	$P=0.12\ C^{1.7}t^{-1.02}$	2.38X	115	6								

[a]Devices with open-collector outputs are not included.

TABLE H.3. (Cont'd)

Summary of ECL models

Model	Input	σ	No. Points	No. Types	Output	σ	No. Points	No. Types	Power	σ	No. Points	No. Types
P_{avg}	$P=0.13\ t^{-0.47}$	3.56X	62	6	$P=0.29\ t^{-0.41}$	2.9X	39	4	$P=0.09\ t^{-0.64}$	1.58X	33	4
I_{avg}	$I=0.75\ t^{-0.266}$	2.22X	49	6	$I=0.16\ t^{-0.21}$	2.03X	39	4	$I=0.086\ t^{-0.31}$	1.48X	33	4
R_{avg}	$R=31.7\ I^{-0.77}$	1.80X	49	6	$R=15.7\ I^{-0.52}$	1.66X	39	4	$R=43.3\ I^{-0.81}$	1.61X	33	4

Summary of DTL models

Model	Input	σ	No. Points	No. Types	Output	σ	No. Points	No. Types	Power	σ	No. Points	No. Types
P_{avg}	$P=0.088\ t^{-0.44}$	2.5X	506	30	$P=0.0065\ t^{-0.69}$	2.1X	305	22	$P=0.093\ t^{-0.55}$	2.4X	178	16
I_{avg}	$I=0.0072\ t^{-0.37}$	1.9X	492	27	$I=0.008\ t^{-0.42}$	1.8X	293	20	$I=0.022\ t^{-0.35}$	2.0X	178	16
R_{avg}	$R=28.85\ I^{-0.84}$	2.0X	543	27	$R=26.6\ I^{-0.73}$	2.4X	293	20	$R=51.5\ I^{-0.75}$	1.9X	178	16

Summary of Linear Models

Model	Input	σ	No. Points	No. Types	Output	σ	No. Points	No. Types	Power	σ	No. Points	No. Types
All Linear												
P_{avg}	$P=0.038\ t^{-0.57}$	4.8X	217	20	$P=0.072\ t^{-0.59}$	3.3X	173	19	$P=0.019\ t^{-0.65}$	3.4X	128	14
I_{avg}	$I=0.03\ t^{-0.29}$	3.4X	217	20	$I=0.078\ t^{-0.3}$	2.2X	167	18	$I=0.046\ t^{-0.32}$	2.6X	126	13
R_{avg}	$R=53.5\ I^{-0.66}$	2.2X	217	20	$R=23.7\ I^{-0.46}$	2.3X	167	18	$R=30.9\ I^{-0.68}$	3.3X	126	13
OP-AMPS												
P_{avg}	$P=0.21\ t^{-0.47}$	4.3X	144	13	$P=0.044\ t^{-0.66}$	2.8X	112	13	$P=0.63\ t^{-0.45}$	3.2X	61	9
I_{avg}	$I=0.06\ t^{-0.25}$	3.4X	144	13	$I=0.11\ t^{-0.30}$	2.2X	106	12	$I=0.024\ t^{-0.22}$	2.44	59	7
Comparators												
P_{avg}	$P=4\times10\ t^{-6\ -1.1}$	4.5X	49	5	$P=0.12\ t^{-0.52}$	4.3X	35	4	$P=0.00085\ t^{-0.84}$	2.6X	27	3
I_{avg}	$I=3.9\times10^{-5}t^{-0.68}$	3.0X	49	5	$I=0.023\ t^{-0.35}$	2.1X	35	4	$I=0.00033\ t^{-0.60}$	2.6X	27	3

TABLE H.4. Comparison of sigma values for current and power vs time regression results for pin-pair polarities considered separately (Ref. H.1).

RTL

Terminal	Sigma	
	Power	Current
In - gnd	2.15X	2.27X
gnd - In	2.08X	2.04X
out - gnd	1.62X	1.43X
gnd - out	1.42X	1.44X
pwr - gnd	1.58X	1.22X
gnd - pwr	1.51X	1.83X

DTL

Terminal	Sigma	
	Power	Current
Ind - gnd	2.56X	1.76X
gnd - In	2.02X	1.96X
out - gnd	2.08X	1.60X
gnd - out	2.15X	1.99X
pwr - gnd	2.08X	1.66X
gnd - pwr	2.38X	1.89X

TTL

Terminal	Sigma	
	Power	Current
In - gnd	2.37X	1.85X
gnd - In	2.53X	1.88X
out - gnd	2.50X	1.94X
gnd - out	2.48X	2.09X
pwr - gnd	2.53X	1.85X
gnd - pwr	3.51X	2.44X

ECL

Terminal	Sigma	
	Power	Current
In - gnd	3.81X	2.34X
gnd - In	1.89X	1.51X
out - gnd	1.28X	1.33X
gnd - out	3.56X	2.11X
pwr - gnd	1.36X	1.66X
gnd - pwr	1.69X	1.39X

Linear

Terminal	Sigma	
	Power	Current
In - gnd	4.99X	4.28X
gnd - In	4.88X	3.39X
out - gnd	2.34X	2.08X
gnd - out	3.00X	2.35X
pwr - gnd	2.39X	1.98X
gnd - pwr	4.74X	4.97X

TABLE H.5. Comparison of sigma values for current and power vs time regression results for pin-pairs, both polarities grouped together (Ref. H.1).

RTL

Terminal	Sigma	
	Power	Current
In	2.2X	2.2X
Out	1.6X	1.6X
Pwr	1.6X	1.6X

DTL

Terminal	Sigma	
	Power	Current
In	2.5X	1.9X
Out	2.1X	1.8X
Pwr	2.4X	2.0Z

TTL

Terminal	Sigma	
	Power	Current
In	2.9X	2.1X
Out	2.4X	2.0X
Pwr	2.5X	2.0X

ECL

Terminal	Sigma	
	Power	Current
In	3.6X	2.2X
Out	2.9X	2.0X
Pwr	1.6X	1.5X

Linear

Terminal	Sigma	
	Power	Current
In	5.1X	3.6X
Out	2.6X	2.2X
Pwr	3.8X	3.1X

TABLE H.6. Failure models for 16 categories of integrated circuit types and terminal pairs developed by Jenkins and Durgin (Refs. H.1, H.15).

No.	Category		$P = At^{-B}$		V^B	R^B	Confidence Interval for A	
	Family	Terminal	A	B	(V)	(ohms)	Lower 95%	Upper 95%
1	TTL	Input	0.00216	0.689	7	16	0.00052	0.00896
2		Output	0.00359	0.722	15	2.4	0.00098	0.013
3	RTL	Input	0.554	0.384	6	40	0.12	2.6
4		Output	0.0594	0.508	5	18.9	0.0090	0.39
5		Power	0.0875	0.555	5	20.8	0.026	0.70
6	DTL	Input	0.0137	0.580	7	25.2	0.0046	0.041
7		Output	0.0040	0.706	1	15.8	0.0012	0.0136
8		Power	0.0393	0.576	1	30.6	0.009	0.17
9	ECL	Input	0.152	0.441	20	15.7	0.045	0.51
10		Output	0.0348	0.558	0.7	7.8	0.0031	0.397
11		Power	0.456	0.493	0.7	8.9	0.22	0.935
12	MOS	Input	0.0546	0.483	30	9.2	0.0063	0.47
13		Output	0.0014	0.819	0.6	11.6	0.00042	0.0046
14		Power	0.105	0.543	3	10.4	0.038	0.29
15	Linear	Input	0.0743	0.509	7	13.2	0.0054	1.01
16		Output	0.0139	0.714	7	5.5	0.0045	0.043

TABLE H.7. 811 NAND gate summary (Ref. H.9).

Terminals pulsed	Test configuration	Pulse duration	No. of M1 gates pulsed	Range of values encountered E(μ J)	R(ohms)	No. of M3 gates pulsed	Range of values encountered E(μ J)	R(ohms)
Y-G	A	4. ns	10	97-168	14-22	17	26-47	7-13
		1. μs	5	38-54	11-22	8	14-26	2-25
		16. μs	3	177-187	10-74	5	39-66	11-18
A(or B)-G	B	4.5ns	3	115-145	13-18	9	80-150	5-10
		1. μs	2	107-122	12-32	4	48-72	2-3
		16. μs	1	350	2-40	3	137-170	2-3
A,B,G-Y	C	4.5ns	6	94-131	12-21	9	25-63	8-10
		1. μs	6	87-176	11-20	8	16-30	5-8
		16. μs	4	133-179	9-17	6	63-82	7-13
V -G co	D	4.5ns	-			4	514	19
		1. μs	-			8	340-457	18-20
		16. μs	-			4	1075	25

At 16 μs and 1 μs numbers entered into resistance column represent extreme values of impedance encountered during the pulse. At 4.5 ns no significant changes in impedance occured during the pulse. M1 and M3 denote different manufacturers.

TABLE H.8. 811 NAND gate summary (Ref. H.9).

Parameters of the curves on Figs. H.7 to H.9

$P = At^{b + c\ln t}$ in W

$R = At^{b + c\ln t}$ in ohms for t in μs

Fig.	Curve	No. of points used	A	b	c	t(min) ns	E(min) μJ
H.7	P(M1)	18	47.32	-.74484	8.1574(-2)	203.3	39.17
	P(M3)	30	20.8	-.81993	5.2005(-2)	177.	17.8
	R(M1)	18	13.94	.17660	4.3859(-2)	-	-
	R(M3)	30	15.81	9.549(-3)	1.3117(-2)	-	-
H.8	P(M1)	6	114.5	-.74094	5.2103(-2)	83.2	82.98
	P(M3)	16	60.41	-.80234	5.4776(-2)	164.6	50.54
	R(M1)	6	22.11	.03246	-6.9156(-3)	-	-
	R(M3)	16	2.23	-.03802	3.0867(-2)	-	-
H.9	P(M3)	23	27.26	-.79656	5.3779(-2)	151.	22.5
	R(M1)	16	14.21	-.05634	-7.3183(-3)	-	-
	R(M3)	23	6.67	.06468	2.5252(-2)	-	-
Not Shown	P(M3)	4	398.5	-.77949	4.9554(-2)	108.	311.77
Not Shown	R(M3)	4	18.95	.06312	1.1582(-2)	-	-

Exceptions $P(M1) = 131.4t^{-.0181\ \ln t}$

$R(M1) = 13.94 - 6.46\log t - 1.77\log^2 t$ both for 16 points

TABLE H.9. Summary of pulse damage models developed for diodes independent of construction type (Ref. H.2).

DIODE TYPE	Z_{SF}	I_{PF}	Z_{DR}	Z_{SR}	I_{PR}
G.E. 1N4148	$\frac{3.4}{(I_{PF})^{0.31}}$	$\left(\frac{37}{t} + \frac{220}{\sqrt{t}}\right)^{0.59}$	$\frac{140}{(I_{PR})^{0.975}}$	$\frac{25.6}{(I_{PR})^{0.85}}$	$\frac{0.17}{t} + \frac{0.306}{\sqrt{t}}$
	σ = 1.12X	σ = 1.16X	σ = 1.06X	σ = 1.59X	σ = 1.58X
Rectifiers, diodes and switches	$\frac{1.15}{(I_0)^{0.42}\ (I_{PF})^{0.38}}$	$\frac{69\ (I_0)^{0.43}}{(t)^{0.35}}$	$\frac{0.9\ (V_Z)^{1.1}}{(I_{PR})^{0.91}}$	$\frac{0.042\ (V_Z)^{1.38}}{(I_{PR})^{0.76}}$	$\frac{1.9\ (I_0)^{0.4}}{(t)^{0.64}}$
	σ = 1.82X	σ = 1.62X	σ = 1.51X	σ = 2.88X	σ = 2.51X
Zener diodes (non-temperature compensated)	$\frac{1.1}{(P_R)^{0.41}\ (I_{PF})^{0.4}}$	$\frac{500(P_R)^{0.88}}{(t)^{0.312}}$	$\frac{1.48\ (V_Z)^{0.72}}{(P_R)^{0.23}\ (I_{PR})^{0.65}}$	$\frac{0.61\ (V_Z)^{0.6}}{(P_R)^{0.36}\ (I_{PR})^{0.5}}$	$\frac{262\ (P_R)^{0.3}}{(V_Z)^{0.25}\ (t)^{0.38}}$
	σ = 1.76X	σ = 2.24X	σ = 2.78X	σ = 2.24X	σ = 2.14X

TABLE H.10. List of symbols used in the diode pulse damage model development shown in the previous table (Ref. 17).

I_o	Maximum average rectified current rating (A) for rectifiers, diodes and switches
I_{PF}	Forward polarity pulse current (A)
I_{PR}	Reverse polarity pulse current (A)
P_R	Power rating for zener diodes (W)
t	Pulse width (μs)
V_{JF}	Forward polarity junction voltage (V)
V_{JR}	Reverse polarity junction voltage (V) $V_{JR} = V_Z$
V_{PF}	Diode forward polarity pulse voltage (V)
V_{PR}	Diode reverse polarity pulse voltage (V)
V_Z	Low current level junction breakdown voltage (V)
Z_{DF}	Forward polarity total device impedance (ohms) $Z_{DF} = \frac{V_{PF}}{I_{PF}}$
Z_{DR}	Reverse polarity total device impedance (ohms) $Z_{DR} = \frac{V_{PR}}{I_{PR}}$
Z_{SF}	Forward polarity surge impedance (ohms) $Z_{SF} = \frac{V_{PF} - V_{JF}}{I_{PF}} \simeq \frac{V_{PF}}{I_{PF}}$
Z_{SR}	Reverse polarity surge impedance (ohms) $Z_{SR} = \frac{V_{PR} - V_Z}{I_{PR}}$

REFERENCES

H.1. Hugh B. O'Donnell and Dante M. Tasca, Development of High Level Electrical Stress Failure Threshold and Prediction Model for Small Scale Junction Integrated Circuits, General Electric Co., Department of the Army, Harry Diamond Laboratories Contract No. DAAG39-76-C (September, 1977).

H.2. D. M. Tasca and S. J. Stokes, III, EMP Response and Damage Modeling of Diodes, Junction Field Effect Transistor Testing and Semiconductor Device Failure Analysis, General Electric Co., Space Division, Philadelphia, PA, Harry Diamond Laboratories Contract DAA G39-74-C-0090, Defense Nuclear Agency Subtask R99AQXEB097, HDL-CR-86-090-1 (April 1976).

H.3. B. M. Kalab, Damage Characterization of Semiconductor Devices for the AN/TRC-145 EMP Study, Harry Diamond Laboratories, Adelphia, MD, (Draft Report - 1978).

H.4. J. R. Miletta, Component Damage from Electromagnetic Pulse (EMP) Induced Transient, Harry Diamond Laboratories, Adelphi, MD, HDL-TM-77-22 (October 1977).

H.5. C. R. Jenkins and D. L. Durgin, An Evaluation of IC EMP Failure Statistics, IEEE Transactions on Nuclear Science, Vol. NS-24, No. 6, December 1977, pp. 2361-2364.

H.6. D. W. Egelkrout, Component Burnout Hardness Assurance Safety Margins and Failure Probability Distribution Models, at IEEE Annual Conf. on Nuclear and Space Radiation Effects, Albuquerque, NM (July 18-21, 1978).

H.7. D. W. Egelkrout, "Component Burnout Hardness Assurance Safety Margins and Failure Probability Distribution Models," Paper submitted to IEEE Transactions on Nuclear Science for NS-25, No. 6 (December 1978).

H.8. R. L. Williams, Semiconductor Device Damage Assessment for the INCA Program--A Probabilistic Approach, Harry Diamond Laboratories, Adelphi, MD, HDL-TR-1833 (March 1978).

H.9. N. Kusnezov and D. L. Crowther, Current Injection Testing of Selected Integrated Circuits, Lockheed Palo Alto Research Laboratory, Palo Alto, CA. LMSC-D506527, U.S. Navy Contract N00030-74-C-0100 (August 1976).

H.10. K. T. LePoer and W. V. Behrens, INCA EMP Assessment of a Foreign Radio (U), Harry Diamond Laboratories, Adelphi, MD, HDL-TM-77-13, September 1977 (title U, report SRD).

H.11. "Volume 1 Safeguard EMP/RFI Lessons Learned Safeguard Ground Facilities," U.S. Army Corps of Engineers, HNDSP-75-35-ED-SR, December 1975.

H.12. S. R. Kahn, Effects of EMP Testing on Semiconductor Long Term Reliability, ITT Research Institute, DNA Contract No. 001-76-C-0243, November 1977.

H.13. EMP Electronic Analysis Handbook, The Boeing Company (in cooperation with Braddock, Dunn, and McDonald, Inc.), May 1973, Air Force Weapons Laboratory, AFWL-TR-74-59, (AD 918 227L).

H.14. Advanced Airborne Command Post GFE Assessment Program Executive Summary Report TRW Systems Group, Redondo Beach, CA, Air Force Weapons Laboratory Contract F29601-74-C-0035 (December 15, 1975).

H.15. Defense Nuclear Agency, EMP Handbook, Vol. 1, Design Principles, Report No. 2114H-1 (August 1974), "CH. 8, Terminal Protection Devices and their Applications".

APPENDIX I.
SHORT PULSE EQUIVALENT

SHORT PULSE EQUIVALENT

In parallel with the rationale for conversion for damage effects for typical EMP signals, a similar expression can be derived for devices exhibited to shorter pulse lengths* and shorter time duration waveforms of a sine wave or damped sine wave nature. Here the assumed form of the damaged failure model is $P = Kt^{-1}$ for short pulse widths. Two cases are given, the forward and reverse conversion factors.

FORWARD CASE

Let t_s = period of sine wave, E = energy, and t_p = duration of pulse

Short Pulse Failure Model

$P_F = Kt_F^{-1}$ power for failure,

$E_F = K$ energy for failure,

or

$K_p = E_p = V_D I_O t_P$,

*An equivalence of this type was needed because of the experiment performed on the LLL Transient Range for nanosecond pulse widths.

where

$$I_o = V_o/R_g \quad .$$

Sine Wave

$$V_g = V_o \sin \omega t = V_o \sin \frac{2\pi t}{t_s} \quad .$$

$$I = I_o \sin \frac{2\pi t}{t_s},$$

$$\text{where } I_o = \frac{V_o}{R_g} \quad .$$

V_D assumed constant $0 \leq t_s/2$.

$$E_s = \int_o^{t_s/2} V_D I_o dt, \text{ energy absorbed during conduction}$$

$$E_s = \int_o^{t_s/2} V_D I_O \sin \frac{2\pi t}{t_s} dt$$

$$E_s = \frac{V_D I_O t_s}{\pi}$$

If the sine wave <u>just</u> causes failure in forward direction, then $t_s/2 = t_F$ and $E_s = E_F$. Substitute this value into the short pulse failure expression

$$K_s = E_F \quad ,$$

$$= \frac{V_D I_O t_s}{\pi} \quad .$$

The equivalence is obtained when $K_p = K_s$. Since

$$K_p = V_D I_0 t_p \quad ,$$

then

$$V_D I_0 t_p = \frac{V_D I_0 t_s}{\pi} \quad ,$$

and the equivalence is

$$t_s = \pi t_p \cong 3t_p \quad .$$

For the forward direction, this value can be compared with the equivalent value for that based on the failure model $p = Kt^{-1/2}$ of

$$t_s = (\pi^2/2)\, t_p \cong 5t_p \quad .$$

REVERSE CASE

For the reverse case, the derivation is slightly more complex. Failure is assumed to occur in the reverse bias direction (generally true). The analysis based on a rectangular pulse is the same as for the forward case with the exception of the expression for the current I_0 through the diode.

$$I_0 = \frac{V_0 - V_{BD}}{R_g} \quad ,$$

where V_{BD} is the breakdown voltage of the device. Damage remains expressed by

$$K_p = V_{BD} I_0 t_p \quad ,$$

where I_0 is as given in the preceding equation.

For a sine wave, $V_g = V_0 \cos \frac{2\pi t}{t_s}$ (cosine wave is used for analysis), the energy absorbed by the device is

$$E_s = \frac{V_{BD} I_0 t_s}{\pi} \left[1 - \left(\frac{V_{BD}}{V_0} \right)^2 \right]^{1/2} .$$

The time required to cause failure of the device is assumed to be the time that the voltage remains above the breakdown level, then

$$E_s = E_F .$$

The damage constant is $K_s = E_F$. The pulse damage constant is $K_p = V_{BD} I_0 t_p$.

The equivalence of these damage constants is

$$K_p = K_s ,$$

or

$$V_{BD} I_0 t_p = \frac{V_{BD} I_0 t_s}{\pi} \left[1 - \left(\frac{V_{BD}}{V_0} \right)^2 \right]^{1/2} ,$$

or upon rearranging,

$$t_s = \frac{\pi}{\left[1 - \left(\frac{V_{BD}}{V_0} \right)^2 \right]^{1/2}} t_p .$$

Thus, the conversion factor depends on the factor by which V_0 exceeds V_{BD}. V_0 is the peak sine wave voltage. (The corresponding factor for the model dependence of $P = Kt^{-1/2}$ is expressed by*

$$t_s = \frac{\cos^{-1}\left(\frac{V_B}{V_0}\right)}{1-\left(\frac{V_{BD}}{V_0}\right)^2}\, t_p \ ,$$

for the values of $V_0/V_{BD} > 1.5$ this factor is between 4 and 5.)

For $V_o/V_{BD} = 2$, the above short-pulse conversion factor is

$$t_s = \pi \frac{2}{\sqrt{3}} t_p \ ,$$

$$t_s = 3.63\ t_p \ .$$

Some values for other ratios:

$$V_0/V_{BD} = 3; \quad t_s = 3.33\ t_p \ ,$$

$$V_0/V_{BD} = 10; \quad t_s = 3.15\ t_p \ ,$$

$$V_0/V_{BD} \longrightarrow \infty; \quad t_s \longrightarrow \pi t_p \ ,$$

$$V_0/V_{BD} = \sqrt{2} \ , \quad t_s = \pi \frac{\sqrt{2}}{1} = 4.44\ t_p \ .$$

---

*Electronic Analysis Handbook, The Boeing Company (in cooperation with Braddock, Dunn, and McDonald, Inc.), May 1973, AFWL, Kirtland AFB, Albuquerque, NM.

APPENDIX J
REVIEW OF SHIELDING AND TERMINAL PROTECTION DEVICE REPORTS

SHIELDING

T. J. Sheppard, Some Considerations in Shielding of Spacecraft Against the Effects of EMP, TRW Systems Group for Lawrence Livermore Laboratory, Livermore, CA, PEM-49 (May 1976).

This report has some information on the variation of shielding effectiveness with frequency and a function of single, double, and triple braided cables.

J. S. Miller, Stripline Test Method for Measuring Transfer Impedance, Rockwell International, B-1 Division, Anaheim, CA, PEM-46 (November 1975).

The important protection parameter is transfer impedance Z_T of riveted joints over the frequency range of 10 kHz to 100 MHz. The stripline approach is used for flat samples as a proven quadraxial test system for cylindrical samples is not suitable. Test anomalies and limitations are discussed.

P. J. Madle, "Cable and Connector Shielding Attenuation and Transfer Impedance Measurements Using Quadraxial and Quintaxial Test Methods," 1975 IEEE Electromagnetic Compatibility Symposium Record, San Antonio, Texas, October 7-9, 1975.

Briefly reviews the shielding attenuation test methods and open wire, coaxial and inverted triaxial, quadriaxial, and quintaxial configurations used.

P. J. Madle, "Introduction to Field Penetration," 1978 IEEE International Symposium on Electromagnetic Compatibility, Atlanta, GA, June 20-22, 1978, pp. 82-85.

This paper reviews some of the sources of error in use and misuse of some conventional shielding viewpoints: Reflection/absorption-planar theory applied to three-dimensional objects, the use of electric, magnetic, and plane wave, and the use of 20 log (I_1/I_2) as a measure of shielding effectiveness.

EMP Protection for AM Radio Broadcast Stations, Defense Civil Preparedness Agency, TR-61-C, July 1976.

There are descriptions and diagrams of protection measures, but no discussions of uncertainty are given.

EMP Protective Systems, Defense Civil Preparedness Agency, TR-61-B, July 1976.

There are descriptions, diagrams, and costs provided, but there are no discussions of uncertainty.

B. D. Faraudo, Protection from an EMP-like Surge on a Wideband Signal Line, Lawrence Livermore Laboratory, Livermore, CA, PEM-54.

The surge arrestor (TPD) was used to protect equipment form fast-rise, high voltage surges. It is a spark gap assembly with gaps available in voltage breakdown ratings from 350 to 3500 Vdc.

J. A. Kreck, Actual Operating Characteristics of Three Terminal Protection Devices Applied to the AN/PRC-77 Field Radio, Harry Diamond Laboratories, Woodbridge, VA, HDL-TR-1826, December 1977.

This report apparently contains some of the most recent and thorough discussions of TPDs and their models. Performance of the spark gap, zener diode, and PIN diode relevant to the high altitude EMP threat was evaluated. A model was developed for the spark gap. Errors enter only as reasonable practical comparisons between computed and experimental results (Figs. 7-1, 7-2, and 7-3)

A Comparison Report of TransZorbs with Metal Oxide Varistor, General Semiconductor Industries Report, Tempe, Az, November 1975.

TransZorbs (General Semiconductor Industries) are silicon PN junction transient voltage suppressors. This report has 12 parameters or characteristics given for comparison of transient suppression devices. Comparisons are given in Figs. 3 and 4 of this report which demonstrate uncertainty variation in clamping voltage with pulse current. No uncertainties in manufacturing variations are given.

E. Malone, Hybrid Spark Gap Surge Arrestors: A High Frequency Receive System Arrestor for Lightning and EMP Protection, Joslyn Electronic Systems, Goleta, CA, PEM-42 (September 1974).

A high frequency receiving antenna system required a combination of lightning and EMP protection. Parameters of arrestor design are the main spark gap, bypass capacitor, parallel bleeder resistor, and a fast responding miniature spark gap for EMP protection. The diagram and a linear equivalent circuit are shown in Figs. J.1 and J.2. The lightning protection gap provides only a 900-V level of clamping at the theoretical 0.73-kV/ns EMP surge voltage ramp.

The miniature spark gap's response at 1800 V is five times faster. Uncertainty in calculated response is introduced by the representation of the complex nonlinear circuit by a linear model as shown.

O. M. Clark, Voltage Clamping Levels for Several Transzorb Transient Suppression Devices, General Semiconductor Industries, Inc. for Lawrence Livermore Laboratory, Livermore, CA, PEM-33 (March 1975).

Data on clamping levels for the 1N5629A (6.8 V), 1N5545A (33 V), 1N5654A (91 V), and 1N5664A (180 V) devices are given in Figs. J.3 for the 80-ns point of a 250-ns pulse duration. Device-to-device variations are usually within +5%.

T. J. Sheppard, Interface Circuit Protection in Satellite Applications, TRW Systems Group for Lawrence Livermore Laboratory, Livermore, CA, PEM-40 (July 1975).

Burnout protection against transients can be accomplished by adding devices (TPDs) to input-output (I/O) lines. Such devices must either limit the current, clamp the voltage or filter a transient without interfering with normal operation. Report discusses transient suppression techniques with first-order analysis for several circuits. Rules or criteria for selection of zener diodes and mechanical layout are given. Series resistors, feed-through filters, and shunt capacitors are discussed briefly as protective devices.

The Boeing Co., Seattle, WA, E-3A Nuclear Hardness Verification Report Summary, D204-10970-1 Contract F19628-70-C-0218, March 1976.

In this report, there are descriptions of the hardening and relative margins given. The types of equipment characteristics and changes with impact on EMP hardness maintenance are listed below.

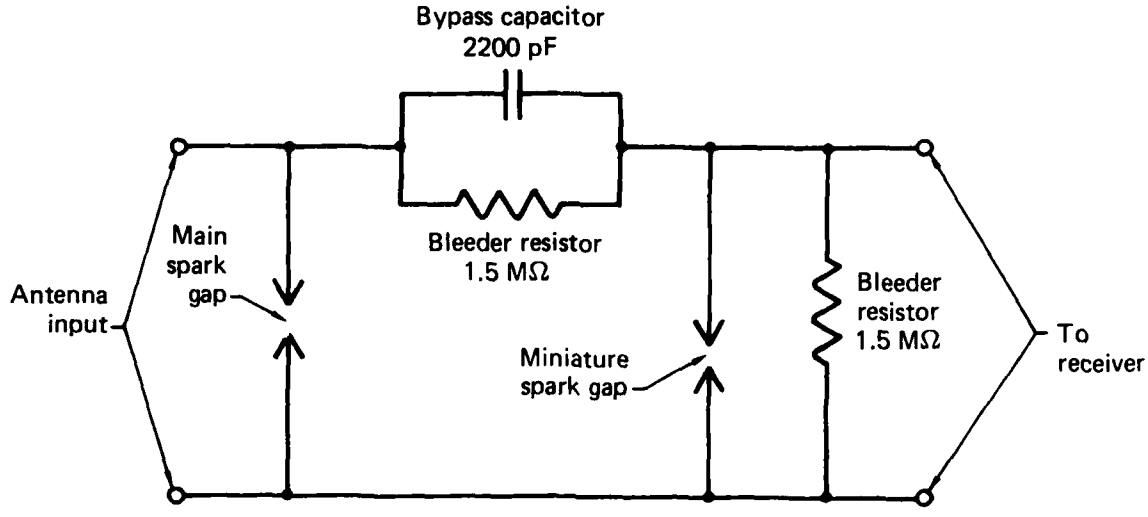

FIG J.1. Components of arrester.

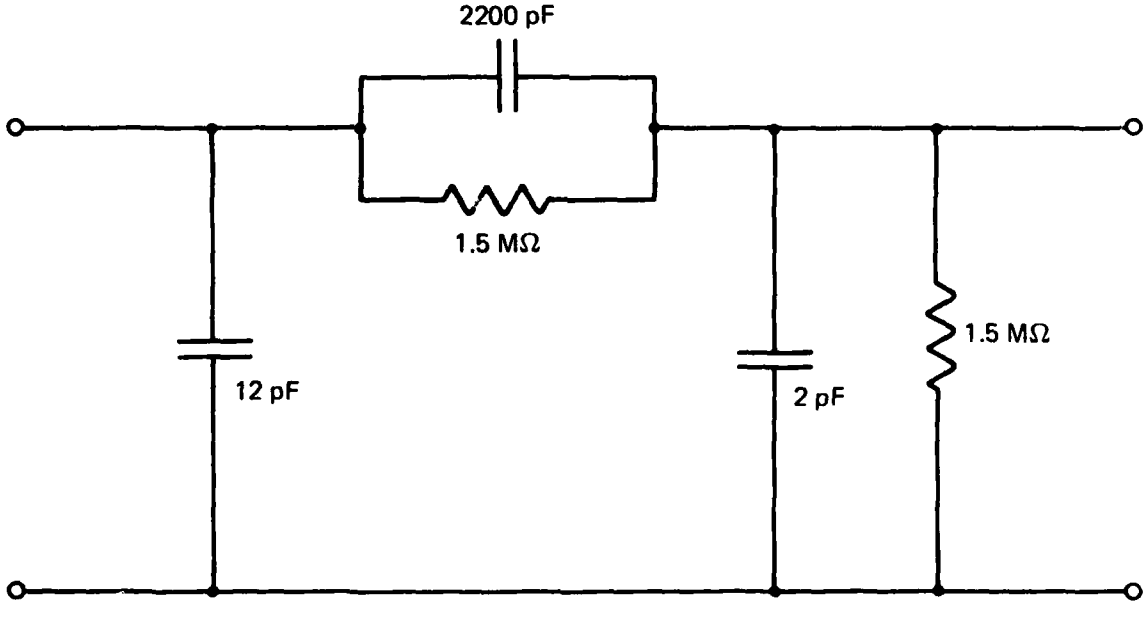

FIG. J.2. Equivalent circuit of the arrester.

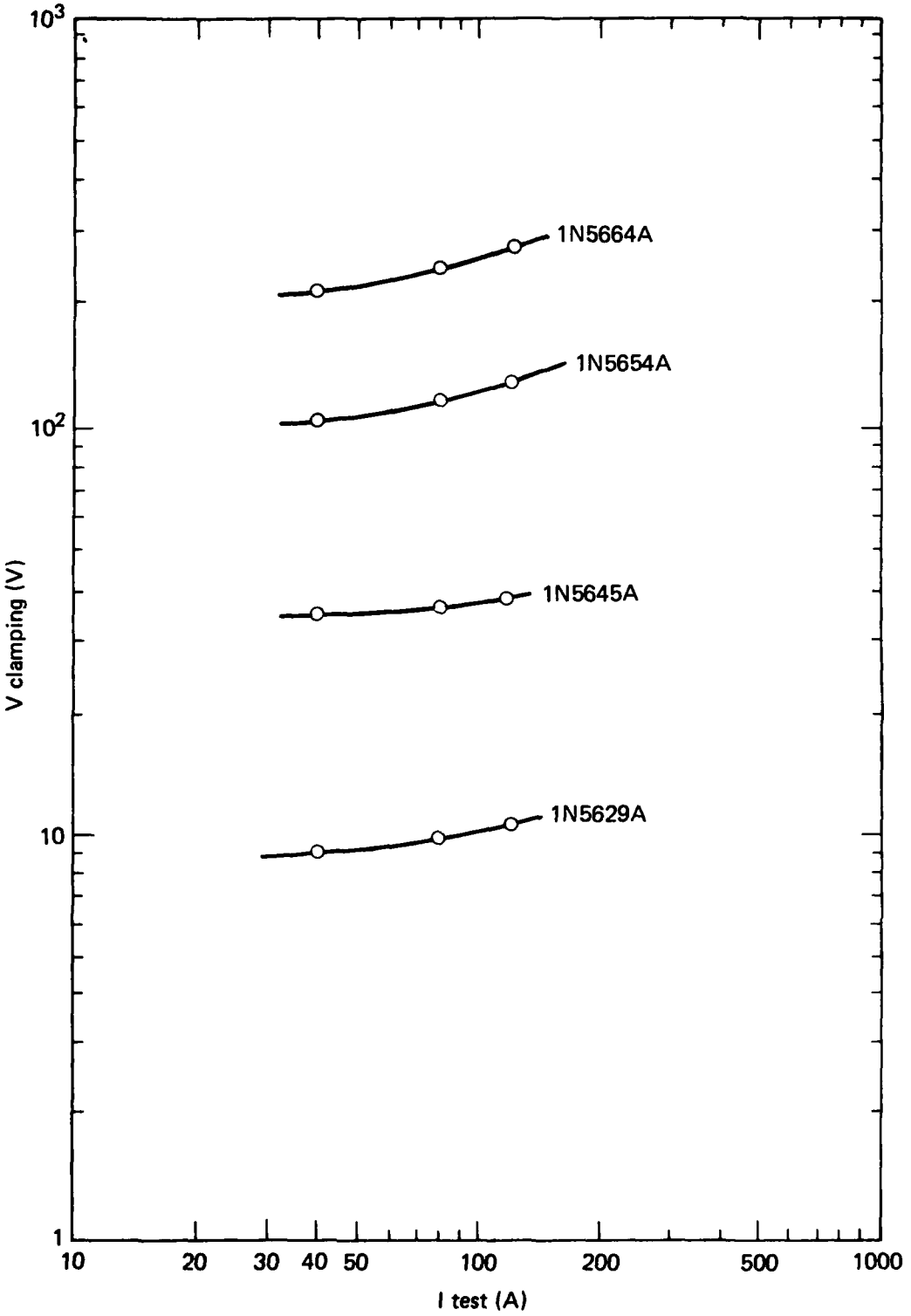

FIG. J.3. Clamping voltage vs test current at 80-ns point for several TransZorb devices.

1. Changes in semiconductor part types and/or electronic circuits.

2. Changes in equipment affecting hardness such as enclosures, filters, protective devices, cable shielding, rack bonding, and rack shielding.

3. Changes in vehicle in shielding and in protection of vulnerable avionics.

    a. Terminal protective devices--such as ESAs, TranZorbs, shunt capacitors, and RF filters.

    b. Wire bundle shields--properly terminated in connector backshells or pigtails to ground.

    c. Dielectric links--installed in control cables and mechanical penetrations of the pressure vessel.

    d. Thermal/EMP shield mask and barrier--installed in flight deck window.

    e. Screens across observation windows and viewing ports.

    f. Bonding and grounding straps.

    g. Conductive ground paths--across structural or mechanical interfaces.

    h. RF fingers.

    i. Waveguides (Below Cutoff)--ducting and tubing.

    j. RF gaskets--on equipment and rack enclosures.

    k. Honeycomb screens--across cooling air ducts.

    l. Embedded wire mesh seals--for all doors, hatches, and cockpit sliding windows.

The above are good examples of items in protection of large aircraft where uncertainty will arise due to changes in the protection features which may occur after the production phase. Lack of controls on such items will present a very difficult problem in estimating the operational hardness of the system.

RAC/tb/rc/11/dp

U. S. Government Printing Office: 1980/11-789-002/5522

END

DATE
FILMED

4-81

DTIC